12-2016

Utilization of ferrioxamine microarrays for the rapid detection of pathogenic bacteria

Nigam Bir Arora
Purdue University

Graduate School Form 30
(Updated 11/20/2014)

PURDUE UNIVERSITY
GRADUATE SCHOOL
Thesis/Dissertation Acceptance

This is to certify that the thesis/dissertation prepared

By Nigam Bir Arora II

Entitled UTILIZATION OF FERRIOXAMINE MICROARRAYS FOR THE RAPID DETECTION OF PATHOGENIC BACTERIA

For the degree of Doctor of Philosophy

Is approved by the final examining committee:

Alexander Wei

Philip S. Low

Kavita Shah

Bruce M Applegate

To the best of my knowledge and as understood by the student in the Thesis/Dissertation Agreement, Publication Delay, and Certification/Disclaimer (Graduate School Form 32), this thesis/dissertation adheres to the provisions of Purdue University's "Policy on Integrity in Research" and the use of copyrighted material.

Alexander Wei

Approved by Major Professor(s): _____

_____

Approved by: Timothy Zwier 11/29/2016

Head of the Department Graduate Program Date

UTILIZATION OF FERRIOXAMINE MICROARRAYS FOR THE RAPID DETECTION OF PATHOGENIC BACTERIA

A Dissertation

Submitted to the Faculty

of

Purdue University

by

Nigam Bir Arora II

In Partial Fulfillment of the

Requirements of the Degree

of

Doctor of Philosophy

December 2016

Purdue University

West Lafayette, Indiana

I dedicate this work to my family; to my father for instilling in me the importance of education and the drive to pursue knowledge, to my mother for providing undying support throughout my education and to my sister for leading the way ever since I can remember.

ACKNOWLEDGMENTS

I would like to acknowledge the educators that played a part in helping me reach this point. First is Professor Stephen Randall who gave me an opportunity to join his lab during my undergraduate education at IUPUI. This is where I got my first taste of laboratory research. Next is Professor Alex Wei who accepted me as a PhD student in his lab in 2012. Since then I have developed greatly as a scientist, a speaker and most importantly as an analytical thinker. I am very appreciative of both these opportunities and the knowledge and experience I have gained along the way. I would also like to thank some of my fellow students who helped me along the way throughout my education. Dr. Gauge Koelher was the first graduate student that I grew to know well. During my time in the Randall lab she never turned down a question and helped me early on establish my foothold in basic laboratory techniques. Dr. Qingshan Wei, the graduate student I worked with during my initial rotation in the Wei lab, introduced me to a whole new side of research related to novel chemistry and fascinating nanoparticle based studies. My experience working with him was a major influence in my decision to join the Wei lab for the remainder of my PhD. Dr. Matt Casselman and Dr. Oscar Morales were the two most senior graduate students when I joined the Wei lab. They took me in and each did their fair share in mentoring me through my early days in the lab. I would also like to thank Karl Williams and his family for taking me into their family home

during my final semester at Purdue. Finally I would like to thank my sister Dr. Natasha Arora. She, more than any other person, has offered me support when I needed it most to keep going throughout my academic career.

TABLE OF CONTENTS

Page

Page

LIST OF TABLES

LIST OF FIGURES

Figure Page

Figure Page

Figure Page

Figure Page

LIST OF SCHEMES

ABSTRACT

Arora, Nigam Bir, II. Ph.D., Purdue University, December 2016. Utilization of Ferrioxamine Microarrays for the Rapid Detection of Pathogenic Bacteria. Major Professor: Alexander Wei.

Siderophores are low-molecular weight species utilized by bacteria for the sequestration of iron, an essential nutrient. Siderophores and their cognate receptors are considered to be virulence factors, due to their prominent role in pathogenicity. The work presented here focuses on ferrioxamine (FOx) as an "immutable" ligand for pathogen detection. A number of bacterial strains expressing high-affinity FOx receptors were identified by a proteomic BLAST search, and screened against microarrays patterned with FOx conjugates for detection using label-free optical imaging. Aspects such as inkjet printing and surface chemistry, iron-limiting conditions and bacterial selection protocols, and linker conjugate design were addressed and optimized.

The label-free optical imaging method is capable of both sensitive and rapid detection of select pathogens, dependent upon bacterial concentration and exposure time. *Y. enterocolitica* could be detected as low as 10^2 cfu/mL after a 1-hour exposure; conversely, several pathogenic bacteria could be detected after just 30 seconds of exposure at 10^7 cfu/mL. Additional studies on pathogen detection at refrigeration temperatures are discussed.

CHAPTER 1. SIDEROPHORES AS IMMUTABLE LIGANDS

1.1 Introduction to Siderophores

Siderophores are a class of small molecules, whose name means "iron bearer" in Greek.[1] As the name implies, siderophores are utilized for acquisition of iron, an element critical to numerous cellular and subcellular processes in both eukaryotic and bacterial cells.[2-5] An astonishingly wide variety of living organisms utilize siderophores as a mechanism for acquisition of this essential nutrient.[6] This chapter focuses on the use of siderophores by bacteria, although some species of fungi and plants also employ these molecules. Hundreds of siderophores have been discovered in bacteria alone, since they were first described in 1949.[6-7]

Siderophores have several defining features: They are generally low molecular-weight species (mw 400–1000), chelate ferric ions (Fe^{3+}) via hexadentate coordination with formation constants ranging from 10^{12}–10^{52}, and are highly soluble in water.[8-10] Siderophores can be further categorized by the chemical functional groups used to chelate iron; these include hydroxamate, phenolate, catecholate and α-hydroxycarboxylate (Figure 1.1).[11-12] Mixed-type siderophores that utilize a combination of chelating groups are also known to exist.

Type: Hydroxamate
Name: Deferoxamine B
Native Producer: *Streptomyces pilosus*

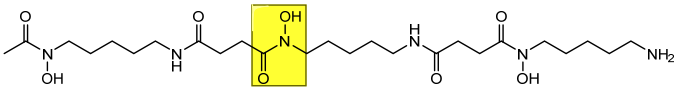

Type: Phenolate
Name: Yersiniabactin
Native Producer: *Yersinia enterocolitica*

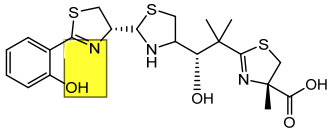

Type: Catecholate
Name: Salmochelin S4
Native Producer: *Salmonella* spp.

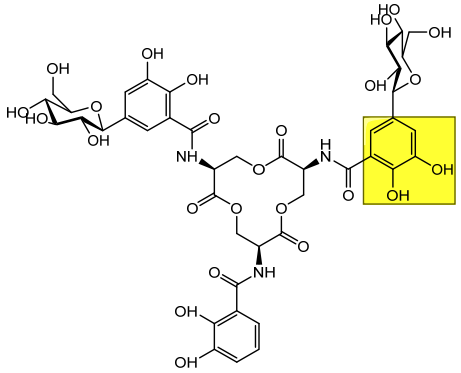

Type: α-hydroxycarboxylate
Name: Achromobactin
Native Producer: *Dickeya dadantii*

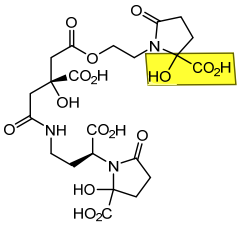

Figure 1.1: Representatives of the four major types of siderophores and their cognate bacterial species. Chemical structures defining the siderophore type are boxed in yellow.

Bacteria often secrete siderophores in response to environmentally low levels of iron.[13] Upon chelation of iron, siderophores are recovered by parent bacteria via cognate receptors presented on their outer membranes.[14] Receptor–siderophore relationships vary widely: in some cases, receptors are highly selective and will only recognize a specific siderophore structure; a well-known example is the selective binding of staphyloferrin A or B by *S. aureus*.[15-16] In other cases, a particular receptor might recognize a few structural congeners from the same siderophore family, as exemplified by the uptake of ferrioxamine, coprogen, or rhodotorulic acid by the same receptor expressed by *E. coli* (K12 strain).[17] The ability of bacteria to bind xenosiderophores (i.e. species other than its native siderophore) is a commonly observed evolutionary adaptation.[12, 18-19] Once bound,

iron-chelated siderophores are internalized through an ABC cassette-type transporter,[1] which for Gram-negative species is usually TonB-dependent.[19] Upon reaching the cytoplasm, the iron is released by enzymatic degradation of the siderophore or by reduction to iron(II), which has greatly reduced affinity for the siderophore.[19] Siderophores are often recycled, as their synthesis is an energetically demanding process.[20]

The idea of exploiting bacteria's affinity for siderophores has been around for some time. The discovery of sideromycins, naturally occurring siderophore–antibiotic conjugates, was the starting point for this field.[21] Since then a variety of synthetic siderophore–antibiotic conjugates have been tested for targeted delivery and increased antibiotic potency.[22] In a similar vein, we and others have used siderophores as ligands for detecting pathogenic bacteria.[16, 23-25] In the next section we present the rationale behind this approach, and earlier work that provides the foundation for this thesis.

1.2 Immutable Ligands for Bacterial Detection

As described in the previous section, the use of siderophores as iron scavengers is an important mechanism by which bacteria obtain this essential mineral.[26] Both siderophores and their corresponding receptors are considered to be virulence factors as they contribute directly to bacterial pathogenicity.[27-28] This is evidenced by severe attenuation or complete loss of pathogenicity in bacteria after deletion of genes responsible for synthesis of siderophores and their receptors.[29-30] Mutants that are unable to export siderophores from cells also exhibit a reduction in virulence.[31] This reliance on

siderophores and their receptors to maintain pathogenicity is a longstanding evolutionary trait and is widespread throughout the bacterial kingdom.[12, 32-33] For this reason, siderophore recognition can be considered to be immutable. In this thesis, we define immutable ligands as molecules with essential roles in pathogenicity and virulence, enabling colonization within a pathogen's requisite host. The use of immutable ligands for detecting pathogenic bacteria offers several fundamental benefits, not the least being their low vulnerability to nonfunctional mutations.

1.2.1 Methods of Pathogen Detection and Associated Pitfalls

A variety of methods for detecting pathogenic bacteria exist, none of which utilize immutable ligands. Most of them are plagued by one or more of the following: (1) slow turnaround time (i.e. time to detection); (2) susceptibility to bacterial mutation (i.e. loss of recognition function); (3) variable performance in different environments (i.e. requirement for laboratory-controlled conditions); (4) reliance on expensive and/or sensitive reagents; and (5) reliance on trained personnel. Traditional bacterial culture methods remain the gold standard for pathogen identification; however, they have many drawbacks for rapid detection. In addition to the need for a controlled laboratory environment and trained personnel, the results can take several days to produce.[34]

Alternatives to culture-based methods have been developed for rapid pathogen detection, although they share one or more of the weaknesses described above. For example, polymerase chain reaction is much faster than culture-based methods but has its own limitations such as the need for expensive instrumentation, trained operators, reliance on sensitive reagents, and potential interference from contaminating DNA

sources.[35] Antibody-based lateral flow assays have the advantage of speed and portability, but may also prove unreliable due to their inherent vulnerability to environmental degradation and also to nonfunctional mutations.[36-38] Regardless, the current state of the field is now focused on methods that are rapid, sensitive, and environmentally robust. In many cases, time to detection of 15 minutes or less has become the expected norm.[39-42]

1.3 Ferrioxamine as an Immutable Ligand for Pathogen Detection

While the promise of siderophores as ligands for pathogen detection is strong, a number of practical challenges must be addressed. One of these is to obtain a steady supply of siderophores for detection assays. The production of siderophores by bacterial fermentation is possible but much time is required for purification and the yields are often low.[11] Total synthesis is another alternative, however only a handful of well-developed procedures have been published for select molecules, and total synthesis in itself is a highly labor-intensive process. Some siderophores are commercially available but at prohibitively high costs, with a single milligram costing over $500 in several cases.

Deferoxamine B (also deferrioxamine or simply dFOx), the cognate siderophore of *Streptomyces pilosus*,[43] offers perhaps the best combination of biological activity and accessibility. Commercially available as deferrioxamine mesylate (Desferal), this compound is widely used as a medical treatment for hemochromatosis and thalassemia.[44-45] Thanks in part to market volume, dFOx is available at a price and purity that makes it appealing for further development as an immutable ligand. It also has a free primary

amine for easy modification, using standard bioconjugate chemistry methods, and the molecule itself is stable in a variety of chemical environments.

1.4 Bacterial Ferrioxamine Receptors

In addition to availability, affordability and robustness, ferrioxamine offers much promise as a low-molecular weight ligand for pathogen detection. As with all siderophores, chelation with iron is achieved readily by simple exposure to solutions containing Fe^{3+} ions (Scheme 1.1); in this thesis, the corresponding metal complex will be referred to simply as FOx.

FOx is known to bind with high affinity to cognate outer-membrane receptors (OMRs) found in many pathogenic bacteria.[12, 19, 46] Three major FOx receptors have been characterized so far: (i) FoxA, which is used by *Yersinia enterocolitica*[47-48] and also by *Salmonella enterica*;[49] (ii) FhuE, which is expressed by *A. baumannii*[50] and several strains of *Escherichia coli*; and (iii) FhuD1/2, whose isoforms are found primarily in *Staphylococcus aureus* but also in certain bacilli.[51-52] All three major FOx receptors have been widely studied, and shown to be important virulence factors in their parent pathogens. Less well-characterized receptors for FOx have also been identified, including DesA in *V. vulnificus*[53-54] and FoxB in certain strains of *E. coli* and *P. aeruginosa*.[55-56]

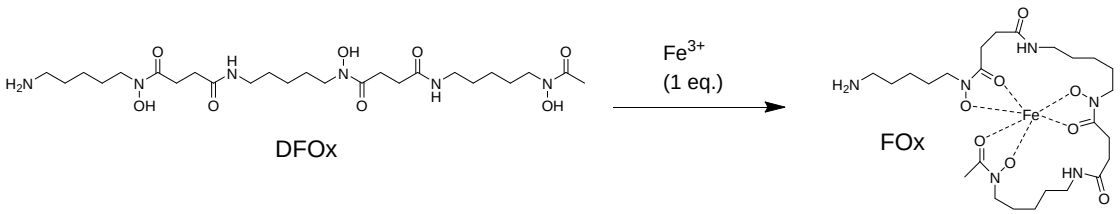

Scheme 1.1: Chelation of dFOx with Fe^{3+} to become FOx.

In the case of *Y. enterocolitica*, the administration of Desferal (dFOx) to treat hemochromatosis has been shown to promote *Yersinia* infections, specifically by strains that use FoxA for iron acquisition.[57] A study of human clinical isolates of *Y. enterocolitica* showed greater than 95% of strains examined utilized FOx for iron acquisition.[58] FoxA mutants are unable to harvest FOx for iron uptake; conversely, transfection of the FoxA gene into *E. coli* strains that do not typically use FOx for iron acquisition bestows the capacity to harvest this siderophore.[47]

The FhuE receptor has been shown to be crucial for the uptake of FOx by *A. baumannii*; studies with FhuE deletion mutants have confirmed the receptor's essential role in FOx uptake.[50] It was also found that expression of FhuE alone, in the absence of other siderophore receptor proteins, was sufficient for *A. baumannii* to harvest FOx.[50] Incidentally, a pan-genomic study including 30 different *A. baumannii* strains revealed the FhuE receptor to be highly antigenic.[59]

In the case of FhuD1 and FhuD2, these lipoprotein receptors are presented on the surfaces of Gram-positive species such as *Staphylococcus aureus*, which lack an outer cell membrane and thus behave differently from OMRs expressed by Gram-negative bacteria. The crystal structures of FhuD2 and its FOx complex was published recently, confirming unequivocally that this receptor is fundamental in the transport of FOx through the bacterial wall.[52] Studies involving FhuD2 deletion mutants of *S. aureus* show expression of this receptor to be critical for establishing initial infection in mammals.[60] The strength of this result led the same group of researchers to begin work toward a vaccine against *S. aureus* using virulence factor FhuD2 to generate immunity.[61] Studies with the methicillin-resistant form of *S. aureus* (MRSA) also show evidence of

the role of FOx in infection.[62] The addition of exogenous FOx enhances infections by MRSA, which express both FhuD1 and FhuD2; in contrast, the level of infection by deletion mutants without these receptors are unaffected by the addition of FOx.

1.5 Protein BLAST Search and Analysis

The basic local assignment search tool (BLAST) is a powerful bioinformatics tool that compares specific sets of genetic or protein data against the vast archives of compiled data. BLAST allows for any amino acid (protein) or nucleotide (gene) sequence to be searched against the proteomes or genomes of a given species. The results of a BLAST search will show whether a sequence of interest is likely to be present in selected species, and also the degree to which they are similar (consensus). In our research, we used BLAST to identify bacterial strains exhibiting outer membrane or lipoprotein receptors capable of binding FOx.

BLAST searches were conducted on two databases, bacteria.ensembl.org and blast.ncbi.nlm.nih.gov. Our efforts were focused on protein rather than gene sequences as we wished to identify actively expressed receptor proteins, although analogous gene-based searches were sometimes performed for confirmation. BLAST searches focused on bacterial proteins[63] identified receptors FoxA, FhuE and FhuD2, whose affinities for FOx were in accord with earlier studies involving bacteria expressing those receptors.[47-52] We also screened for FOx receptors in several drug-resistant bacterial strains, for potential expansion into the rapid detection of these public health menaces.[64] A summary of all BLAST searches focused on FOx receptors are presented in Table 1.1.

Table 1.1: Bacterial strains subjected to BLAST search based on expression of FOx receptors

Bacterial Strain	ATCC #[a]	FOx Receptor(s)
Available laboratory strains		
Acinetobacter baumannii	19606	FhuE
Aliivibrio fischeri	7744	None
Bacillus anthracis		None
Bacillus cereus	14579	FhuD2
Bacillus megaterium	14581	None
Bartonella henselae	49882	None
Campylobacter jejuni	33560	None
Chlamydia trachomatis	VR-571B	None
E. coli (Migula)	25922	FhuE
E. coli (O157:H7)	43895	None
E. coli K12 MG1655	700926	FhuE
E. coli O104:H21	BAA-178	None
Enterobacter aerogenes	13048	FoxA
Klebsiella pneumoniae	27736	FoxA
Listeria monocytogenes	19115	None
Mycobacterium smegmatis		None
Neisseria gonorrhoeae	49226	None
Pseudomonas aeruginosa	47085	FoxA
Rhodospirillum rubrum	9791	None
Salmonella enterica	35664	FoxA, FhuE
Shigella spp.		None
Staphylococcus aureus	10537	FhuD2
S. aureus, methicillin-resistant (MRSA)	BAA-1720	FhuD2
Staphylococcus epidermidis	155	None
Streptococcus pneumoniae	BAA-255	None
Vibrio cholerae	39541	None
Yersinia enterocolitica	51871	FoxA
Drug-resistant Strains[64]		
Carbapenem-Resistant Enterobacteriaceae (*E. coli*)		FoxA
Carbapenem-Resistant Enterobacteriaceae (*K. pneumoniae*)		FoxA
Vancomycin-Resistant Enterococcus (VRE; *Enterococcus faecium*; ATCC 700221)		None
Methicillin-Resistant *Staphylococcus pseudintermedius* (MRSP; 49051)		FhuD2
Clostridium Difficile (C-DIFF)		None
Salmonella enterica serovar Typhi*;* ATCC 19430		FoxA
Vancomycin-Resistant *Staphylococcus aureus* (VRSA)		None

Of available laboratory strains, 11 were identified by BLAST search of the three major FOx receptors. In particular searches against *Y. enterocolitica, S. enterica, A. baumannii, S. aureus, P. aeruginosa, K. pneumoniae* and MRSA were performed against the exact ATCC strains used in our laboratories. Interestingly, a BLAST search with *S. enterica* (ATCC 35664) was found to express receptors FoxA and FhuE, although the latter has not been reported in literature previously.[47-49]

1.6 Conclusions

Siderophores, like so many useful natural products, have been shaped by evolutionary pressures into a sophisticated and structurally diverse group of molecular species. In particular, many pathogenic bacteria have developed siderophores for the acquisition of iron, an important virulence factor. For this reason, siderophores can be considered as immutable ligands that enable the recognition and capture of specific bacteria with high affinity. Unlike antibodies, nonfunctional mutations cannot cause siderophore recognition to fail, as pathogenic bacteria will always have a need for iron. Exploiting siderophore recognition for pathogen detection thus avoids many of the common pitfalls associated with antibody-based recognition.

FOx is an ideal siderophore as an immutable ligand for bacterial detection: it is employed by numerous pathogen receptors, and is readily available at an affordable cost. A variety of human pathogens present outer membrane and lipoprotein receptors with high affinity for FOx, as verified by protein BLAST searches.

1.7 Materials and Methods

BLAST search. Amino acid sequences for receptors FhuD2 (Q7BGA5_STAAU) and FhuE (A0A009HL84_ACIBA) were found on UniProt.org.[65] The sequence for FoxA has been described in the literature.[47] BLAST searches were performed using the website bacteria.ensembl.org. From the home page BLAST was selected from the main menu. Once on this page the amino acid sequence for a single receptor protein was copied and pasted into the box labelled "sequence data". Underneath this box the option for "Protein" was selected in order to search against known amino acid sequences. The next box titled "search against" allowed for selection of up to 25 bacterial strains from the list of tens of thousands available to search against. For each receptor protein multiple searches were performed in order to accommodate all strains from Table 1.1. Underneath this box, the option for "protein database" was selected and the next box labeled "search tool" was automatically set to "BLASTX". The box labeled "search sensitivity" was set to "normal". After each of these steps was complete search was started by clicking the "run" button.

Upon completion of the search a list of jobs would come up. For each job a section titled "view results" was selected for more detailed information. This information gave several indicators about the quality of the hit. The length of the sequence should match that which was input. The E-val should be below 10^{-4}, with lower values indicating a better match. %ID was also shown, indicating the amount of homology between the sequence search and the one being viewed. For a definitive hit this should be near 99% or above. Furthermore, by clicking the name of the protein a written description would come up. A description such as "ferrioxamine receptor" was a further

indicator of a good hit. If all these identifiers were positive it was considered a positive hit. The strain exhibiting the examined protein was then added to the list of positive hits displayed in Table 1.1.

1.8 References

1. Saha, R.; Saha, N.; Donofrio, R. S.; Bestervelt, L. L., Microbial siderophores: a mini review. *J Basic Microbiol.* **2013,** *53* (4), 303-317.

2. Messenger, A. J. M.; Barclay, R., Bacteria, iron and pathogenicity. *Biochem Educ.* **1983,** *11* (2), 54-63.

3. Andrews, S. C.; Robinson, A. K.; Rodríguez-Quiñones, F., Bacterial iron homeostasis. *FEMS Microbiol Rev.* **2003,** *27* (2-3), 215-237.

4. Dlouhy, A. C.; Outten, C. E., The Iron Metallome in Eukaryotic Organisms. *Met Ions Life Sci.* **2013,** *12*, 241-278.

5. Frawley, E. R.; Fang, F. C., The Ins and Outs of Bacterial Iron Metabolism. *Mol Microbiol.* **2014,** *93* (4), 609-616.

6. Hider, R. C.; Kong, X., Chemistry and biology of siderophores. *Nat Prod Rep.* **2010,** *27* (5), 637-657.

7. J. Francis, J. M., H. M. Macturk and G. A. Snow, Isolation from Acid-Fast Bacteria of a Growth-Factor for *Mycobacterium johnei* and of a Precursor of Phthiocol. *Nature* **1949,** *163*, 365.

8. Neilands, J. B., Microbial Envelope Proteins Related to Iron. *Annu Rev Microbiol.* **1982,** *36* (1), 285-309.

9. Crosa, J. H.; Walsh, C. T., Genetics and Assembly Line Enzymology of Siderophore Biosynthesis in Bacteria. *Microbiol Mol Biol Rev.* **2002,** *66* (2), 223-249.

10. Oves-Costales, D.; Kadi, N.; Challis, G. L., The long-overlooked enzymology of a nonribosomal peptide synthetase-independent pathway for virulence-conferring siderophore biosynthesis. *Chem. Commun.* **2009,** (43), 6530-6541.

11. Bister, B.; Bischoff, D.; Nicholson, G. J.; Valdebenito, M.; Schneider, K.; Winkelmann, G.; Hantke, K.; Süssmuth, R. D., The structure of salmochelins: C-glucosylated enterobactins of *Salmonella enterica*. *Biometals* **2004,** *17* (4), 471-481.

12. Miethke, M.; Marahiel, M. A., Siderophore-Based Iron Acquisition and Pathogen Control. *Microbiol Mol Biol Rev.* **2007,** *71* (3), 413-451.

13. Ratledeg, C.; Dover, L. G., Iron Metabolism in Pathogenic Bacteria. *Annu Rev Microbiol.* **2000,** *54*, 881.

14. Stintzi, A.; Barnes, C.; Xu, J.; Raymond, K. N., Microbial Iron Transport via a Siderophore Shuttle: A Membrane Ion Transport Paradigm. *Proc Natl Acad Sci USA* **2000,** *97* (20), 10691-10696.

15. Grigg, J. C.; Cheung, J.; Heinrichs, D. E.; Murphy, M. E. P., Specificity of Staphyloferrin B Recognition by the SirA Receptor from Staphylococcus aureus. *J. Biol. Chem.* **2010,** *285* (45), 34579-34588.

16. Pandey, R. K.; Jarvis, G. G.; Low, P. S., Chemical synthesis of staphyloferrin A and its application for *Staphylococcus aureus* detection. *Org Biomol Chem.* **2014,** *12* (11), 1707-1710.

17. Sauer, M.; Hantke, K.; Braun, V., Sequence of the fhuE outer-membrane receptor gene of *Escherichia coli* K12 and properties of mutants. *Mol Microbiol* **1990,** *4* (3), 427-37.

18. Winkelmann, G., Ecology of siderophores with special reference to the fungi. *Biometals* **2007,** *20* (3), 379-392.

19. Caza, M.; Kronstad, J. W., Shared and distinct mechanisms of iron acquisition by bacterial and fungal pathogens of humans. *Front Cell Infect Microbiol.* **2013,** *3*, 80.

20. Imperi, F.; Tiburzi, F.; Visca, P., Molecular basis of pyoverdine siderophore recycling in *Pseudomonas aeruginosa*. *Proc Natl Acad Sci USA* **2009,** *106* (48), 20440-20445.

21. Braun, V.; Pramanik, A.; Gwinner, T.; Koberle, M.; Bohn, E., Sideromycins: tools and antibiotics. *Biometals* **2009,** *22* (1), 3-13.

22. Page, M. G. P., Siderophore conjugates. *Ann N Y Acad Sci.* **2013,** *1277* (1), 115-126.

23. Doorneweerd, D. D.; Henne, W. A.; Reifenberger, R. G.; Low, P. S., Selective Capture and Identification of Pathogenic Bacteria Using an Immobilized Siderophore. *Langmuir* **2010,** *26* (19), 15424-15429.

24. Kim, Y.; Lyvers, D. P.; Wei, A.; Reifenberger, R. G.; Low, P. S., Label-free detection of a bacterial pathogen using an immobilized siderophore, deferoxamine. *Lab Chip* **2012,** *12* (5), 971-976.

25. Adak, A. K.; Boley, J. W.; Lyvers, D. P.; Chiu, G. T.; Low, P. S.; Reifenberger, R.; Wei, A., Label-Free Detection of *Staphylococcus aureus* Captured on Immutable Ligand Arrays. *ACS Appl Mater Interfaces* **2013,** *5* (13), 6404-6411.

26. Chu, B.; Garcia-Herrero, A.; Johanson, T.; Krewulak, K.; Lau, C.; Peacock, R. S.; Slavinskaya, Z.; Vogel, H., Siderophore uptake in bacteria and the battle for iron with the host; a bird's eye view. *Biometals* **2010,** *23* (4), 601-611.

27. Holden, V. I.; Bachman, M. A., Diverging roles of bacterial siderophores during infection. *Metallomics* **2015,** *7* (6), 986-995.

28. Beare, P. A.; For, R. J.; Martin, L. W.; Lamont, I. L., Siderophore-mediated cell signalling in *Pseudomonas aeruginosa*: divergent pathways regulate virulence factor production and siderophore receptor synthesis. *Mol Microbiol.* **2003,** *47* (1), 195-207.

29. Register, K. B.; Ducey, T. F.; Brockmeier, S. L.; Dyer, D. W., Reduced Virulence of a *Bordetella bronchiseptica* Siderophore Mutant in Neonatal Swine. *Infect Immun.* **2001,** *69* (4), 2137-2143.

30. Dale, S. E.; Doherty-Kirby, A.; Lajoie, G.; Heinrichs, D. E., Role of Siderophore Biosynthesis in Virulence of *Staphylococcus aureus*: Identification and Characterization of Genes Involved in Production of a Siderophore. *Infect Immun.* **2004,** *72* (1), 29-37.

31. Wells, R. M.; Jones, C. M.; Xi, Z.; Speer, A.; Danilchanka, O.; Doornbos, K. S.; Sun, P.; Wu, F.; Tian, C.; Niederweis, M., Discovery of a Siderophore Export System Essential for Virulence of *Mycobacterium tuberculosis*. *PLoS Pathog.* **2013,** *9* (1), e1003120.

32. Lee, W.; van Baalen, M.; Jansen, V. A. A., An evolutionary mechanism for diversity in siderophore-producing bacteria. *Ecol Lett.* **2012,** *15* (2), 119-125.

33. Kümmerli, R.; Schiessl, K. T.; Waldvogel, T.; McNeill, K.; Ackermann, M., Habitat structure and the evolution of diffusible siderophores in bacteria. *Ecol Lett.* **2014,** *17* (12), 1536-1544.

34. Washington, J. A., Principles of Diagnosis. In *Medicinal Microbiology*, 4 ed.; S., B., Ed. University of Texas Medical Branch: Galveston, 1996.

35. Olsen, J. E.; Aabo, S.; Hill, W.; Notermans, S.; Wernars, K.; Granum, P. E.; Popovic, T.; Rasmussen, H. N.; Olsvik, Ø., Probes and polymerase chain reaction for detection of food-borne bacterial pathogens. *Int J Food Microbiol.* **1995,** *28* (1), 1-78.

36. Paddle, B. M., Biosensors for chemical and biological agents of defence interest. *Biosens Bioelectron.* **1996,** *11* (11), 1079-1113.

37. Nugaeva, N.; Gfeller, K. Y.; Backmann, N.; Lang, H. P.; Düggelin, M.; Hegner, M., Micromechanical cantilever array sensors for selective fungal immobilization and fast growth detection. *Biosens Bioelectron.* **2005,** *21* (6), 849-856.

38. Savran, C. A.; Knudsen, S. M.; Ellington, A. D.; Manalis, S. R., Micromechanical Detection of Proteins Using Aptamer-Based Receptor Molecules. *Anal Chem.* **2004,** *76* (11), 3194-3198.

39. Amini, K.; Kraatz, H.-B., Recent advances and developments in monitoring biological agents in water samples. *Rev Environ Sci Biotechnol* **2015,** *14* (1), 23-48.

40. Li, B.; Yu, Q.; Duan, Y., Fluorescent labels in biosensors for pathogen detection. *Crit Rev Biotechnol.* **2015,** *35* (1), 82-93.

41. Thissen, J. B.; McLoughlin, K.; Gardner, S.; Gu, P.; Mabery, S.; Slezak, T.; Jaing, C., Analysis of sensitivity and rapid hybridization of a multiplexed Microbial Detection Microarray. *J Virol Methods* **2014,** *201* (C), 73-78.

42. Mai, J.; Abhyankar, V. V.; Piccini, M. E.; Olano, J. P.; Willson, R.; Hatch, A. V., Rapid detection of trace bacteria in biofluids using porous monoliths in microchannels. *Biosens Bioelectron.* **2014,** *54*, 435-441.

43. Müller, G.; Raymond, K. N., Specificity and mechanism of ferrioxamine-mediated iron transport in *Streptomyces pilosus*. *J Bacteriol.* **1984,** *160* (1), 304-312.

44. Bernhardt, P. V., Coordination chemistry and biology of chelators for the treatment of iron overload disorders. *Dalton Trans.* **2007,** (30), 3214-3220.

45. Nick, H., Iron chelation, quo vadis? *Curr Opin Chem Biol.* **2007,** *11* (4), 419-423.

46. Sheldon, J. R.; Heinrichs, D. E., Recent developments in understanding the iron acquisition strategies of gram positive pathogens. *FEMS Microbiol Rev.* **2015,** *39* (4), 592-630.

47. Báumler, A. J.; Hantke, K., Ferrioxamine uptake in *Yersinia enterocolitica*: characterization of the receptor protein FoxA. *Mol Microbiol.* **1992,** *6* (10), 1309-1321.

48. Deiss, K.; Hantke, K.; Winkelmann, G., Molecular recognition of siderophores: A study with cloned ferrioxamine receptors (FoxA) from *Erwinia herbicola* and *Yersinia enterocolitica*. *Biometals* **1998,** *11* (2), 131-137.

49. Kingsley, R. A.; Reissbrodt, R.; Rabsch, W.; Ketley, J. M.; Tsolis, R. M.; Everest, P.; Dougan, G.; Bäumler, A. J.; Roberts, M.; Williams, P. H., Ferrioxamine-Mediated Iron(III) Utilization by *Salmonella enterica*. *Appl Environ Microbiol.* **1999,** *65* (4), 1610-1618.

50. Funahashi, T.; Tanabe, T.; Mihara, K.; Miyamoto, K.; Tsujibo, H.; Yamamoto, S., Identification and Characterization of an Outer Membrane Receptor Gene in *Acinetobacter baumannii* Required for Utilization of Desferricoprogen, Rhodotorulic Acid, and Desferrioxamine B as Xenosiderophores. *Biol Pharm Bull.* **2012,** *35* (5), 753-760.

51. Sebulsky, M. T.; Shilton, B. H.; Speziali, C. D.; Heinrichs, D. E., The Role of FhuD2 in Iron(III)-Hydroxamate Transport in *Staphylococcus aureus*. *J. Biol. Chem.* **2003,** *278* (50), 49890-49900.

52. Podkowa, K. J.; Briere, L.-A. K.; Heinrichs, D. E.; Shilton, B. H., Crystal and Solution Structure Analysis of FhuD2 from *Staphylococcus aureus* in Multiple Unliganded Conformations and Bound to Ferrioxamine-B. *Biochemistry* **2014,** *53* (12), 2017-2031.

53. Aso, H.; Miyoshi, S.-i.; Nakao, H.; Okamoto, K.; Yamamoto, S., Induction of an outer membrane protein of 78 kDa in *Vibrio vulnificus* cultured in the presence of desferrioxamine B under iron-limiting conditions. *FEMS Microbiol Lett.* **2002,** *212* (1), 65-70.

54. Funahashi, T.; Tanabe, T.; Maki, J.; Miyamoto, K.; Tsujibo, H.; Yamamoto, S., Identification and characterization of *Aeromonas hydrophila* genes encoding the outer membrane receptor of ferrioxamine B and an AraC-type transcriptional regulator. *Biosci Biotechnol Biochem.* **2014,** *78* (10), 1777-1787.

55. Nelson, M.; Carrano, C.; Szaniszlo, P., Identification of the ferrioxamine B receptor, FoxB, in *Escherichia coli* K12. *Biometals* **1992,** *5* (1), 37-46.

56. Ó Cuív, P.; Keogh, D.; Clarke, P.; O'Connell, M., FoxB of *Pseudomonas aeruginosa* Functions in the Utilization of the Xenosiderophores Ferrichrome, Ferrioxamine B, and Schizokinen: Evidence for Transport Redundancy at the Inner Membrane. *J Bacteriol.* **2007,** *189* (1), 284-287.

57. Bottone, E. J., *Yersinia enterocolitica*: Revisitation of an Enduring Human Pathogen. *Clin Microbiol Newsl.* **2015,** *37* (1), 1-8.

58. Chambers, C. E.; Sokol, P. A., Comparison of siderophore production and utilization in pathogenic and environmental isolates of *Yersinia enterocolitica*. *J Clin Microbiol.* **1994,** *32* (1), 32-39.

59. Hassan, A.; Naz, A.; Obaid, A.; Paracha, R. Z.; Naz, K.; Awan, F. M.; Muhmmad, S. A.; Janjua, H. A.; Ahmad, J.; Ali, A., Pangenome and immuno-proteomics analysis of *Acinetobacter baumannii* strains revealed the core peptide vaccine targets. *BMG Genomics* **2016,** *17*, 732.

60. Mishra, R. P. N.; Mariotti, P.; Fiaschi, L.; Nosari, S.; Maccari, S.; Liberatori, S.; Fontana, M. R.; Pezzicoli, A.; De Falco, M. G.; Falugi, F., et al., *Staphylococcus aureus* FhuD2 Is Involved in the Early Phase of Staphylococcal Dissemination and Generates Protective Immunity in Mice. *J Infect Dis.* **2012,** *206* (7), 1041-1049.

61. Mariotti, P.; Malito, E.; Biancucci, M.; Lo Surdo, P.; Mishra, Ravi P. N.; Nardi-Dei, V.; Savino, S.; Nissum, M.; Spraggon, G.; Grandi, G., et al., Structural and functional characterization of the *Staphylococcus aureus* virulence factor and vaccine candidate FhuD2. *Biochem. J.* **2013,** *449* (3), 683-693.

62. Arifin, A. J.; Hannauer, M.; Welch, I.; Heinrichs, D. E., Deferoxamine mesylate enhances virulence of community-associated methicillin resistant *Staphylococcus aureus*. *Microbes Infect.* **2014,** *16* (11), 967-972.

63. Kersey, P. J.; Allen, J. E.; Armean, I.; Boddu, S.; Bolt, B. J.; Carvalho-Silva, D.; Christensen, M.; Davis, P.; Falin, L. J.; Grabmueller, C., et al., Ensembl Genomes 2016: more genomes, more complexity. *Nucleic Acids Res.* **2016,** *44* (D1), D574-D580.

64. *Antibiotic/Antimicrobial Resistance*; Centers for Disease Control and Prevention: Septemeber 8, 2016.

65. Consortium, T. U., UniProt: a hub for protein information. *Nucleic Acids Res.* **2015,** *43* (D1), D204-D212.

CHAPTER 2. OPTIMIZATION OF MICROARRAYS FOR DETECTION OF FERRIOXAMINE-BINDING PATHOGENS

2.1 Introduction to Microarrays for Detection of Pathogenic Bacteria

The method presented here was designed to afford straightforward, reliable and rapid detection of pathogenic bacteria. The method has evolved over time and has benefited from incremental improvement through the efforts of previous work in our laboratories. The label-free pathogen detection method with FFT readout was first reported by Doorneweerd *et al.* in 2010.[1] In brief, a bacteria binding molecule (pyoverdine) was conjugated to bovine serum albumin (BSA) and patterned onto substrates as a linear grating by microcontact printing using PDMS stamps. The capture of pathogenic *P. aeruginosa* onto the array could be imaged under optical darkfield conditions, and quantified by converting images into spectra by fast Fourier transform followed by peak analysis. Later that year, a second report published by Adak *et al.*[2] demonstrated that a glycan conjugated to a bishydrazide linker could also be tethered onto BSA for presentation on substrates as periodic microarrays, with the successful detection of *P. aeruginosa* at 10^3 cfu/mL.

In 2012, Kim *et al*.[3] showed that the siderophore ferrioxamine (FOx) could also be used for pathogen capture and detection. These microarrays were screened against multiple species of live pathogens including *Y. enterocolitica*, *P. aeruginosa* and *S.*

aureus. A formal limit of detection for *Y. enterocolitica* was established to be 10^3 cfu/mL after a 1 hour exposure. In 2013, Adak *et al*. demonstrated the use of non-contact inkjet printing for patterning conjugates as dot-matrix microarrays onto activated glass substrates.[4] FFT analysis of simulated microarrays was examined in detail, and noted for its fault tolerance and potential application toward multiplex detection. Since the introduction of these methods, further progress has been made with regard to inkjet deposition and substrate conditioning. The work presented in this chapter represent the most significant advances in the inkjet printing of immutable ligand microarrays.

2.2 Chip Preparation and Optimization

The process begins with an immutable ligand that is recognized by bacterial strains of interest. While FOx is featured for reasons described in Section 1.4, the methodology is readily adaptable to many other ligands. In this work, we conjugate FOx to a bis-isothiocyanate (ITC) linker for its optimal presentation to bacterial receptors. The conjugates dissolve readily in mildly basic buffers and can be deposited onto activated glass substrates by inkjet printing. Ligand concentration, ionic strength, pH, and surfactant additives are all important factors for "ink" optimization.

Inks are loaded into cartridges for piezoelectric deposition using a Dimatix materials printer (DMP-2800). Droplets (10-pL) jetted by the printhead nozzle are controlled via a programmable waveform that allows all the piezoelectric pulse to be customized. The waveform along with several other DMP settings needs to be adjusted for every ink, to enable their optimized deposition into periodic dot-matrix arrays.

Droplets are deposited onto 1.25-cm^2 glass substrates coated with epoxysilane (Nexterion E), and incubated overnight in a 75% relative humidity chamber to allow complete bonding of the printed conjugate to the epoxy-coated substrate. After curing, substrates are washed and blocked against nonspecific binding using BSA. From this point forward, the printed, washed and blocked substrate will be referred to simply as a "chip."

Chips can be used immediately in pathogen detection experiments, or stored in a desiccator under an argon atmosphere for later use. Chips are typically handled by their edges with forceps, and exposed to bacterial suspensions by the drop-on-chip method (discussed in Section 3.3) or briefly immersed by the horizontal submersion method (discussed in Section 3.4). Following exposure to bacteria, chips are rinsed by applying a jet of water on their backside, dried under a stream of nitrogen, then imaged under darkfield conditions.

2.2.1 Preparation of Ferrioxamine Conjugates

FOx has the qualities of an immutable ligand for pathogen detection, but its presentation on substrates for optimal interaction with bacterial receptors remains to be defined. Initial attempts to reproduce the conjugation of FOx onto a generic protein carrier such as BSA were largely unsuccessful;[3] however, we found that conjugating a bis-isothiocyanate (bis-ITC) linker onto FOx enabled its attachment onto a variety of molecules and substrates.

2.2.1.1 FOx–BSA Conjugates and Associated Pitfalls

FOx–BSA conjugates were previously used for presenting ligands to bacterial receptors, following their immobilization onto substrates via covalent attachment of their exposed cysteine and lysine residues.[3] Conjugation of FOx onto BSA was performed using 1-ethyl-3-(3-dimethylaminopropyl)carbodiimide (EDC), followed by purification using a 10-kDa cutoff spin filter. Characterization using matrix-assisted laser desorption ionization (MALDI) mass spectrometry confirmed a successful conjugation reaction (Figure 2.1), with an average of eight FOx ligands per BSA. The FOx–BSA conjugates were then patterned onto epoxy-coated substrates as chips for pathogen detection, and tested against live *Y. enterocolitica* at concentrations of 10^3–10^6 cfu/mL using an incubation time of 1 hour. Unfortunately, chips prepared in this manner proved to be relatively insensitive: FFT analysis showed that detection was only achieved at 10^6 cfu/mL, and not at lower concentrations (Figure 2.2).

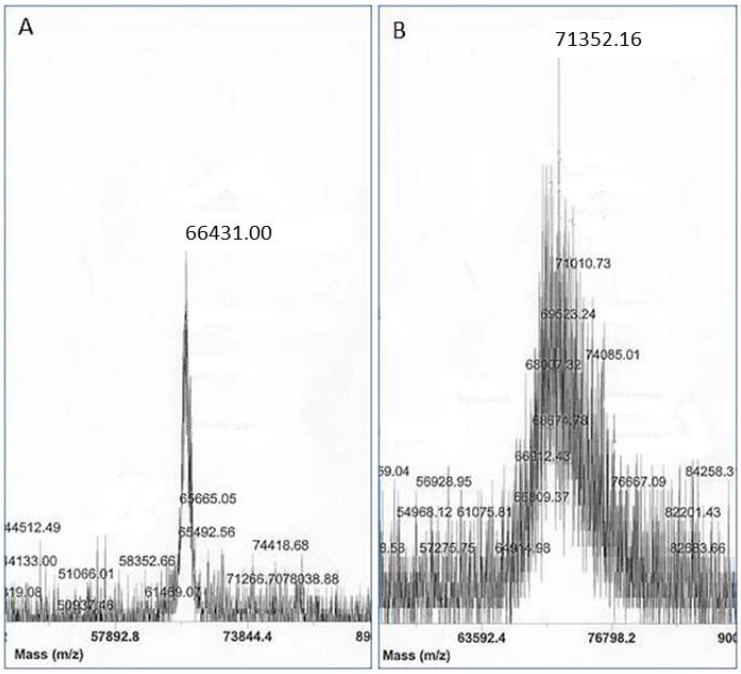

Figure 2.1: MALDI analysis of (A) unmodified BSA and (B) FOx–BSA conjugate, with an average of eight FOx molecules per BSA.

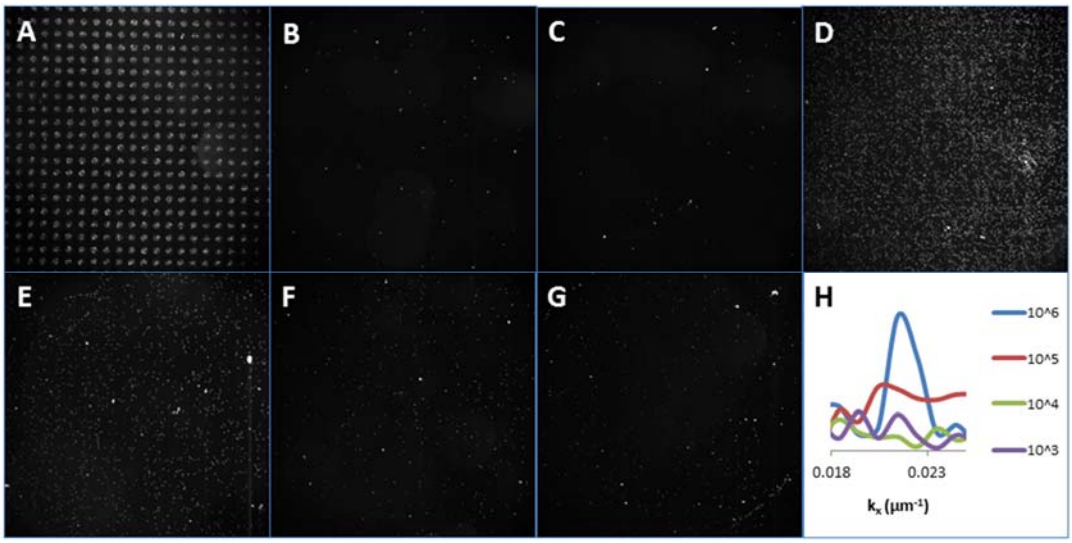

Figure 2.2: Darkfield images of FOx–BSA patterned chips, following 1 hour exposure to *Y. enterocolitica*. (A–C) Images of chips post print, post block, and post exposure to PBS, respectively. (D–G) Images of chips after 1-hour exposure to bacteria at 10^6–10^3 cfu/mL. (H) FFT analysis of images D–G; significant signal is produced only at the highest concentration (Chip D; 10^6 cfu/mL).

2.2.1.2 Synthesis of Bis-isothiocyanate (ITC) Linkers

FOx attached to BSA may not have achieved its optimal presentation. We first considered that attaching FOx directly onto the chip, rather than as a protein conjugate, may support a configuration necessary for binding to receptors. This was tested experimentally by patterning FOx (0.66 mg/mL or 1 mM) onto activated substrates, which were screened against four strains known to express FOx-binding receptors (Figure 2.3); unfortunately, this did not yield any improvements.

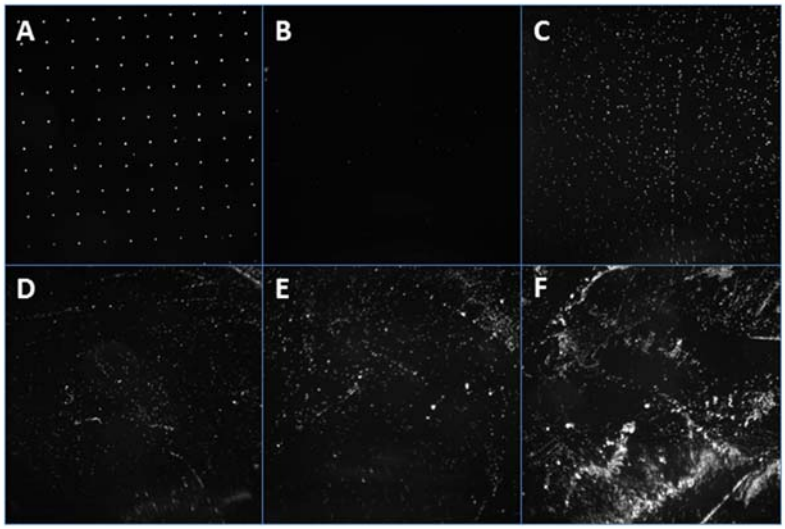

Figure 2.3: Darkfield images of FOx patterned chips following (A–B) printing and blocking respectively and after 30 minute exposure to (C) *Y. enterocolitica*, (D) *S. aureus*, (E) *S. enterica* and (F) *A. baumannii*.

We then hypothesized that introducing a linker to FOx–BSA conjugates might improve its accessibility to FOx receptors, using ITCs for conjugation. Linkers containing terminal ITCs were appealing for at least two reasons. First, they react readily with primary amines, and are thus well suited for coupling FOx (which has a terminal

amine) with an amine-presenting substrate. Second, ITCs can be hydrolyzed under moderately basic conditions into primary amines, thereby changing its role from electrophile to nucleophile.

Three α,ω-diamines were converted into bis-ITCs **1**–**3** using the two-step method by Munch *et al*. (Scheme 2.1):[5] (i) 1,4-diaminobutane, a short and hydrophobic linker; (ii) *p*-xylylenediamine, which is also hydrophobic and more rigid than diaminobutane; and (iii) 2,2'-(ethylenedioxy)bis(ethylamine), a flexible, hydrophilic linker. All of these were prepared in high yields, and coupled with the terminal amine of FOx to yield derivatives **1a**–**3a** (Scheme 2.2).

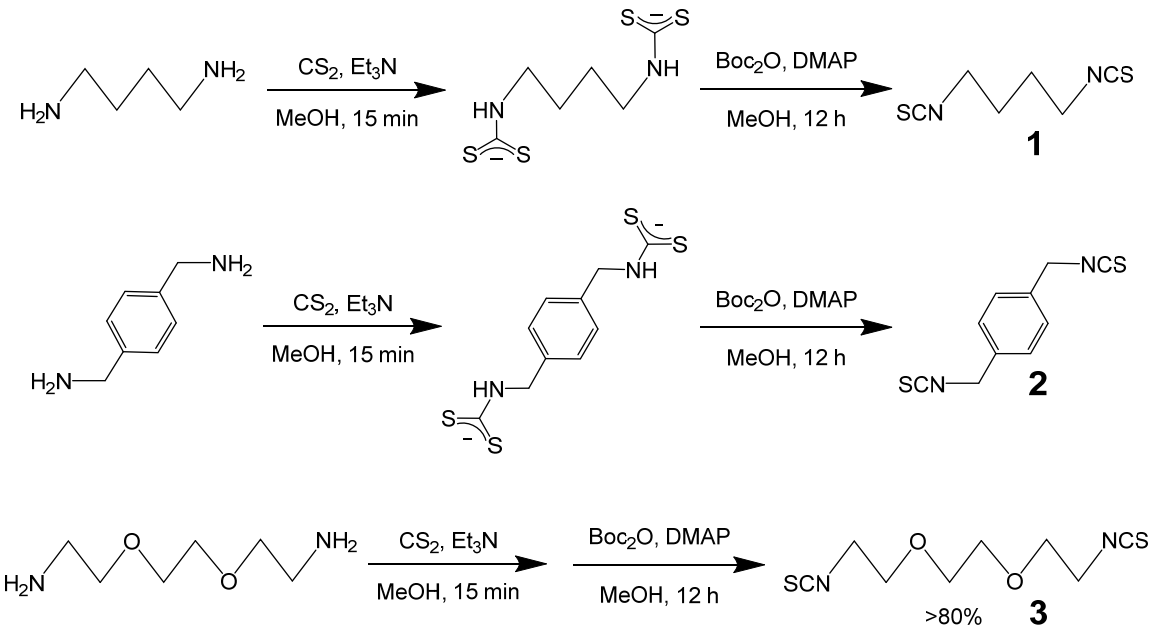

Scheme 2.1: Synthesis of 1,4-butanediisothiocyanate (butylene bis-ITC), *p*-xylylene diisothiocyanate (xylylene bis-ITC), and 2,2'-(ethylenedioxy)bis(ethylisothiocyanate).

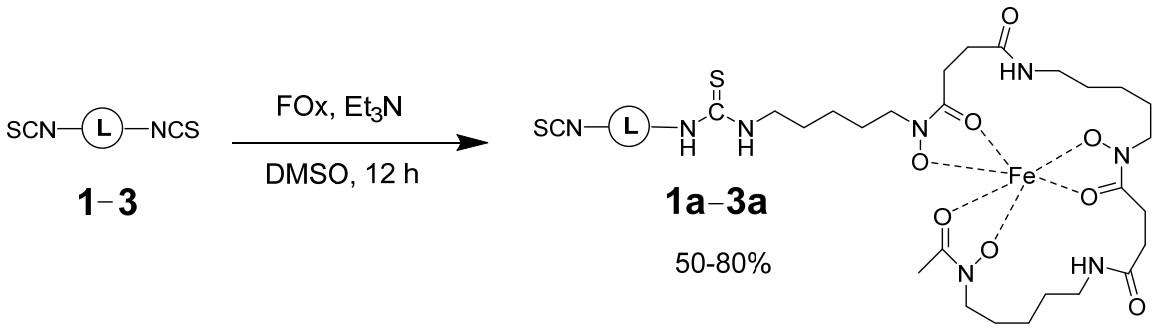

Scheme 2.2: Synthesis of FOx-bis-ITC conjugates **1a–3a**.

FOx–bis-ITC derivative **3a** was then conjugated onto BSA at different concentrations, yielding conjugates with average ligand–protein ratios of 1.2, 6.5, and 14.7. Conjugates were evaluated in microarray format for the detection of *Y. enterocolitica*. We hypothesized that the additional freedom provided by the linkers would improve the presentation of FOx to cognate bacteria. However, detection with the BSA conjugates proved to be inconsistent and afforded low sensitivity, typically requiring bacterial concentrations of 10^7 cfu/mL to achieve positive signals. In addition, the inks prepared from these BSA conjugates began to degrade in as little as five days, even when stored at 4 °C. We thus discontinued the development of chips based on patterned FOx–BSA conjugates.

2.2.1.3 Synthesis of Low-Molecular Weight FOx Conjugates

After multiple uninspiring attempts to capture bacteria of interest using BSA-based conjugates, we hypothesized that chips patterned directly with derivatives **1a–3a** might be useful for pathogen detection. However, conjugation of these molecules onto epoxysilane-activated slides required their conversion into nucleophiles. This was

achieved simply by hydrolysis of the remaining ITC group into a primary amine (**3b**) at high pH;[6] a second approach involved converting the ITC into a thiosemicarbazide ($NH(CS)NHNH_2$) by hydrazine addition. These modifications were performed on FOx-bis-ITC conjugate **3a**, derived from the hydrophilic linker 2,2'-(ethylenedioxy)bis(ethyl-ITC), by gradual hydrolysis at pH 10–11 to generate amine derivative **3b**, or by treatment with hydrazine hydrate to generate thiosemicarbazide **3c** (Scheme 2.3).

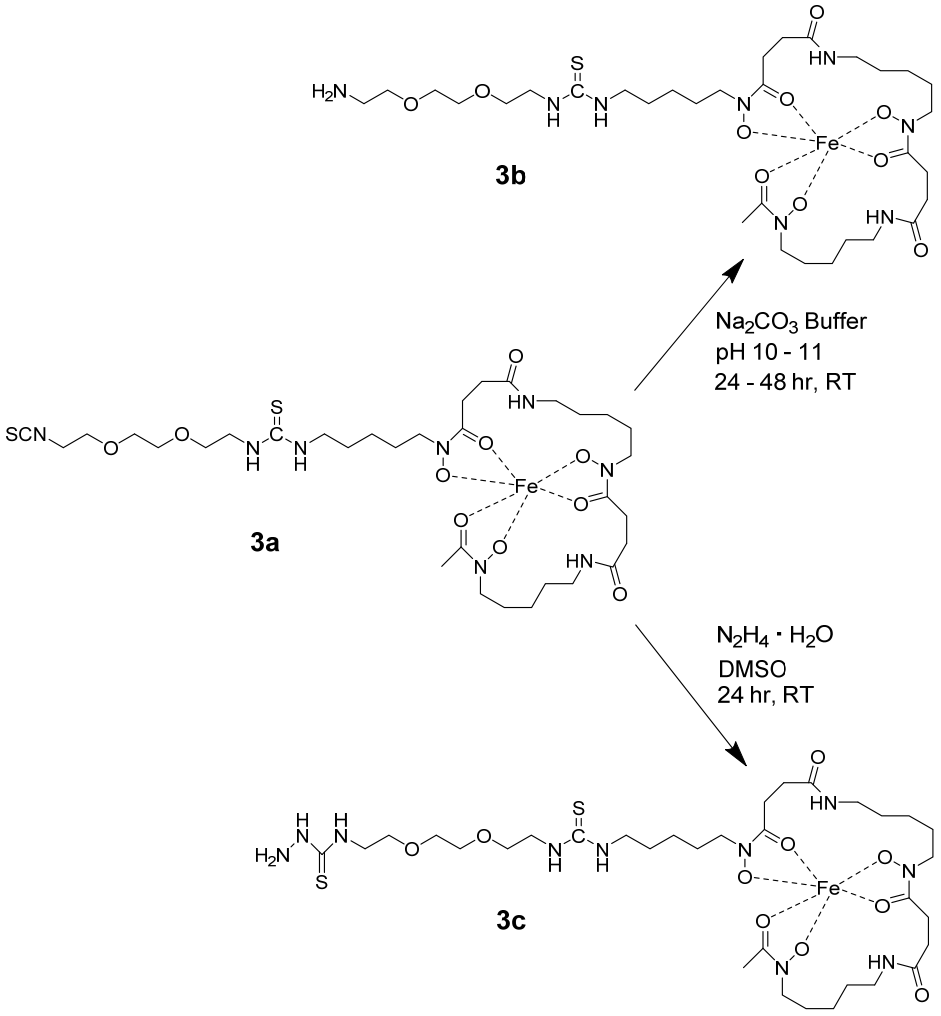

Scheme 2.3: Conversion of FOx–bis-ITC derivative **3a** into nucleophiles **3b** and **3c**.

The hydrolysis of **3a** to **3b** was studied using several different pH conditions. Samples of **3a** were dissolved in pH 7 PBS buffer, pH 9 sodium bicarbonate buffer, and pH 11 sodium carbonate buffer, each at a concentration of 100 mM. All samples were allowed to sit overnight at room temperature followed by analysis using positive-ion ESI mass spectrometry (Figure 2.4); hydrolysis was also confirmed by IR (Figure 2.5).

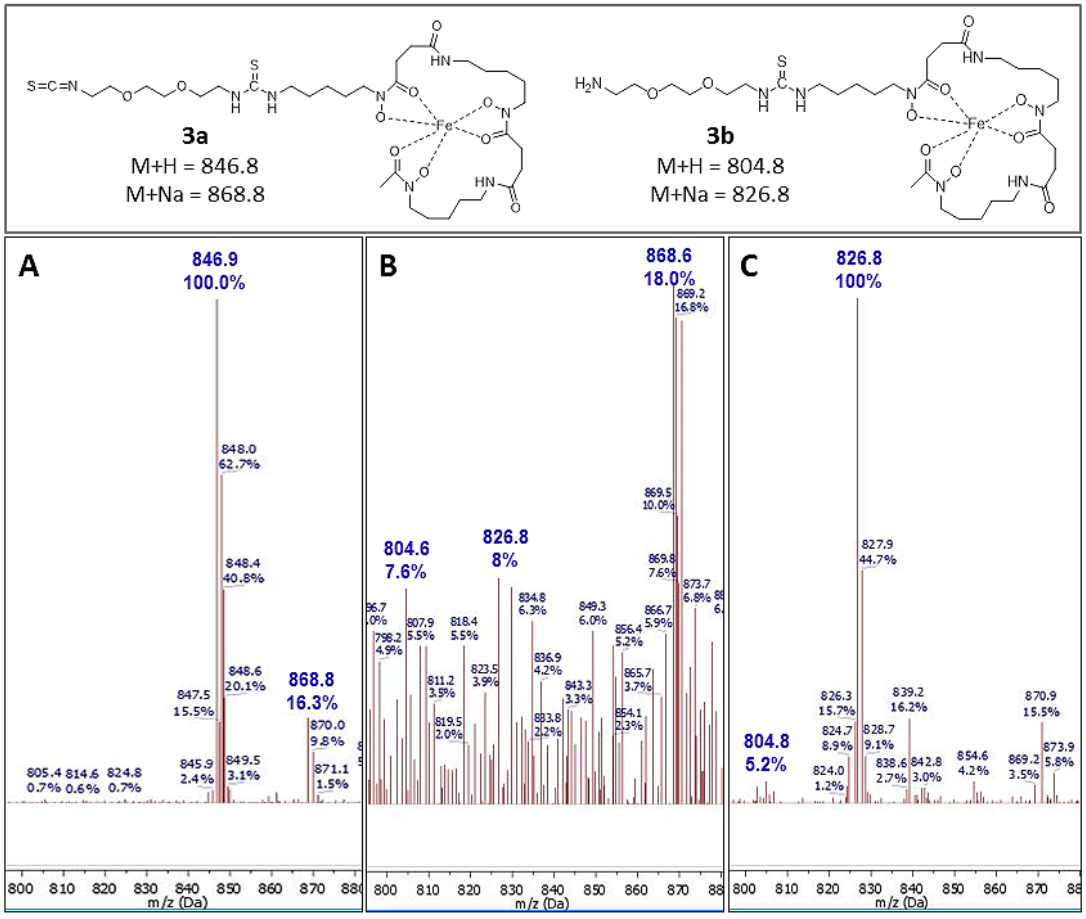

Figure 2.4: FOx-bis-ITC **3a** and desired hydrolysis product **3b** are depicted in the top panel, along with associated molecular ion peaks (M+H and M+Na) by positive-mode ESI mass spectrometry. The lower panels show mass spectra of samples treated with buffers at pH (A) 7, (B) 9 and (C) 11; only the latter produced strong evidence of **3b**.

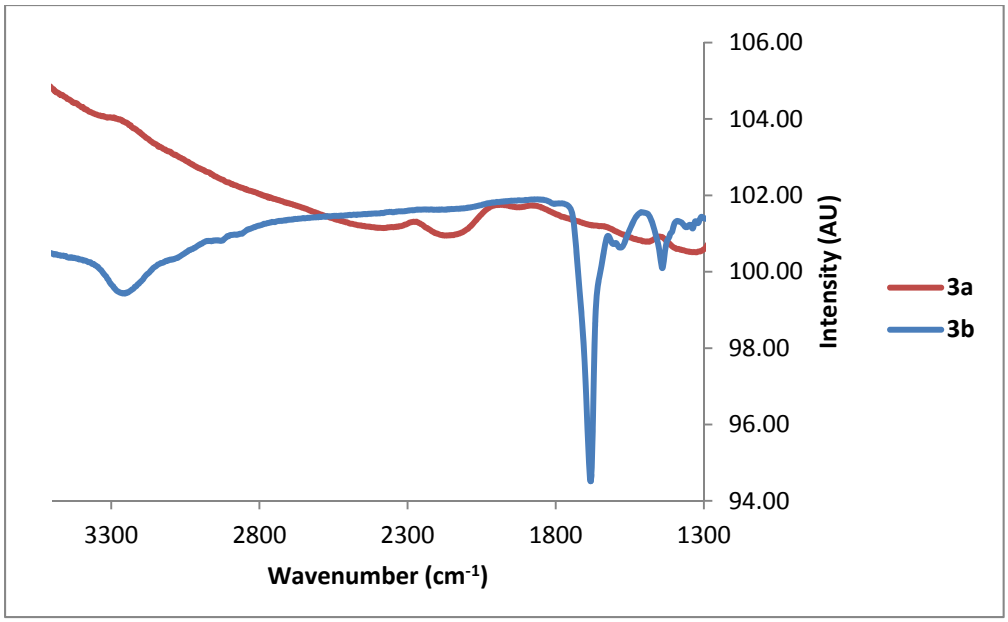

Figure 2.5: IR spectra of **3a** and **3b.**

Attempts to hydrolyze **3a** at pH 7 did not produce any free amine, whereas partial conversion was observed at pH 9 and full conversion was observed at pH 11. It was later determined that hydrolysis could be performed at pH 10 over a longer reaction time (10 mM Na_2CO_3 buffer, 48–72 hours). This condition allows us to avoid the more basic buffer, with less residual salt after inkjet printing.

2.2.2 Optimization of Chip Preparation

2.2.2.1 Synthesis of FITC Conjugate for Optimization of Chip Preparation

The reliability and uniformity of ligand printing is a fundamental factor in chip preparation. In particular, it is important to gauge how efficiently an amine-terminated conjugate can be attached to the epoxy-coated substrate. To accomplish this, we

conjugated a diamine linker to fluorescein isothiocyanate (FITC) to produce conjugate **4** (Scheme 2.4). FITC is similar in size and molecular weight as FOx and should validate the quality of surface functionalization. Very importantly, compound **4** can be viewed by fluorescence microscopy and be used to evaluate every step of microarray production.

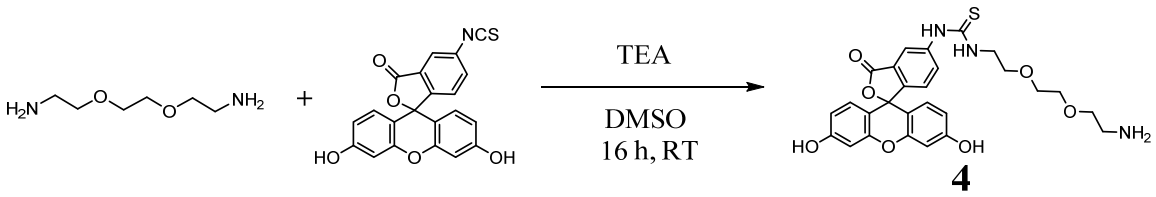

Scheme 2.4: Synthesis of FITC conjugate **4**.

2.2.2.2 Optimization of pH and Humidity Conditions with FITC Conjugate

A variety of inkjet conditions were assessed using **4** as the test ink. We first analyzed the alkalinity of the buffer at pH 7 and 11 (Figure 2.6). While both conditions enabled substrate labeling by **4**, higher fluorescence intensity was observed using the more basic solution. Negative control studies without **4** or using FITC without diamine did not show any fluorescence after blocking, as expected.

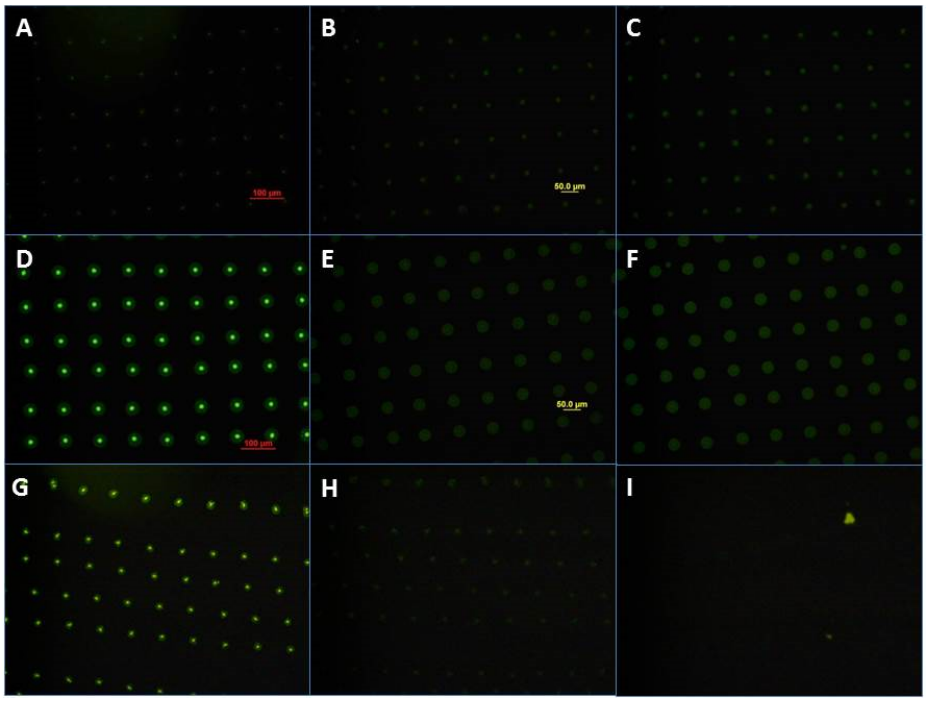

Figure 2.6: Fluorescence microscopy of substrates printed with **4** or FITC. (A–C) Substrates labeled with **4** at pH 7 after printing, washing and blocking respectively; (D–F) substrates labeled with **4** at pH 11 after printing, washing and blocking; (G–I) substrates printed with FITC at pH 11 after printing, washing and blocking.

Relative humidity during curing of patterned substrates was also evaluated. After printing at pH 11, substrates were stored overnight in an airtight chamber with a container filled with water halfway and saturated with salt such that one inch of solute remained at the bottom. NaCl, $Mg(NO_3)_2$, and $MgCl_2$ were used to achieve a relative humidity (RH) of 75%, 53%, and 33% respectively. After curing for 12 hours at room temperature, substrates were removed and subjected to standard washing and blocking procedures.

Substrates cured at variable RH were imaged by fluorescence microscopy (Figure 2.7), which revealed variations due to different RH conditions. Spots on substrate cured at 33% RH clearly showed a uniform ring of higher intensity surrounding a less uniform

central region. This phenomenon, known as contact line pinning,[7] was also observed in substrates cured at 53% RH, although to a lesser extent. Spots on substrates cured at 75% RH show the greatest uniformity of cases studied. From these results, it was determined that 75% RH was optimal for curing.

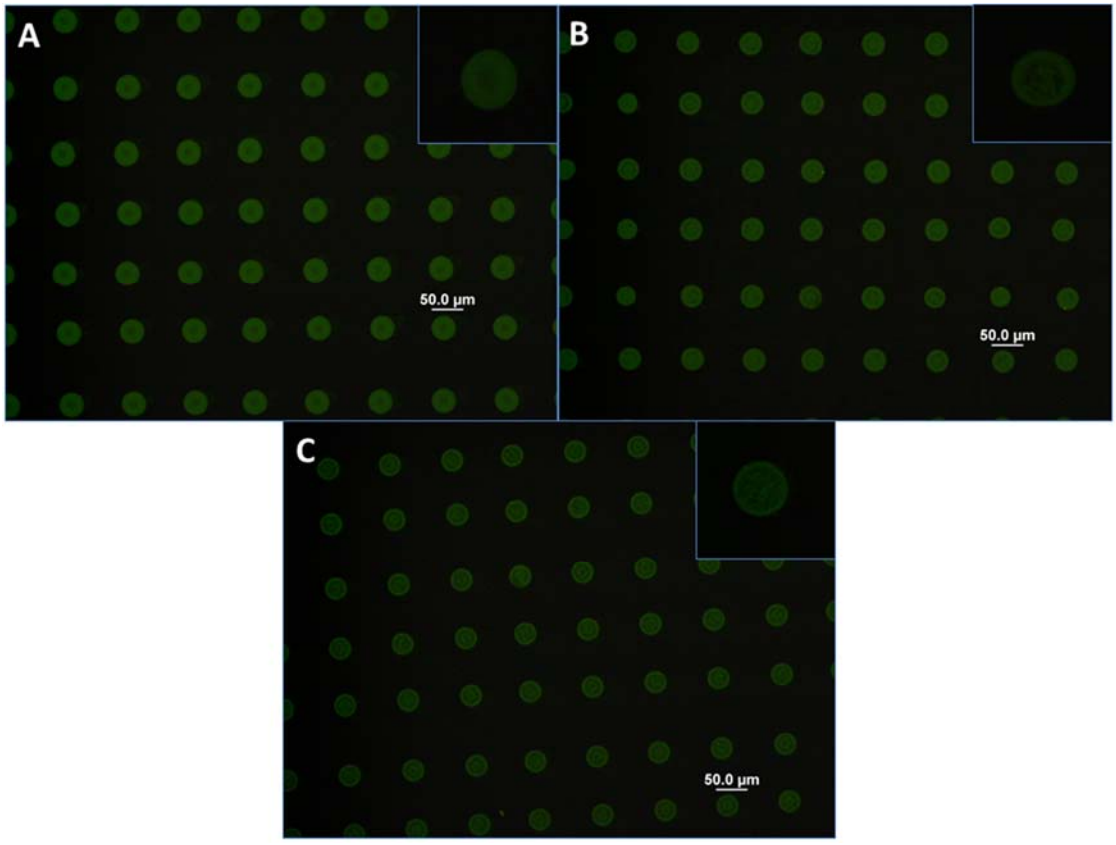

Figure 2.7: Fluorescence images of substrates patterned with **4** and cured overnight at (A) 75% RH, (B) 53% RH, or (C) 33% RH.

2.2.2.3 Minimization of Background Noise

After completion of the rinsing and blocking steps, there should be no visual evidence of the printed microarray: darkfield imaging of the chips should appear

essentially blank. This is important as the pattern should only be visible after exposure to cognate bacteria, caused by scattering from immobilized cells. As standard practice, blocked chips were routinely imaged prior to exposure to bacteria to ensure minimum background.

Microarrays generated from FOx conjugate **3b** gave rise to a persistent background, despite copious washings. This was likely due to the use of unpurified conjugate after hydrolysis. In regards to detection of target bacteria, **3b** performed adequately so making changes to the conjugate itself was not considered a viable option. The situation called for a method to remove visible background from chips, while preserving the detection capability provided by **3b**.

The issue of background visibility was remedied by making a few key changes to the method of chip preparation. The first change was to replace the 100 mM sodium carbonate buffer (pH 11) with 10 mM (pH 10) for hydrolysis of **3a** to **3b**. The second was to alter the rinsing method used after printing and blocking. Previously a dip rinse had been utilized, in which the substrate was gripped with forceps and dipped vertically into rinsing solutions (PBS 1X containing Tween-20, followed twice by deionized water), then agitated by hand for 10 seconds. This was replaced by submersion of substrate(s) printed side up in a buffer-filled petri dish, with orbital shaking at 40 rpm for 15 minutes. The third change was to increase the Tween-20 concentration in the first rinse from 0.05% to 0.25% (v/v). Implementing these modifications resolved nearly all issues related to systematic background noise.

It is worth mentioning that several other variables were also tested that either failed to reduce background or resulted in loss of detection capability. These included

increasing the concentration of BSA in the blocking solution from 0.1 to 1.0% (w/v), introduction of 0.05% Tween-20 into the BSA blocking solution, and inclusion of DMSO in the inkjet formulation. Sonication of chips submerged in cleaning solution was also investigated and observed to have an adverse effect on detection capability, likely due to the aggressive removal of surface-bound conjugate.

2.3 Culturing of Pathogenic Bacteria in Iron-Restricted Media

Bacteria of interest were cultured in standard liquid media and monitored for changes in optical density at 600 nm (OD_{600}). At the end of their log growth phase, bacteria were centrifuged to pellets and rinsed three times with phosphate buffered saline (PBS). Finally, bacterial suspensions were diluted serially with PBS and exposed to chips for pathogen detection experiments.

In detection studies described previously by Kim *et al*,[3] a relatively low dose of 2,2'-bipyridine (bipy; 80 μM) was added to growth media for *Y. entericolitica*. Bipy limits the available iron, but not to the point where requisite growth to late log phase is inhibited. The culturing of bacteria under iron-restricted conditions can activate the Fur system and promote expression of siderophore receptors.[8-10] However, each type of bacteria has a unique response to environmental stress, requiring tailoring of culture conditions. In other words, to achieve maximal expression of FOx-binding receptors, optimization of iron-limiting conditions for each strain of interest is requisite.

For the data shown in Table 2.1, strains were grown in culture tubes with 10 mL of broth with incubation at 37 °C (unless otherwise noted) and 220 rpm shaking. First-

generation cultures were inoculated from previously frozen (–80 °C) stocks; subsequent generations were inoculated as 1% (v/v) solutions using active strains. As standard practice, strains were grown out for a minimum of three generations prior to inoculation in bipy-treated media. These cultures were handled exclusively with acid-washed materials to eliminate the possibility of iron contamination. For optimization, strains were cultured in broth with variable bipy concentrations ranging from 0.05–3 mM, to determine the highest restriction of iron while still permitting steady growth. For many strains, a clear concentration threshold could be determined above which bacteria did not proliferate. Other strains could proliferate at even the highest bipy concentrations; in these cases, optimal conditions were determined by consistency of culture growth and/or by the quality of the detection experiments.

Table 2.1: List of bacterial strains optimized for growth under iron-restricted conditions

Bacterial strain	Broth	Max. [bipy], in mM
Y. enterocolitica	Luria-Bertani	3
Y. enterocolitica (4 °C)	Luria-Bertani	0.05
S. aureus	Tryptic Soy	1
MRSA	Tryptic Soy	1
P. aeruginosa	Luria-Bertani	0.3
S. enterica	Luria-Bertani	0.1
A. baumannii	Nutrient Broth	0.1
K. pneumoniae	Nutrient Broth	0.1

2.4 Pathogen Detection

Bacterial adhesion onto patterned chips could be imaged in a label-free manner using optical darkfield microscopy, based on the light scattering from the bacteria themselves.[1-4] Chips without exposure to bacteria should appear nearly blank when viewed under darkfield conditions, whereas those exposed to bacteria should support a periodic pattern commensurate with concentration. However, visual inspection is not sufficiently objective to determine whether bacterial adhesion to the ligand microarrays is significant, especially in cases of high background or low signal intensity. To address this issue, darkfield images can be analyzed by fast Fourier Transform (FFT) to convert periodic signals into reciprocal lattice peaks, as represented schematically in Figure 2.8.

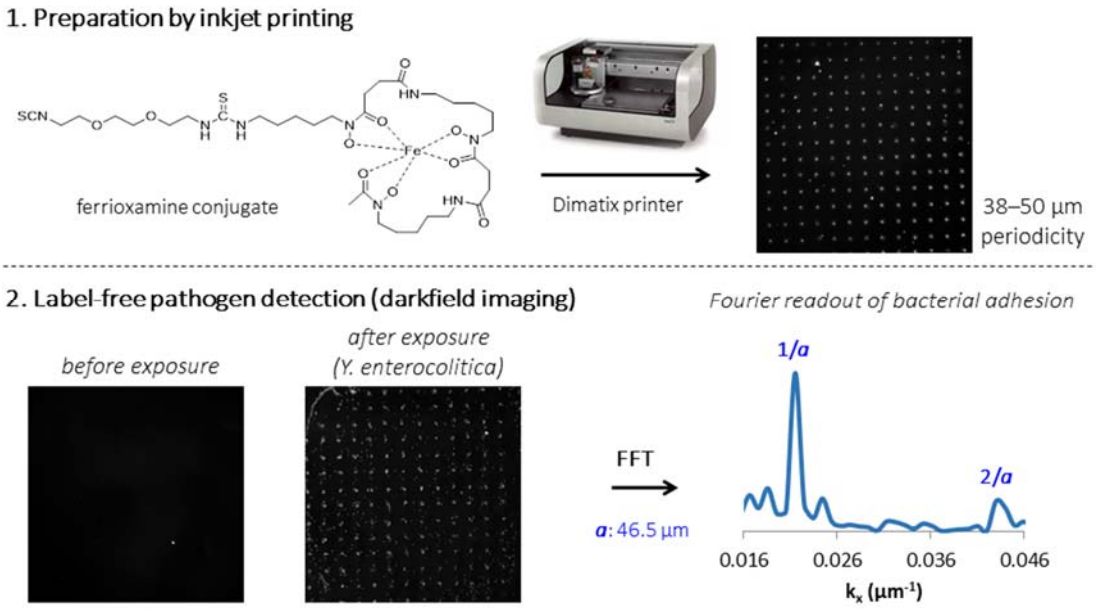

Figure 2.8: Overview of detection methodology, with FFT readout.

FFT analysis of the bacterial adhesion patterns allows signals to be compared quantitatively against noise or local background intensities, referred to here as *S/N* and *S/B* respectively, where *N* is based on the standard deviation of *B*:

$$\frac{S}{N} = \frac{S - B}{\sigma_B}$$

In this study, a 2D-FFT algorithm was applied using WSxM software,[11] followed by a linescan along the *x*-direction to produce a one-dimensional Fourier spectrum. Background intensities were estimated after applying a logarithmic weighting function to suppress low-frequency (1/*f*) noise (see Section 2.9, Materials and Methods).

2.5 Initial Use of Small-Molecule Conjugates for Screening Bacteria

Detection experiments were performed following the basic methodology outlined in Section 2.2, using inks composed of 1 mM of **3a** (0.8 mg/mL) dissolved in a 5:1 ratio of 100 mM carbonate buffer (pH 9) and dimethylformamide (DMF) containing 0.005% Tween-20 (v/v). The basic pH was expected to promote hydrolysis of the ITC to the corresponding amine, and covalent binding by ring opening of the epoxy groups on the substrate surface. Tween-20 was included to promote consistent jetting of droplets from the nozzles of inkjet printer cartridge, and also to prevent clogging. Following inkjet printing and curing and rinsing steps, substrates were blocked against non-specific binding using 0.1% (w/v) BSA in PBS, rinsed to remove unbound BSA, and dried under a stream of nitrogen.

Chips were screened for detection against four bacterial strains shown to have receptors for FOx by literature precedent or by BLAST search as described in Section

1.5. Selected strains include *Y. enterocolitica*, *S. aureus*, *S. enterica* and *A. baumannii*. Some of these were subjected to a competitive binding test to establish that adhesion of bacterial cells to chips patterned with **3a** was specific to ferrioxamine: A suspension of *Y. enterocolitica* was dosed with 1 mM dFOx 30 minutes prior to exposure to the chip, in order to saturate all available receptors and inhibit binding to the FOx microarray. *E. coli* Nissle 1917 (a non-pathogenic strain not expected to bind FOx) was also screened as a negative control. As a second negative control, a chip treated only with PBS was carried through the entirety of the experiment. All strains were cultured in iron-deficient media to mimic physiological conditions and to ensure the expression of FOx receptors, and initially surveyed at a concentration of 10^7 cfu/mL. Chips were exposed to bacterial suspensions for 30 minutes using the drop-on-chip method (see Section 3.3), then rinsed, dried, and imaged as shown in Figure 2.9.

The results of this initial screening showed all strains to have affinity for the FOx microarrays. All negative controls also performed as expected, and did not produce any significant evidence of FOx-mediated adhesion. The competitive inhibition experiment is especially noteworthy: The absence of binding validated the assumption that bacterial adhesion was mediated by receptor–ligand interactions. The lack of binding by *E. coli* Nissle 1917 supported the notion that pathogen capture was specific to strains expressing FOx-binding receptors. Finally, the lack of visible signals in the PBS control eliminated the possibility of nonspecific sources of light scattering from the patterned microarray.

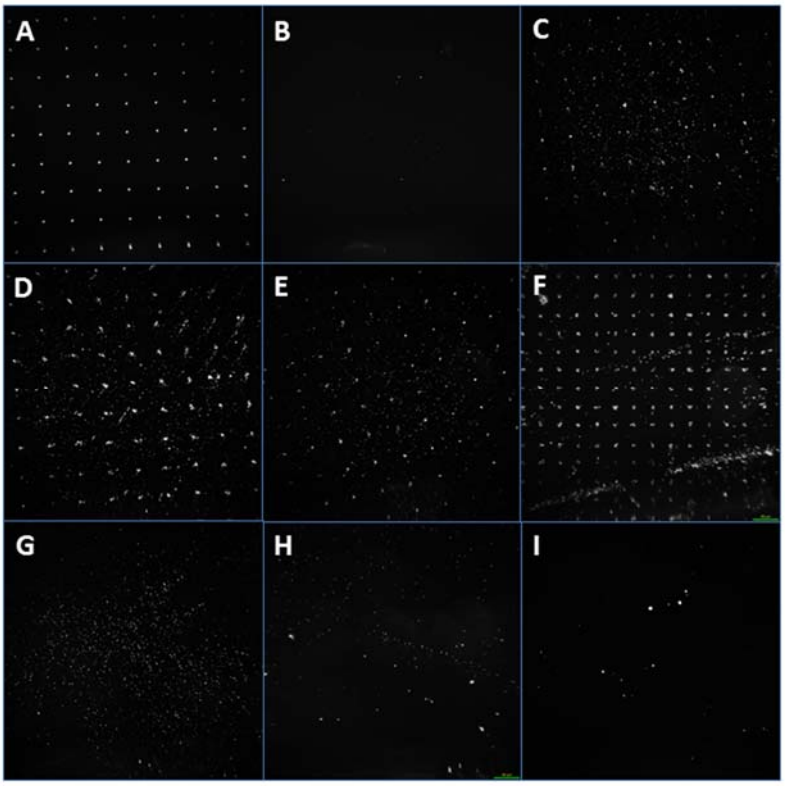

Figure 2.9: Darkfield images from preliminary screening of FOx-binding bacteria using FOx microarrays. Chips are shown (A) post print, (B) post block, and after 30-min exposure to (C) *Y. enterocolitica*, (D) *S. aureus*, (E) *S. enterica* and (F) *A. baumannii*. Chips used as negative controls include (G) competitive inhibition of *Y. enterocolitica* using free dFOx, (H) exposure to *E. coli* and (I) exposure to PBS buffer.

Despite this initial success, we found that bacteria screened at concentrations below 10^7 cfu/mL were not detected in any case. We hypothesized that the rate of hydrolysis at pH 9 was only sufficient to convert a small percentage of FOx-bis-ITC **3a** into the corresponding amine **3b.** As a result, only a small amount of FOx conjugate was attached to the substrate surface, therefore limiting sensitivity. Subsequent studies indicated hydrolysis at pH 10–11 drastically increased the amount of **3b** (Figure 2.4). Inkjet printing of these solutions was found to produce reliable and uniform array

elements on epoxysilane-functionalized substrates, with greatly improved limits of detection.

2.6 Limit of Detection Using Ferrioxamine Microarrays

In these studies, the ink used for printing FOx microarrays consisted of 3 mg/mL **3b** in 10 mM sodium carbonate buffer (pH 10) containing 0.005% Tween-20 (v/v). Substrates post-printing were subjected to the curing and rinsing protocol described previously prior to blocking. *Y. enterocolitica* was cultured under iron-minimal conditions as described in Section 2.3.

To determine the limit of detection (LOD) for *Y. enterocolitica*, five chips were exposed to bacterial suspensions at concentrations between 10^6 and 10^2 cfu/mL. A negative control chip was exposed to PBS buffer and also carried through all parts of the experiment. Chip exposure time was 1 hour using the drop-on-chip method (Section 3.3). Chips were imaged under darkfield conditions (Figure 2.10), then subjected to FFT analysis for an objective determination of positive capture (Figure 2.11). In some cases, bacteria-treated chips were treated with propidium iodide (PI) to confirm that optical scattering was primarily due to immobilized *Y. enterocolitica*. Chips were first sterilized with UV light irradiation (254 nm) for four hours, then exposed to 3 μg/mL PI in a pH 7 sodium chloride/sodium citrate buffer for 10 minutes before rinsing with water, drying with compressed air, and imaging with a fluorescence microscope (Figure 2.12).

PI staining confirmed that the patterns visualized by darkfield imaging were in fact due to scattering from immobilized bacteria. This was reinforced by images taken with the 100X objective, showing individual stained cells clustered on printed spots. We

can thus conclude that the LOD for *Y. enterocolitica* is 10^2 cfu/mL, given an exposure time of one hour. Under the same conditions, *A. baumannii* and MRSA achieved a LOD of 10^5 and 10^4 cfu/mL respectively. Nevertheless, these results confirmed that chips printed with amine-terminated FOX conjugate **3b,** formed in situ by hydrolysis of FOX-bis-ITC **3a** at pH 10–11**,** could provide high sensitivity for pathogen detection.

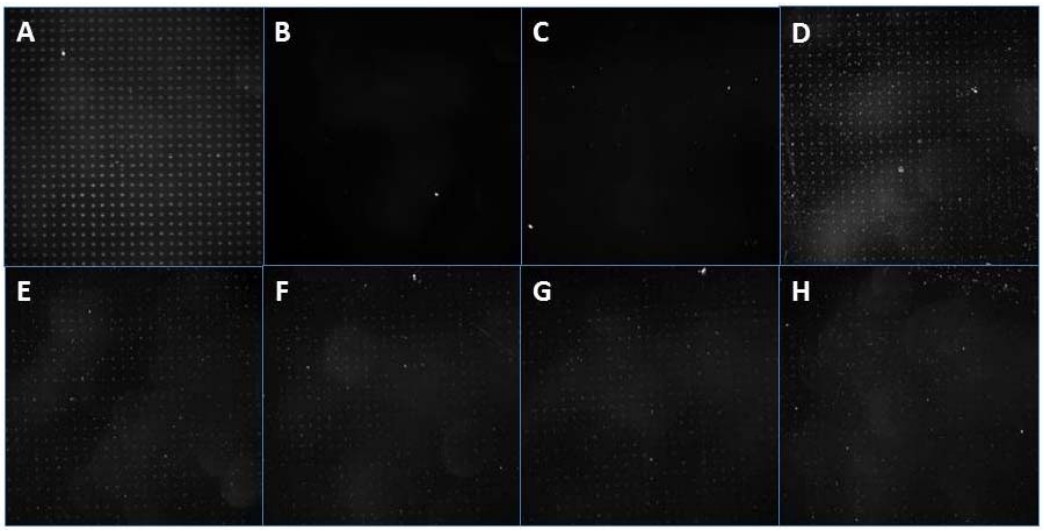

Figure 2.10: Darkfield images depicting chips from LOD study with *Y. enterocolitica*. (A) post print, (B) post block, (C) after exposure to PBS only, and (D–H) after exposure to bacteria at concentrations of 10^6 – 10^2 cfu/mL respectively.

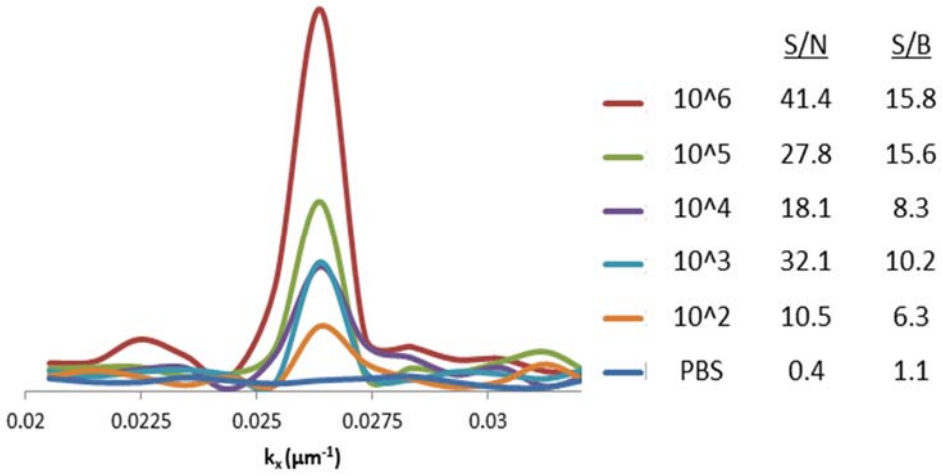

Figure 2.11: FFT signals from darkfield images of LOD experiment, with associated S/N and S/B values.

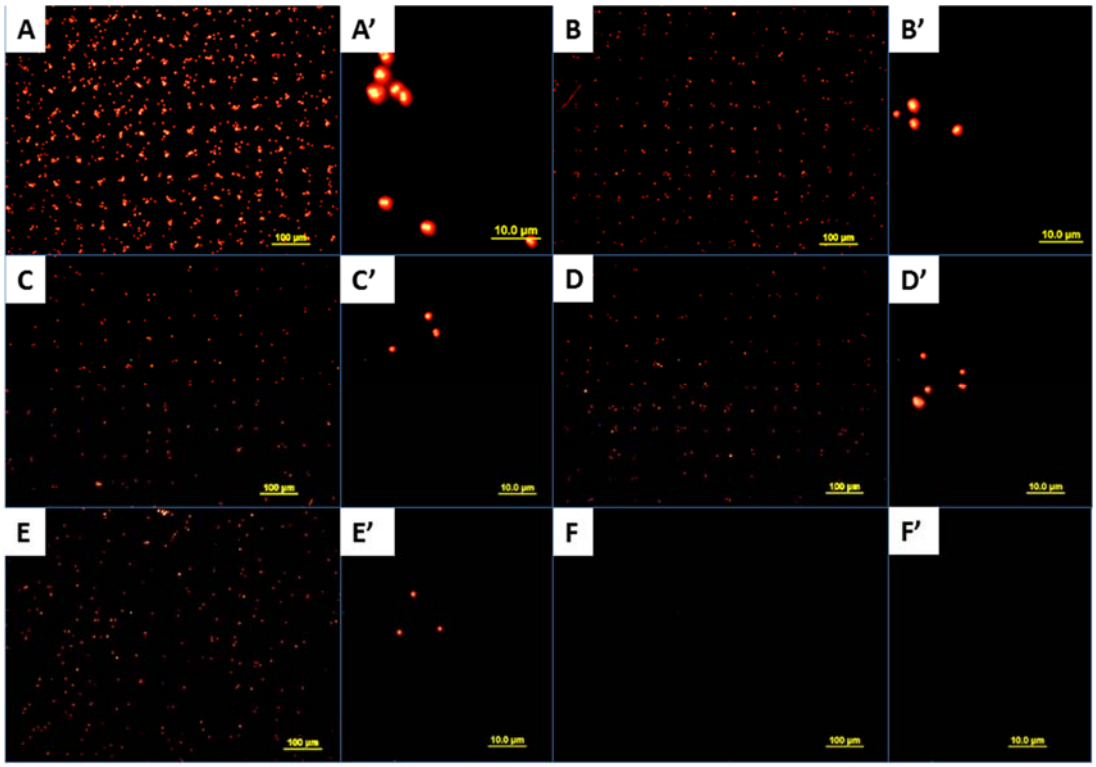

Figure 2.12: Fluorescence images of all chips used in LOD experiment, after treatment with PI. Low-magnification images with 10X objective (A–E) and images of individual array elements spots with 100X objective (A'–E') are represented for chips exposed to bacteria at 10^6, 10^5, 10^4, 10^3, and 10^2 cfu/mL, respectively. Negative control chips treated with PBS buffer (F and F') appear blank, indicating absence of immobilized bacteria.

It should be noted that all chips, printed with **3a** or **3b**, were able to produce visible patterns by darkfield imaging, including negative controls, given sufficient image exposure times. For this reason, FFT analysis is necessary to establish significant bacterial adhesion in an objective manner, with rejection of signals from negative controls. When properly established, S/N and S/B values confirmed that detection was possible even at the lowest bacteria concentration of 10^2 cfu/mL. Overall, both S/N and S/B decrease with bacterial concentration; importantly, imaging setting can be set such that PBS controls show no appreciable signals, with S/N at $1/a$ below three, the standard threshold of significance.

2.7 Optimization of PathoTest Device (Mark V)

Earlier work related to this project involved the design and construction of a semi-automated benchtop instrument (PathoTest) that combined label-free pathogen detection with FFT readout.[12] This instrument went through several rounds of development; the last version, dubbed Mark V, was capable of detecting bacteria adhesion in real time, albeit at rather high concentrations. The device comprised a USB camera, 3X zoom lens, cuvette for viewing chips mounted vertically, and a LED ring lamp for wide-angle illumination (Figure 2.13A). The camera and lens were mounted together on an adjustable track allowing for changes in focal length, and the distance between the ring lamp and the sample could be adjusted independently.

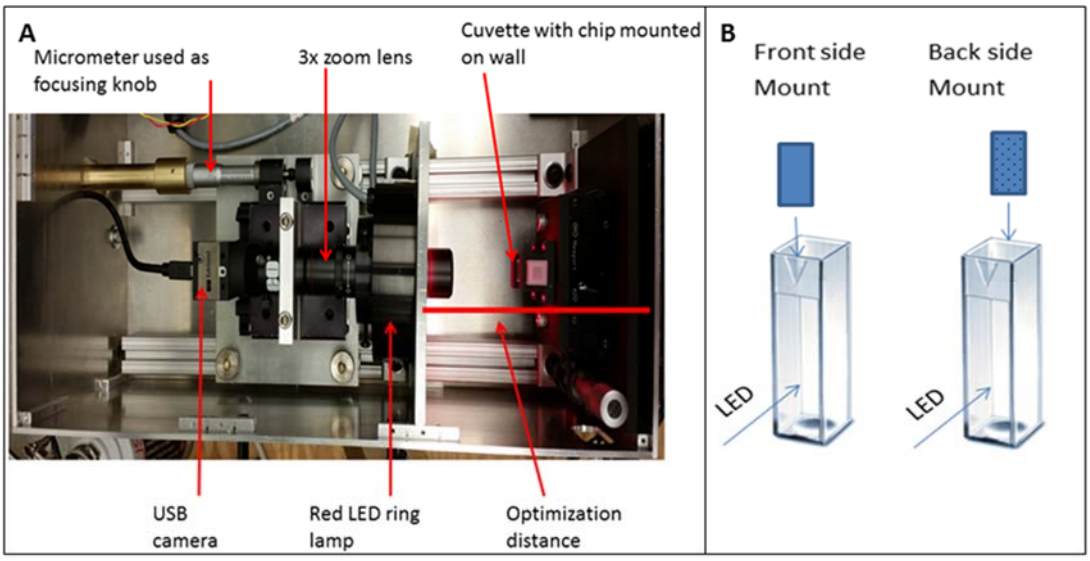

Figure 2.13: PathoTest Mark V. (A) Bird's eye view of major components; (B) two methods of mounting chips on cuvette walls. In the "front side mount" configuration, the microarray is facing away from camera.

We attempted to use the PathoTest Mark V to detect *Y. enterocolitic*a with FOx-conjugated microarrays. Optimization steps for chip imaging include adjusting the focal length to 3.5 cm, and mounting chips on the front side of the cuvette for better optical contrast (Figure 2.13B). By utilizing simple capillary forces, the chip could be effectively stuck to the cuvette wall with either a drop of water or NVM index-matching fluid. Water provided higher signal intensities, but NVM fluid provided superior contrast and was used in subsequent studies.

The position of the ring lamp was also assessed systematically for maximum off-axis illumination. Using the "front side mount" configuration, the lamp was moved in 1-cm increments from the focal plane, with an image taken at each position. FFT analysis of these images indicated 8 cm to provide the highest intensity FFT signals. These

optimized imaging conditions were applied toward chips from the LOD study with *Y. enterocolitica* (10^6–10^2 cfu/mL), with analysis by FFT (Figure 2.14).

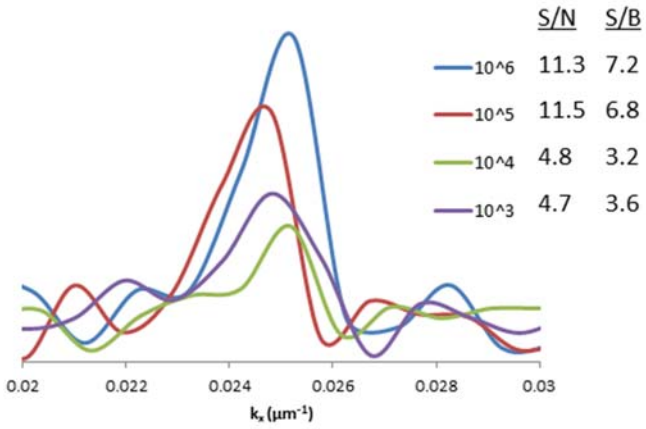

Figure 2.14: FFT analysis of chips imaged with PathoTest Mark V.

Unfortunately, the S/N of the reciprocal lattice peak ($k_x = 1/a$) were weak compared to those derived from images acquired under darkfield conditions (Figure 2.11), and the chip treated with bacteria at 10^2 cfu/mL did not produce any notable signal after FFT analysis. The PathoTest Mark V system was thus not able to compete with darkfield microscopy when it came to samples prepared at lower bacterial concentrations. In addition, the printed microarrays themselves generated sufficient background under the imaging conditions described above, possibly due to a high level of residual organic material generated during the in situ hydrolysis of **3a**. For these reasons, work with the Mark V was discontinued. However, it is worth noting that subsequent studies with purified **3b (conjugate 5)** and also **6** produced much lower levels of background, leaving the door open to a re-investigation of portable systems for point-of-care analysis.

2.8 Conclusions

The methodologies utilized for detection of pathogenic bacteria were systematically optimized, enabling a limit of detection at 10^2 cfu/mL in the best cases. FITC conjugate **4** proved useful for optimizing the conditions of ink pH and relative humidity during post print curing for uniform and reproducible spot formation. An improved procedure for removing residual materials from the FOX conjugate arrays post printing also proved fruitful for reducing background levels. Progress was made toward optimizing iron-restricted conditions for culturing multiple pathogens of interest. This was important, as individual bacterial strains respond differently to iron deprivation. The synthesis of several linkers and FOx conjugates was also achieved, and two conjugates, **3a** and **3b**, were used successfully for detecting pathogens of interest. In situ hydrolysis of **3a** was shown to be capable of capturing *Y. enterocolitica*, *S. aureus*, *S. enterica* and *A. baumannii*; by increasing its efficient conversion to **3b**, a limit of detection for *Y. enterocolitica* of 10^2 cfu/mL could be achieved.

2.9 Materials and Methods

Fast Fourier transform (FFT) analysis. Raw images were loaded into WSxM software in greyscale TIFF format, where they were adjusted to 1 micron per pixel and sized to 1004 x 1002 pixels (Figure 2.15) The periodic array images were slightly tilted off-axis to avoid artifacts created by boundary effects. FFT processing produced an output image measureable in frequency units. A line profile through the x-axis produced a one-dimensional Fourier spectrum which could be evaluated quantitatively for peak signal intensities (S) at $1/a$ (in μm^{-1}), where a represents the periodicity of the printed

microarray (in μm). It should be noted that many Fourier spectra also produced a significant secondary harmonic at 2/*a*.

To estimate background (*B*) and noise (*N*) values, fundamental and secondary harmonic peaks were edited from the Fourier spectrum, followed by a logarithmic baseline correction. Mean background intensities near the 1/*a* peak were calculated using the range of *x* values between 0.016 and 0.046; the *S*/*N* value was calculated as $S–B/\sigma_B$ (see Section 2.3).

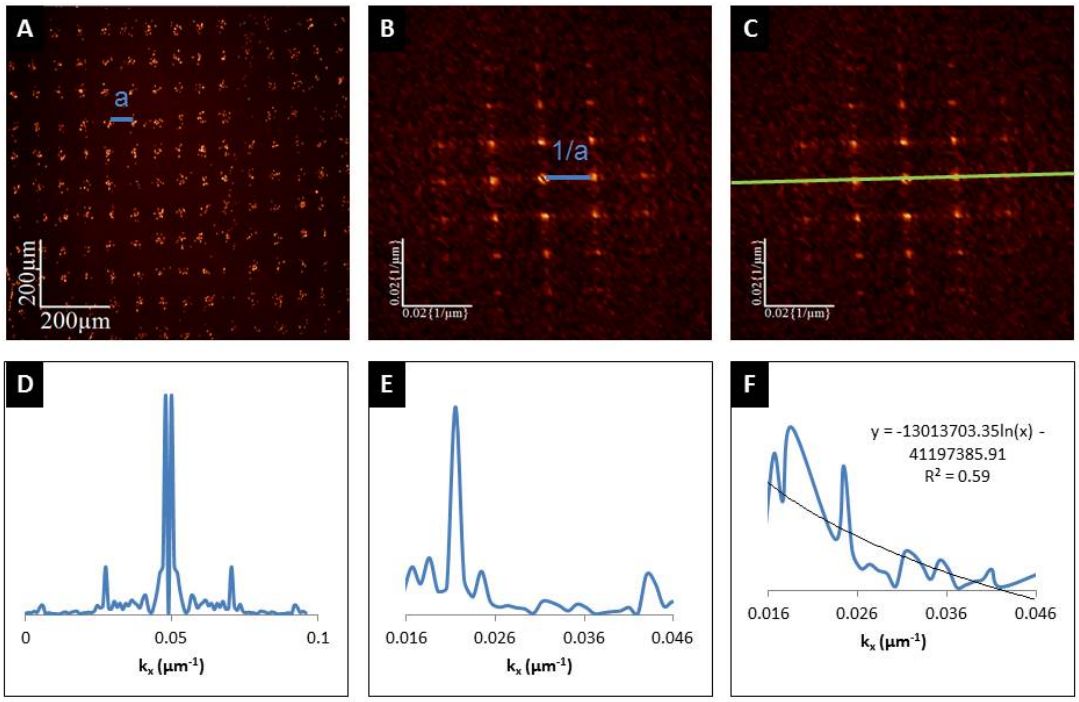

Figure 2.15: Overview of steps involved in FFT analysis. (A) Darkfield images of microarrays (periodicity = *a*) are rescaled to 1 micron per pixel. Image is slightly tilted to avoid artifacts created by boundary effects. (B) FFT processing yields a 2D image in the frequency domain ($k_x = 1/a$). (C,D) Line profile along the *x*-direction yields Fourier spectrum. (E) Expansion of Fourier spectrum containing fundamental and secondary harmonic peaks (1/*a*, 2/*a*). (F) Peak signals are edited from Fourier spectrum, followed by application of a logarithmic fit to remaining data points for baseline correction. The corrected spectral values were used to determine *S*/*N* and *S*/*B*.

Synthesis of 2,2'-(ethylenedioxy)bis(ethylisothiocyanate) (3a). To a solution of 2,2'-(ethylenedioxy)bis(ethylamine) (322 µL in 5 mL dry methanol) was added triethylamine (612 µL) and carbon disulfide (400 µL). The reaction was stirred at room temperature and monitored for changes in optical extinction using Cary 50 UV-vis spectrometer. Formation of the bis-dithiocarbamate (DTC) intermediate was observed at 5 minutes; the reaction was deemed complete at 15 minutes. The reaction vessel was cooled to 0 °C in an ice bath. Di-*tert*-butyl dicarbonate (1.19 g in 1.25 mL dry methanol) was added to the reaction mixture, followed by 4-dimethylaminopyridine (DMAP; 8.1 mg in 1mL dry methanol), and the reaction was warmed to room temperature. UV spectroscopy showed reduction in DTC absorption at 255 and 290 nm within 5 minutes at room temperature, and emergence of an absorption band at 225 nm corresponding to the isothiocyanate (Figure 2.16). The reaction mixture was stirred for 1 hour, then concentrated by rotary evaporation to a clear yellow oil (418 mg, 82% yield). ITC formation was confirmed by ^{13}C NMR (Figure 2.17). Bis-ITC **3a** was used without further purification.

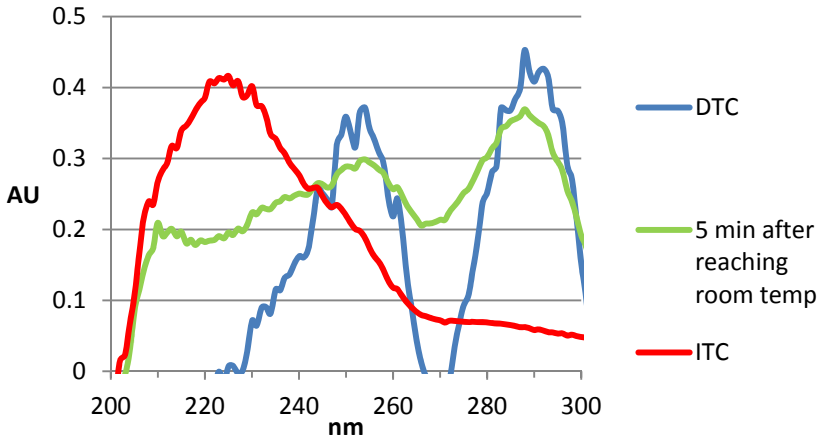

Figure 2.16: UV spectra of reaction mixture during the synthesis of 2,2'-(ethylenedioxy)bis(ethylisothiocyanate) (**3a**).

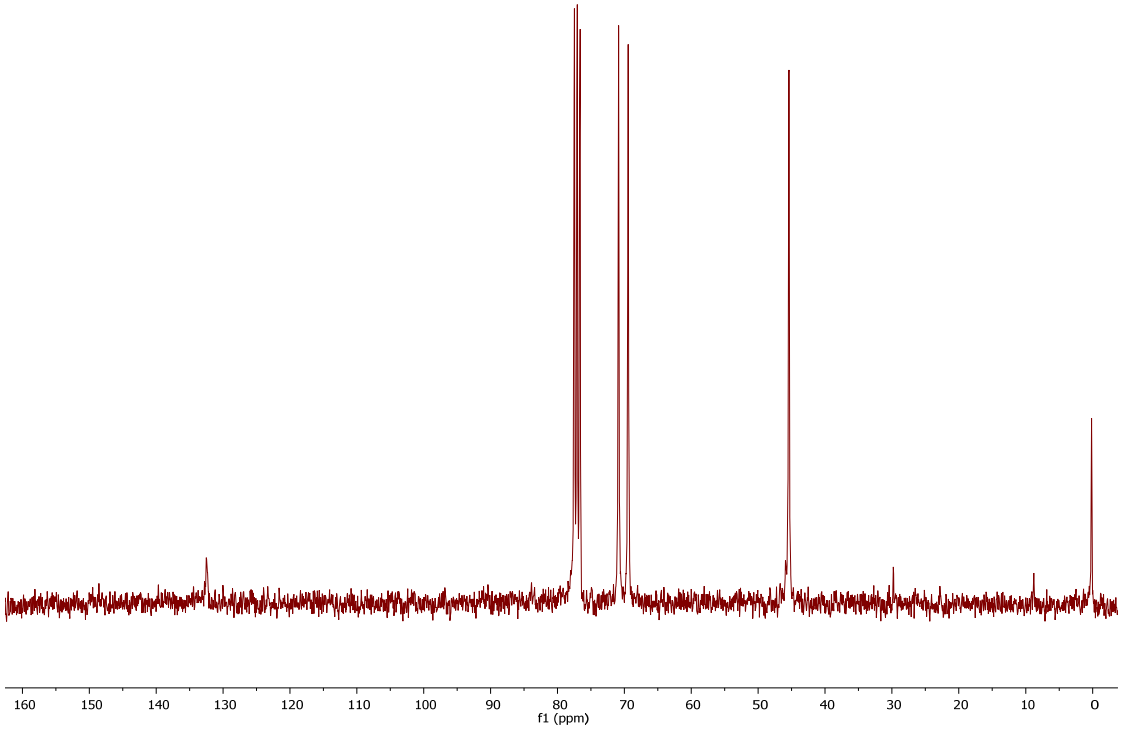

Figure 2.17: ^{13}C NMR (300 MHz, $CDCl_3$) of bis-ITC **3a**.

Synthesis of *p*-xylylenediisothiocyanate (3b). To a solution of *p*-xylenediamine (50 mg in 10 mL dry methanol) was added triethylamine (102 µL) and carbon disulfide (67 µL). The reaction was stirred at room temperature and monitored by UV-vis spectrometry. Formation of the bis-DTC intermediate was observed at 5 minutes, and the reaction was deemed complete at 15 minutes. The reaction vessel was cooled to 0°C, treated with di-*tert*-butyl dicarbonate (337 mg in 500 µL dry methanol) followed by DMAP (1.35 mg in 500 µL dry methanol), then warmed to room temperature. Within 2 hours, UV spectroscopy again showed reduction in DTC absorbance peaks and emergence of a peak corresponding to ITC formation. The reaction mixture was stirred for at least 12 hour at room temperature to ensure complete conversion to **3b** (Figure 2.18); reaction monitoring

by ATR-IR spectroscopy indicated a large increase in ITC (Figure 2.19). The reaction mixture was then concentrated by rotary evaporation to a tan paste (60 mg, 82% yield). ITC formation was confirmed by ^{13}C NMR (Figure 2.20).

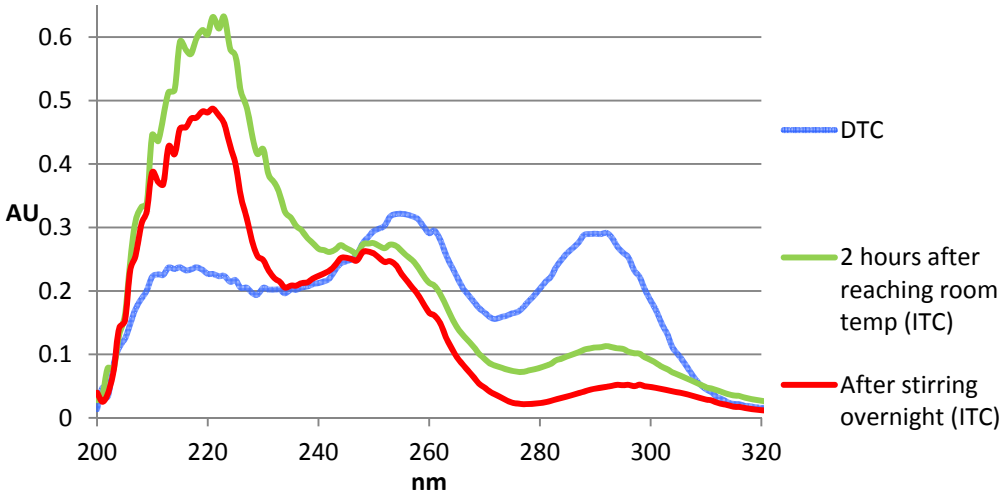

Figure 2.18: UV spectra during synthesis of *p*-xylylenediisothiocyanate (**3b**).

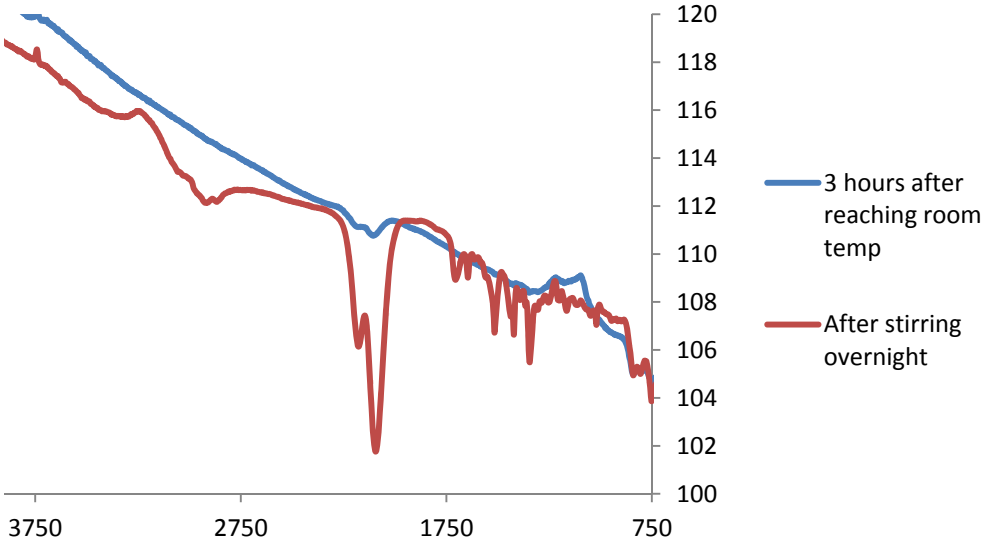

Figure 2.19: ATR-IR monitoring during synthesis of **3b**.

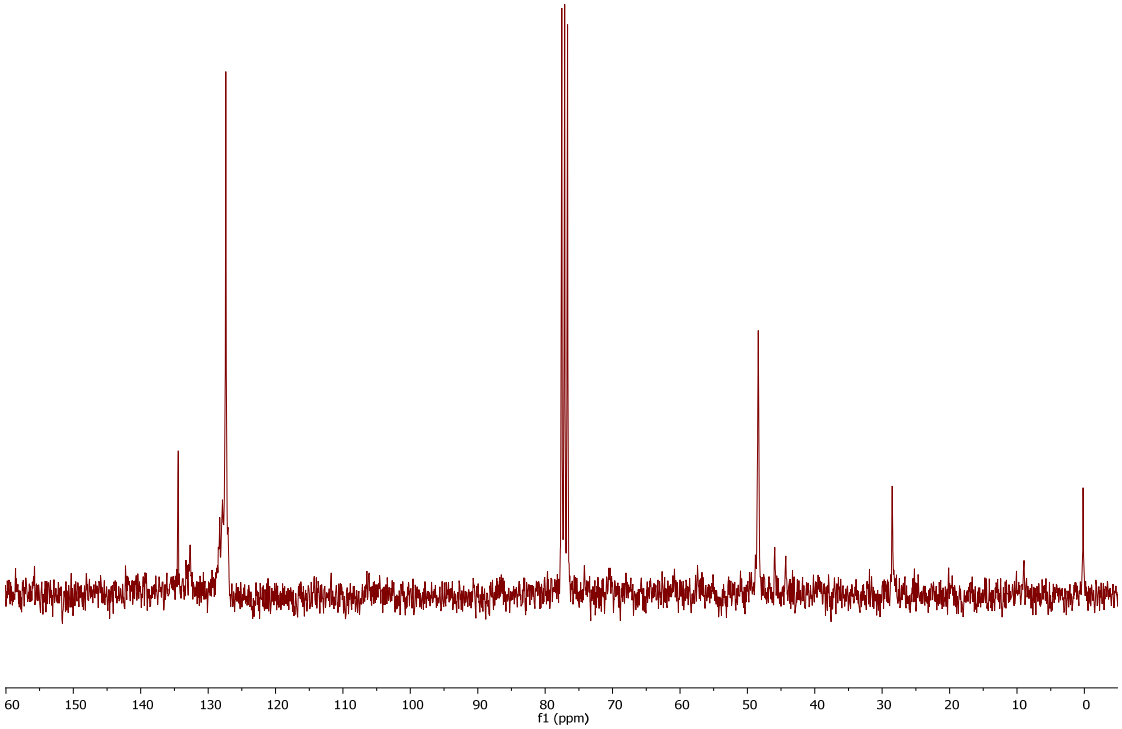

Figure 2.20: ^{13}C NMR (300 MHz, $CDCl_3$) of *p*-xylylenediisothiocyanate (**3b**).

Synthesis of 1,4-diisothiocyanatobutane (3c). To a solution of 1,4 diaminobutane (36.9 µL in 10 mL dry methanol) was added triethylamine (102 µL) and carbon disulfide (67 µL). The reaction was stirred at room temperature and monitored by UV-vis spectroscopy; formation of the bis-DTC intermediate was observed at 5 minutes and the reaction was deemed complete at 15 minutes. The reaction vessel was cooled to 0°C and treated with di-*tert*-butyl dicarbonate (320 mg in 500 µL dry methanol) and DMAP (1.35 mg in 500 µL dry methanol), then warmed to room temperature and allowed to stir for at least 12 hours, then concentrated by rotary evaporation (53 mg, 95% mass recovery). ATR-IR and ^{13}C NMR spectroscopy both showed the presence of ITC groups as well as

some peaks not associated with the product, likely due to residual di-tert-butyl dicarbonate.

Conjugation of FOx to bis-ITC linkers. A solution of iron(III) chloride (4.9 mg in 1 mL DMSO) was treated with 18.5 mg of dFOx to form the corresponding iron chelate (FOx). The dark red reaction was mixed for 10 min at room temperature until a homogeneous solution was obtained, then treated with dry triethylamine (15 µL) and 2,2'-(ethylenedioxy)bis(ethylisothiocyanate) (14 µL) and allowed to stir for at least 12 hours. Product formation and the disappearance of FOx were monitored by ESI mass spectrometry (Figure 2.21). Purification was performed by HPLC (Waters) using a C18 reverse-phase column (Phenomenex 250 x 21 mm) with a gradient of 25–75% acetonitrile in water, at a constant flow rate 10 mL/min (Figure 2.21). Fractions containing the desired conjugate were concentrated first by rotary evaporation (to remove acetonitrile), followed by lyophilization. The conjugates were obtained as orange powders, with isolated yields on the order of 60%.

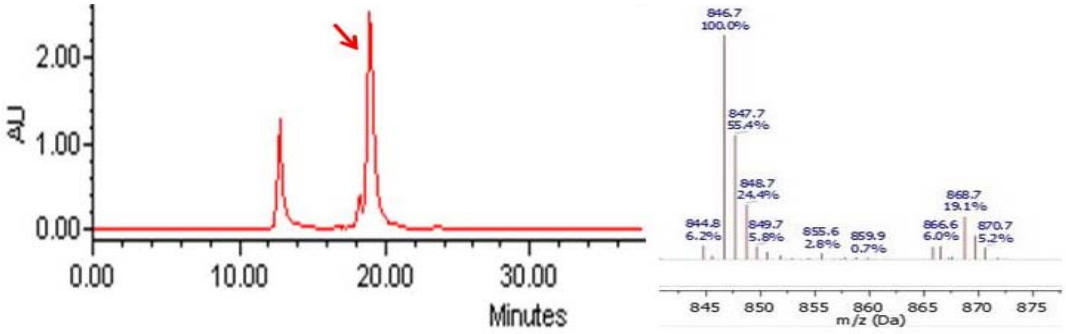

Figure 2.21: Left panel shows HPLC chromatogram from purification of compound **4a**. The red arrow denotes the product peak. The small ridge just before the product peak is a known contaminant and was not collected with the product. The right panel shows the resulting ESI+ mass spectra of the purified product peak.

Inkjet printing. 1–2 mL of FOx conjugate (0.8 – 3 mg/mL) was filtered through a 0.22-μm PTFE membrane filter, prior to loading into the Dimatix cartridge reservoir (10 pL drop size). The cartridge print head was attached to the reservoir, with care taken to remove air bubbles from the reservoir neck by pressing (but not connecting) the two parts together with reservoir side down. The assembly was then inverted (reservoir side up), allowing ink to flow through the neck into the print head. As soon as ink was observed passing through the neck, the two pieces were connected; this was done quickly to avoid spilling ink outside the reservoir. The assembled cartridge was then tapped directly on the neck of the reservoir several times, using a finger or reverse side of a small screwdriver, to promote the release of any small bubbles that may have been trapped. Finally, the inkjet cartridge was loaded into the Dimatix printer.

All standard operating procedures were performed according to the Dimatix operator manual, with the exception of the cartridge settings which were adjusted to ensure proper jetting and droplet formation. Standard inks consisted of 3 mg/mL conjugate dissolved in 10 mM Na_2CO_3 buffer containing 0.005% Tween-20 (v/v). A jetting voltage between 18 and 25 V was used in conjunction with the waveform shown in Figure 2.22; jetting was limited to a single nozzle for reliable control over droplet deposition. The voltage and waveform settings have the greatest influence on droplet formation; other noteworthy settings include cartridge temperature (30°C), meniscus setpoint (3.0), and cartridge print height (1.000 mm). Settings under the cleaning cycle are also important, with all categories set to “spit purge spit”. The cycle was run every 200 bands or 180 seconds during active printing, and every 300 seconds while idle.

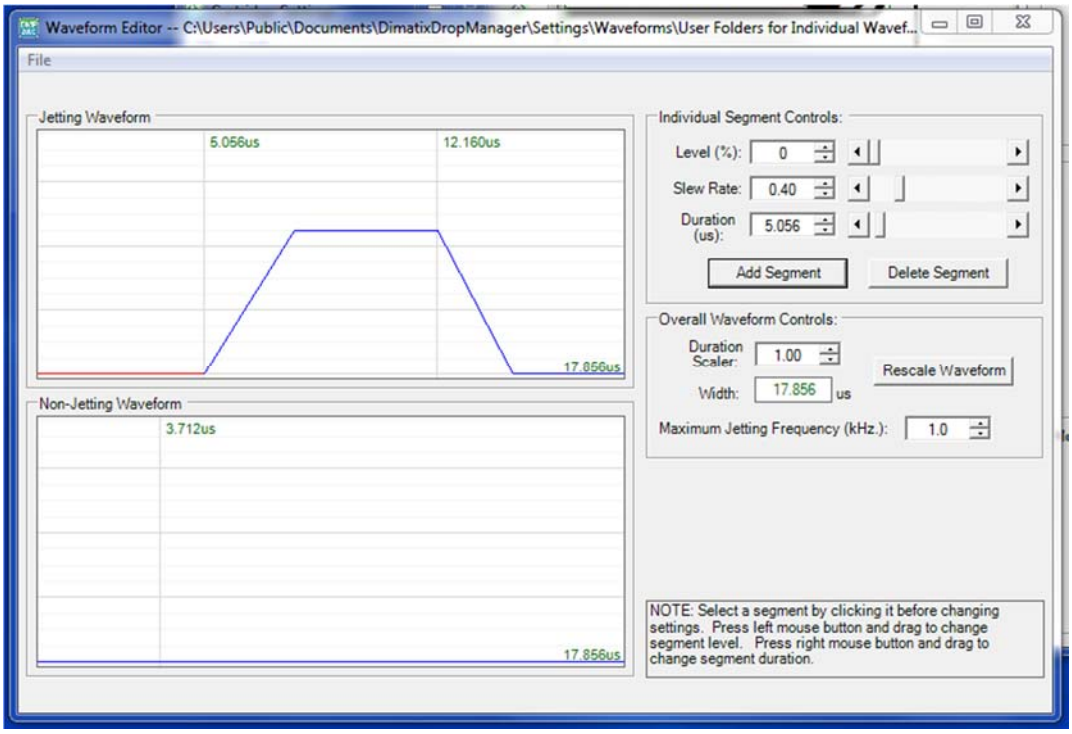

Figure 2.22: Screenshot depicting the waveform used for patterning chips with FOx conjugates, using the Dimatix inkjet printer. The values shown under "individual segment controls" correspond with the initial (red) section of the timeline.

Acid-treated materials. Microcentrifuge tubes and pipet tips were acid-washed prior to use with bacterial suspensions in iron-minimal media. An acid bath comprised of 1–2% HNO_3 in deionized water was prepared in a large glass container (>3 L). Acid-treated materials were fully submerged and allowed to soak for at least one hour, with stirring every 15 minutes. The acid bath was then discarded, and treated materials were washed with freshly dispensed deionized water for a minimum of six times. Materials were placed into autoclavable boxes and autoclaved at 121 °C.

2.10. References

1. Doorneweerd, D. D.; Henne, W. A.; Reifenberger, R. G.; Low, P. S., Selective Capture and Identification of Pathogenic Bacteria Using an Immobilized Siderophore. *Langmuir* **2010,** *26* (19), 15424-15429.

2. Adak, A. K.; Leonov, A. P.; Ding, N.; Thundimadathil, J.; Kularatne, S.; Low, P. S.; Wei, A., Bishydrazide Glycoconjugates for Lectin Recognition and Capture of Bacterial Pathogens. *Bioconjugate Chem.* **2010,** *21* (11), 2065-2075.

3. Kim, Y.; Lyvers, D. P.; Wei, A.; Reifenberger, R. G.; Low, P. S., Label-free detection of a bacterial pathogen using an immobilized siderophore, deferoxamine. *Lab Chip* **2012,** *12* (5), 971-976.

4. Adak, A. K.; Boley, J. W.; Lyvers, D. P.; Chiu, G. T.; Low, P. S.; Reifenberger, R.; Wei, A., Label-Free Detection of *Staphylococcus aureus* Captured on Immutable Ligand Arrays. *ACS Appl Mater Interfaces* **2013,** *5* (13), 6404-6411.

5. Munch, H.; Hansen, J. S.; Pittelkow, M.; Christensen, J. B.; Boas, U., A new efficient synthesis of isothiocyanates from amines using di-tert-butyl dicarbonate. *Tetrahedron Lett.* **2008,** *49* (19), 3117-3119.

6. Pecháček, R.; Velíšek, J.; Hrabcová, H., Decomposition Products of Allyl Isothiocyanate in Aqueous Solutions. *J Agric Food Chem.* **1997,** *45* (12), 4584-4588.

7. Kalinin, Y. V.; Berejnov, V.; Thorne, R. E., Contact Line Pinning by Microfabricated Patterns: Effects of Microscale Topography. *Langmuir : the ACS journal of surfaces and colloids* **2009,** *25* (9), 5391-5397.

8. Neilands, J. B., Siderophores: Structure and Function of Microbial Iron Transport Compounds. *J. Biol. Chem.* **1995,** *270* (45), 26723-26726.

9. Venturi, V.; Weisbeek, P.; Koster, M., Gene regulation of siderophore-mediated iron acquisition in *Pseudomonas*: not only the Fur repressor. *Mol Microbiol* **1995,** *17* (4), 603-10.

10. Troxell, B.; Hassan, H. M., Transcriptional regulation by Ferric Uptake Regulator (Fur) in pathogenic bacteria. *Front Cell Infect Microbiol* **2013,** *3*, 59.

11. Horcas, I.; Fernandez, R.; Gomez-Rodriguez, J. M.; Colchero, J.; Gomez-Herrero, J.; Baro, A. M., WSXM: a software for scanning probe microscopy and a tool for nanotechnology. *Rev Sci Instrum* **2007,** *78* (1), 013705.

12. Lyvers, D. P. PhD Thesis. Purdue University, 2012. Chapter 3.

CHAPTER 3: ULTRA-RAPID DETECTION OF BACTERIAL PATHOGENS

3.1 Introduction to Rapid Pathogen Detection

Time is a crucial factor in the detection of actively virulent pathogens. All strains in this study have earned reputations as public health threats when left unchecked. *S. enterica* is the single largest cause of bacterial foodborne illness in the United States with an estimated 1,027,561 cases each year, including 19,000 hospitalizations and 380 deaths.[1-2] *Y. enterocolitica* is also of concern in food safety, and is known to thrive at refrigerator and even freezer temperatures.[3-11] *S. aureus* and its methicillin-resistant strains (MRSA) are leading causes of nosocomial infections in the United States,[12-14] and are included in the group of pathogens referred to as ESKAPE bacteria, along with *A. baumannii*.[15] Many ESKAPE pathogens are resistant against currently available antibiotics, and have become a menace in hospitals and other health clinics.[16]

Early detection provides the opportunity to respond to these threats in a quick and targeted fashion,[17-18] reducing the overreliance on blanket remedies such as broad-spectrum antibiotics, which only serve to exacerbate the issues of poor patient outcomes[19-20] and the creation of multidrug-resistant strains.[21]

However, standard methods of bacterial detection lack the fast turnaround time necessary to combat these dangerous pathogens. This issue is well known to the scientific community, as evidenced by the current drive to develop more rapid detection methods.[22-25] Federal and international health agencies have echoed the call for further development of rapid, cost-effective methods for the detection of pathogenic bacteria.[26-28] Numerous approaches to pathogen detection are being explored, but many have been plagued by one or more pitfalls, as described in Section 1.2.1.

The use of siderophores such as FOx and other small-molecule conjugates provide valuable entry points for the development of new rapid pathogen detection methods, as described in several publications from our laboratory.[29-31] Reducing time to detection (TTD) has become our primary objective, in our drive to push detection methods toward useful applications. In previous studies, time points for detection were held constant at 30 or 60 minutes in some cases.[32] In this Chapter, we probe the practical limits of our system and find that detection can be easily achieved within 30 seconds, which we have dubbed "ultra-rapid detection." In particular, we find that the method of sample preparation is crucial for enabling TTD in the ultra-rapid domain.

With all parameters optimized, FOx microarrays on chips were able to capture five pathogenic bacterial strains with high levels of sensitivity. In the case of *Y. enterocolitica*, detection was achieved at bacterial concentrations as low as 10^2 cfu/mL within 60 minutes. In this chapter, we systematically studied bacterial detection as a function of exposure time to determine the TTD for each strain. In particular, we considered the rates of binding between FOx and specific bacterial receptors, to better

understand the molecular aspects of siderophore-mediated bacterial adhesion in our detection platform.

It was previously shown that the appropriate presentation of FOx is crucial for rapid binding of cognate bacteria to chip surfaces. FOx patterned onto chips without a linker was incapable of binding effectively to *Y. enterocolitica* or other FOx binding strains. In order to improve presentation, FOx conjugates **5** and **6** (section 3.2) were synthesized then patterned onto substrate to produce chips used in TTD experiments for the five strains of interest. Initially experiments were performed using the drop-on-chip method described in Chapter 2 (also see Section 3.3), which enabled detection to be achieved in as little as five minutes, but in a rather capricious fashion. We hypothesized that the drop-on-chip method introduced turbulent flow that discouraged planktonic bacteria from activating their virulence factors (see Section 3.4), and considered alternative methods of exposing capture chips to bacteria that might further reduce TTD.

We thus developed the "horizontal submersion method," in which chips were fully submerged into a still bacterial suspension, lying flat with the microarray facing upward. This method of sampling provided a drastic improvement in TTD for all five strains, with strong signals achieved within 30 seconds of exposing chips to bacteria. Additional experiments were performed to monitor detection at exposure times for up to 15 minutes. Negative control experiments confirmed that detection was mediated by ligand–receptor interactions; the binding of strains expressing FOx receptors onto chips could be reduced by competitive inhibition with free dFOx, prior to exposure.

3.2 Synthesis of Ferrioxamine Conjugates

In the course of optimizing experimental design parameters, it became evident that the surface chemistry for presenting FOx conjugates (see Sections 2.2.2 and 2.5) needed to be optimized as well. FOx conjugated with 2,2'-(ethylenedioxy)bis-(ethylisothiocyanate) (**3a**) was subject to hydrolysis in 10 mM Na_2CO_3 buffer (pH 10). The major product (identified as **3b** in its crude form) was purified by reverse-phase HPLC to yield conjugate **5**. Electrospray ionization mass spectrometry (ESI-MS) in positive mode showed a major peak at the expected *m/z* ratio (Figure 3.1). Taking advantage of the modular nature of the bis-ITC linker, **5** was then treated with 2,2'-(ethylenedioxy)bis(ethylamine) and purified by reverse-phase HPLC to yield conjugate **6** (Figure 3.2). The syntheses of both conjugates are shown in Scheme 3.1.

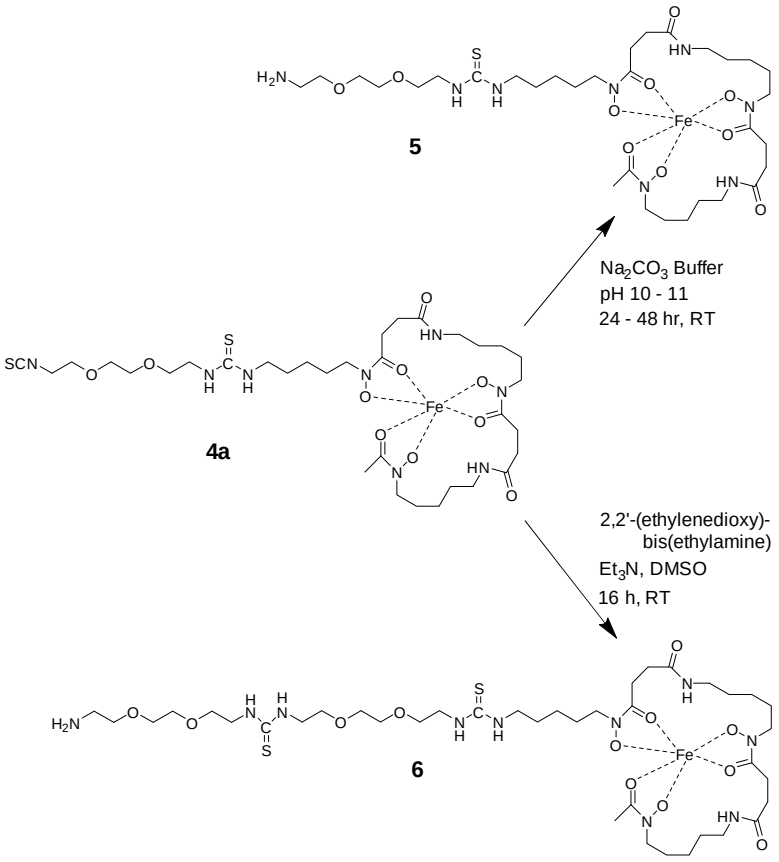

Scheme 3.1: Synthesis of conjugates **5** and **6**

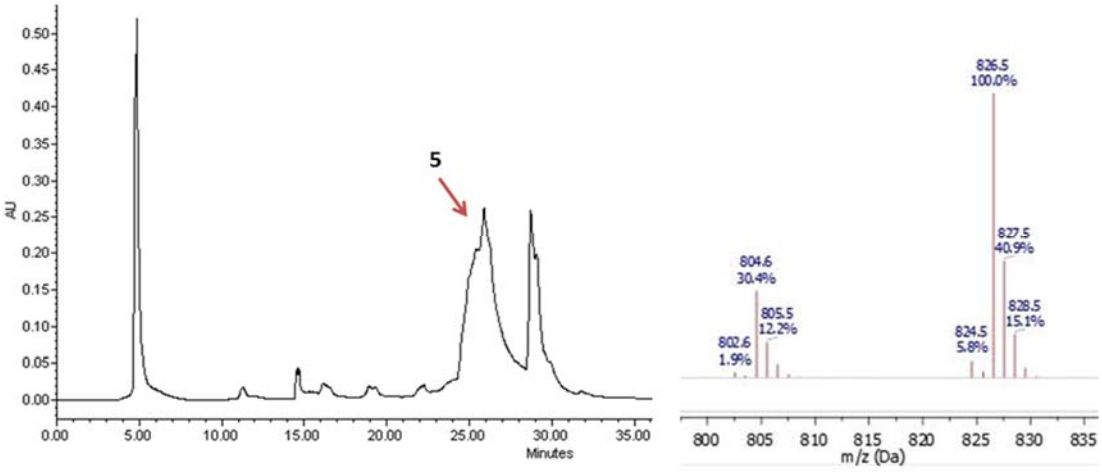

Figure 3.1: Purification and characterization of **5**. *Left*, HPLC trace for purification of **5**, with the red arrow pointing to the product peak. *Right*, ESI mass spectrum of purified **5**. $[M+H]^+$: calcd *m/z* = 804, actual = 804.6; $[M+Na]^+$: calcd *m/z* = 826, actual = 826.5.

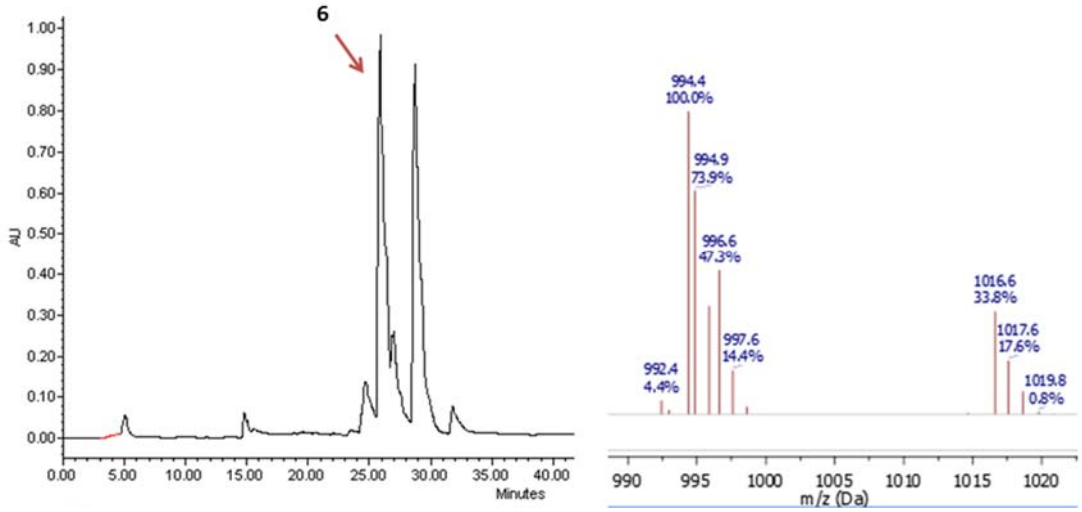

Figure 3.2: Purification and characterization of **6.** *Left*, HPLC trace from purification of **6**, with the red arrow pointing to the product peak. *Right*, ESI mass spectrum of purified **6**. $[M+H]^+$: calcd *m/z* = 994, actual = 994.4; $[M+Na]^+$: calcd *m/z* = 1016, actual = 1016.6.

3.3 Preliminary Studies Utilizing Drop-on-Chip Method

The drop-on-chip method was employed for all experiments described in Chapter 2. This method involved placing the capture substrate horizontally in a petri dish with patterned side facing up. A suspension of a given bacteria at a given concentration was prepared in PBS. A portion of this suspension (200–400 µL) was then pipetted directly onto the patterned substrate using a 1-mL micropipetman. Optimally the suspension would cover 80–90% of the substrate surface (1.25 cm^2) but would not reach to the corners. The substrates was covered with a petri dish lid immediately following placement of the liquid, with care taken not to cause any mechanical disturbance to the sample.

The goal of these experiments was to determine the TTD for each bacterial strain identified as a binding partner for FOx by BLAST search from Section 1.5. Of

the strains identified, seven were available in our lab for testing: *Y. enterocolitica, S. aureus,* MRSA, *S. enterica, A. baumannii, K. pneumoniae* and *P. aeruginosa.* Each of these strains was tested at a concentration of 10^7 cfu/mL with 15-minute and 5-minute exposure times, and 10^6 cfu/mL with 15-min exposure times, using substrates patterned with **6**. All strains other than *P. aeruginosa* were also tested under identical conditions using substrates patterned with **5**. These experiments could determine whether detection was reliable with exposure times of 15 minutes or less, and whether linker length in **5** and **6** was a significant factor in TTD. While it was clear that a linker was necessary for bacterial detection from the experiments described in Section 2.5.2, it was unknown whether further increasing its length would provide any advantages. The results presented in Table 3.1 neatly address this question.

Table 3.1: Summary of S/N values from bacterial detection studies using the drop-on-chip method

Strains (receptors)	Conjugate 5			Conjugate 6		
	10^7 cfu/mL		10^6 cfu/mL	10^7 cfu/mL		10^6 cfu/mL
	Exposure time (min)			Exposure time (min)		
	15	5	15	15	5	15
Yersinia enterocolitica (FoxA)	21.8	ND[a]	ND[a]	26.7	8.2	ND[a]
Staphylococcus aureus (FhuD2)	15.0	3.1	ND[a]	ND[a]	ND[a]	--[b]
MRSA (FhuD2)	11.8	3.7	ND[a]	ND[a]	ND[a]	--[b]
Acinetobacter baumannii (FhuE)	3.7	ND[a]	ND[a]	7.4	ND[a]	ND[a]
Klebsiella pneumoniae (FoxA)	ND[a]	ND[a]	ND[a]	ND[a]	ND[a]	ND[a]
Salmonella enterica (FoxA, FhuE)	ND[a]	ND[a]	ND[a]	8.6	ND[a]	ND[a]
Pseudomonas aeruginosa (FoxA)	--[b]	--[b]	--[b]	ND[a]	ND[a]	ND[a]

[a] ND indicates no detection was achieved; [b] -- indicates experiment was not attempted.

Darkfield images of chips and their associated FFT analyses using **5** and **6** are represented in Figures 3.3 and 3.4 respectively. In the case of **5**, four bacteria were detectable after a 15-minute exposure, with *Y. enterocolitica* providing the highest S/N, followed by *S. aureus* and MRSA, then *A. baumannii* near the threshold of detection. However, with 5-minute exposure times only *S. aureus* and MRSA produced signals near the threshold of detection. In the case of **6**, three bacteria were detectable after a 15-minute exposure, with *Y. enterocolitica* again providing the strongest signal, followed by *S. enterica* and *A. baumannii*. However, only *Y. enterocolitica* could be detected within 5 minutes.

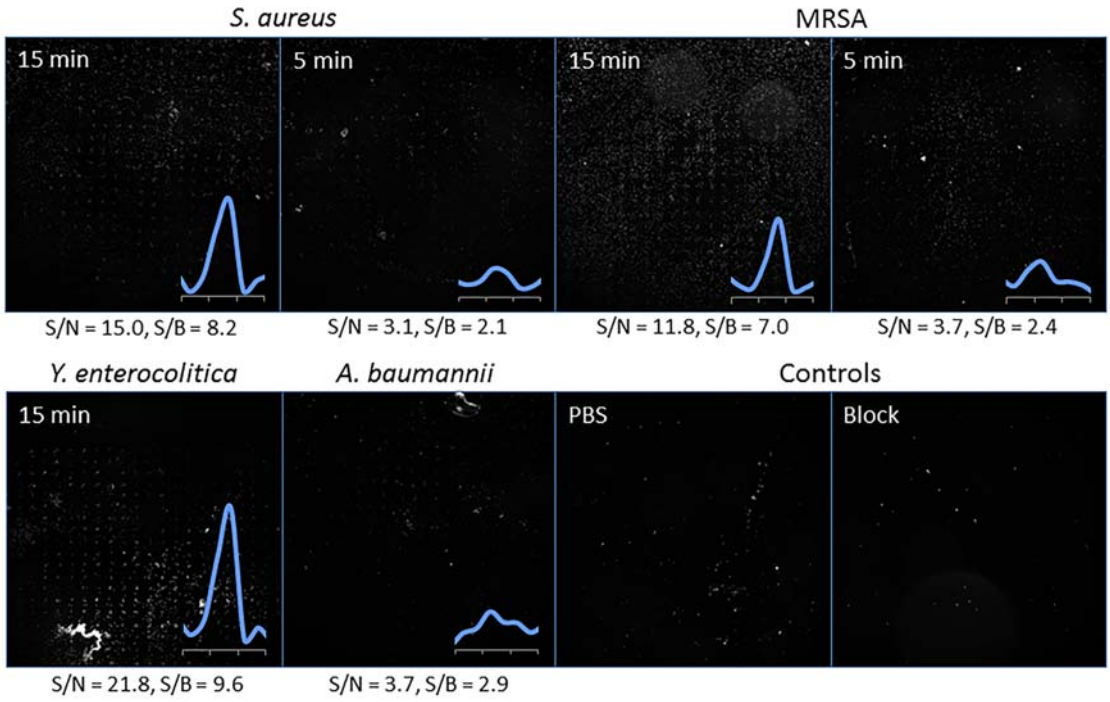

Figure 3.3: Representative raw images and FFT analysis (where appropriate) from experiments using drop-on-chip method with chips patterned with **5**. Appropriate controls appear essentially blank.

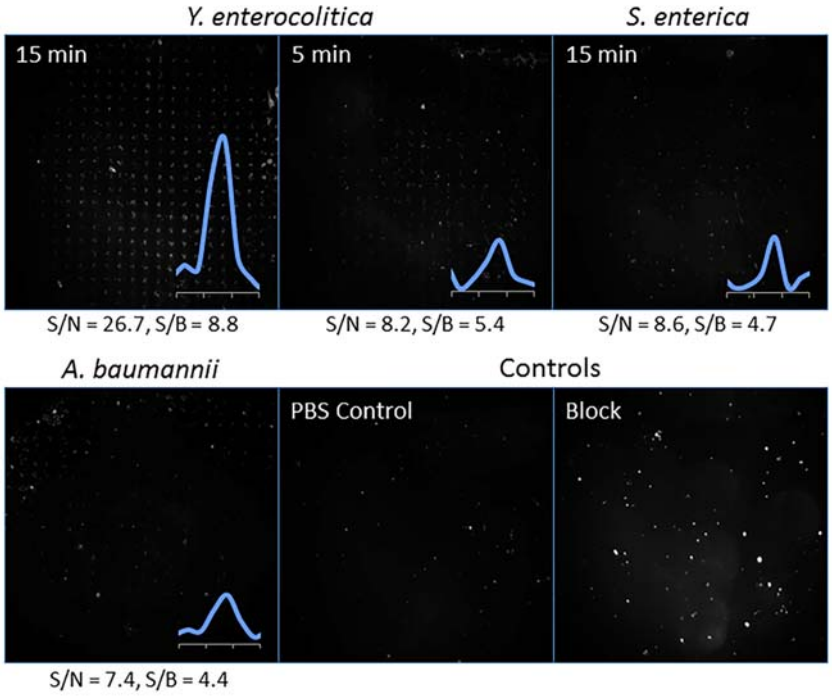

Figure 3.4: Representative raw images and FFT analysis (where appropriate) from experiments using drop-on-chip method with chips patterned with **6**. Appropriate controls and blocked microarrays appear essentially blank prior to bacterial exposure.

Several other observations of the experiments above are also noteworthy. First, bacterial concentrations of 10^7 cfu/mL were required for signal generation; at the lower concentration of 10^6 cfu/mL, detection was not achieved in any case. Second, the capture profiles of substrates patterned with **5** and **6** were highly variable. Conjugate **6** performed best for the detection of strains expressing the FoxA and FhuE receptors. *Y. enterocolitica*, which expresses the FoxA receptor,[33-34] was captured by both conjugates but **6** supported a higher S/N ratio and also a faster time to detection. *A. baumannii*, which expresses the FhuE receptor,[35] was also captured by both conjugates with a 15-minute exposure, but chips prepared using **6** again produced higher S/N ratios. These trends were further reinforced by experiments with *S. enterica*, which expresses both FoxA and FhuE receptors,[36] and was detected only by conjugate **6**. Conversely, *S.*

aureus and MRSA, which express the FhuD2 receptor,[37-39] were only detected by conjugate **5**.

3.4 Pathogen Detection Using the Horizontal Submersion Method

Use of the drop-on-chip method provided good results during LOD studies when all data points were collected at 30 minutes, but was less than optimal when data points were collected at 15 minutes or less. This suggests that planktonic bacteria needed 15–30 minutes to resume their fully active state following pipet transfer. We postulated that the motion associated with pipetting bacterial suspensions onto chips was enough to activate a self-protective response in planktonic cells that suppresses surface adhesion, as shear forces are known to do.[40-41] These types of disturbances should be avoided to keep bacteria primed for adhesion.[42-44]

To circumvent this problem, an alternative method of exposing chips to bacterial suspensions was devised, described here as "horizontal submersion." Once the bacterial suspension had been washed with PBS, an aliquot was pipetted into a 3-dram vial and diluted to the desired concentration with a final volume of 3–4 mL. The diluted suspension was then mixed very gently using pipet action, then left standing without further disturbance for a minimum of 20 minutes, prior to the pathogen detection experiment. Chips were then gripped by forceps on a predesignated corner and lowered vertically into the vial, edge-first, with minimum mechanical disturbance. The submerged chip was then released and allowed to rest horizontally on the vial floor with patterned side facing up (Figure 3.5).

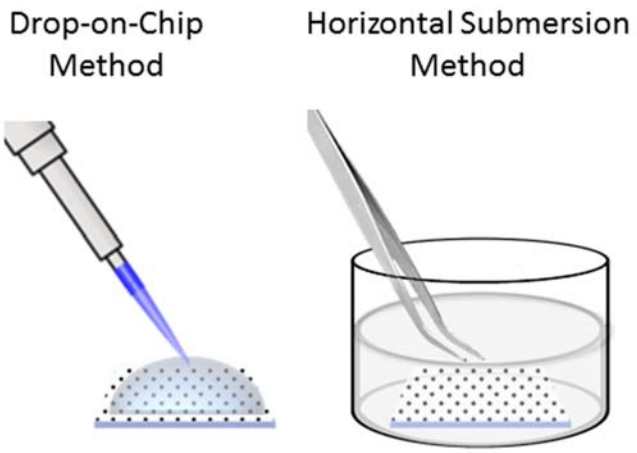

Figure 3.5: Visual comparison of chip exposure methods. In the drop-on-chip method, chips were laid flat and bacterial suspension was pipetted directly onto the patterned face of the chip. In the horizontal submersion method, chips were gripped with forceps and lowered onto the floor of a vial with a bacterial suspension that had been undisturbed for at least 20 minutes, patterned side face up.

With the horizontal submersion method, bacterial detection became possible within 30 seconds. "Vertical submersion" was also attempted: In one instance, chips were held in the vertical orientation and dipped into solution without resting on any surface, for times ranging from 30 seconds to 2 minutes; however, capture of bacteria was not observed. In another instance, chips were left leaning against the inner wall of the vial while submerged in still suspension, but required at least 5 minutes for detection to occur. We thus conclude that chips added to a still suspension and laid in a horizontal state are necessary conditions for ultra-rapid bacterial adhesion.

3.5 Ultra-rapid Detection of *Y. enterocolitica*, *S. aureus*, *S. enterica* and *A. baumannii*

TTD experiments were performed for five strains of interest using the horizontal submersion method, with exposure times of 15 minutes, 5 minutes, 2 minutes, and 30 seconds. The first two time points allowed for direct comparison to the drop-on-chip method, while the latter two validated detection in the ultra-rapid time domain. Each condition was tested using **5** and **6**, to determine if variability based on tether length was a factor, as observed earlier with the drop-on-chip method. For all cases, bacteria were cultured in iron-deficient media in order to mimic physiological conditions, achieved by adding 2,2-bipyridyl (bipy) to media prior to autoclaving. Optimization of bipy concentrations for each strain are described in Section 2.3, with final values listed in Tables 3.2 and 3.3.

In the cases of *S. aureus* and MRSA, we applied an additional culturing technique prior to performing TTD experiments. These strains were selected over several generations utilizing FOx as a source of iron. This was achieved by cycling growth media between stock TS broth and TS broth dosed with both bipy (1 mM) and FOx (50 μM) several times. FOx-selected cultures were then cultured in a standard iron-deficient media (TS with 1 mM bipy) for use in TTD experiments. This method of selection was also employed for *A. baumannii*, but only for the TTD experiment performed using **6**. As shown in Section 3.3, detection of *S. aureus*, MRSA and *A. baumannii* within 15 minutes is still possible without FOx selection pressure. However, we have found that selective feeding is important to lower the TTD to the ultra-rapid domain, to ensure that receptors of interest were being expressed. In contrast, neither *Y. enterocolitica* (37 °C or 4 °C) nor *S. enterica* were subject to any type of selection; both

were grown in standard LB broth prior to inoculation of iron-deficient media, prior to TTD experiments.

For a given pair of conjugate and bacterial strain, chips were employed at each time point and imaged by darkfield optical microscopy at three different ROIs. Each image was independently processed by FFT analysis to determine both S/N and S/B. These values were then averaged to give a value representative of the entire capture chip as minor variability was known to exist. The same process was repeated for each strain (Figure 3.6).

Tables 3.2 and 3.3 summarize all processed results, including S/N and S/B. Overall these experiments proved to be successful as detection (S/N > 3) was achieved in nearly every condition tested. Furthermore, control experiments involving competitive inhibition with excess free ligand confirmed the specificity of bacterial adhesion to be mediated by FOx–receptor interactions. For these experiments, separate bacterial suspensions were first treated with 250 μM dFOx, 5 or 20 minutes prior to chip exposure, with the hypothesis that excess dFOx would saturate bacterial receptors and reduce binding to tethered conjugates. In all cases except one, chips exposed to dFOx-treated bacteria did not demonstrate detection within 30 seconds. In the singular case of *A. baumannii*, pre-incubation with dFOx for 5 minutes was not sufficient to suppress pathogen adhesion, however inhibition was achieved with 20 minutes of pre-incubation.

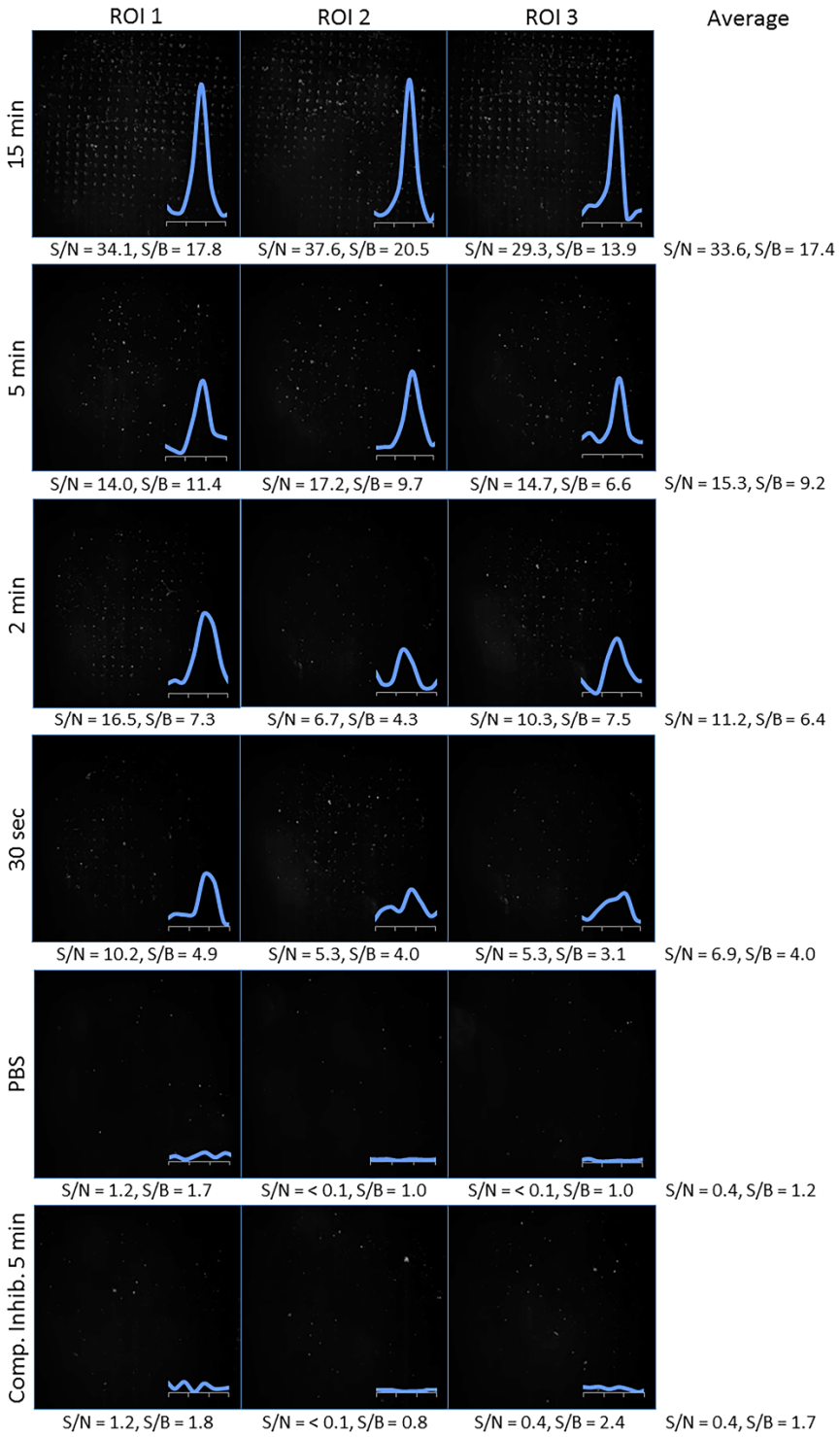

Figure 3.6: Detection of *Y. enterocolitica* using chips patterned with conjugate **6**, using the horizontal submersion method. Raw images of three ROIs and their associated FFT signals are depicted for each time point, using S/N and S/B values as quantitative metrics; averages are shown at far right.

Table 3.2: Summary of time-to-detection experiments utilizing the horizontal submersion method, with mean S/N values from three independent FFT analyses

Strains (receptors)	[bipy], mM[d]	Conjugate 5				Conjugate 6					
		Exposure time (min)				Exposure time (min)					
		15	5	2	0.5	15	5	2	0.5	0.5 (dFOx 5)[e]	0.5 (dFOx 20)[e]
Yersinia enterocolitica (FoxA)	3	6.6	5.7	10.4	9.6	33.6	15.3	11.2	6.9	0.4	0.6
Yersinia enterocolitica @ 4 °C	0.05	--[b]	--[b]	--[b]	--[b]	19.3	12.4	9.2	19.7	--[b]	--[b]
Staph aureus (FhuD2)	1	18.9	14.6	ND[a]	ND[a]	--[b]	--[b]	--[b]	--[b]	--[b]	--[b]
Staph aureus (FhuD2) (FOx^+)[c]	1	17.6	13.2	8.2	20.6	37.2	11.6	20.4	12.0	0.4	1.0
MRSA (FhuD2) (FOx^+)[c]	1	22.4	21.1	15.8	6.5	14.2	ND[a]	11.5	10.5	0.1	0.4
Acinetobacter baumannii (FhuE)	0.1	12.9	10.5	ND[a]	ND[a]	--[b]	--[b]	--[b]	--[b]	--[b]	--[b]
Acinetobacter baumannii (FhuE) (FOx^+)[c]	0.1	--[b]	--[b]	--[b]	--[b]	28.3	22.1	11.9	11.8	10.2	0.7
Salmonella enterica (FoxA, FhuE)	0.1	17.0	11.5	10.3	5.7	11.0	8.2	5.7	4.2	0.3	1.0

[a] ND indicates no detection was achieved. [b] -- indicates experiment was not attempted. [c] Entries annotated with (FOx^+) indicate bacteria were pre-selected for FOx recognition. [d] [bipy] represents the concentration of 2,2-bipyridine used to create iron-deficient conditions. [e] Competitive inhibition using chips pre-incubated with 250 µM dFOx for 5 min (dFOx 5) or 20 min (dFOx 20), prior to bacterial exposure.

Table 3.3: Summary of time-to-detection experiments utilizing the horizontal submersion method, with mean S/B values from three independent FFT analyses

Strains (receptors)	[bipy] mM[d]	Conjugate 5				Conjugate 6					
		Exposure time (min)				Exposure time (min)					
		15	5	2	0.5	15	5	2	0.5	0.5 (dFOx 5)[e]	0.5 (dFOx 20)[e]
Yersinia enterocolitica (FoxA)	3	4.3	3.2	4.9	4.5	17.4	9.2	6.4	4.0	1.7	1.2
Yersinia enterocolitica @ 4 °C	0.05	--[b]	--[b]	--[b]	--[b]	7.5	7.0	6.3	10.3	--[b]	--[b]
Staph aureus (FhuD2)	1	10.7	8.4	ND[a]	ND[a]	--[b]	--[b]	--[b]	--[b]	--[b]	--[b]
Staph aureus (FhuD2) (FOx^+)[c]	1	11.7	7.8	5.2	11.0	18.7	8.2	10.9	7.5	1.4	1.5
MRSA (FhuD2) (FOx^+)[c]	1	14.1	9.5	8.9	3.1	5.6	ND[a]	6.2	6.1	1.1	1.2
Acinetobacter baumannii (FhuE)	0.1	8.9	6.0	ND[a]	ND[a]	--[b]	--[b]	--[b]	--[b]	--[b]	--[b]
Acinetobacter baumannii (FhuE) (FOx^+)[c]	0.1	--[b]	--[b]	--[b]	--[b]	10.1	11.6	6.6	6.7	6.1	1.3
Salmonella enterica (FoxA, FhuE)	0.1	10.1	5.9	6.8	3.4	5.1	4.9	3.1	2.7	1.2	1.5

See previous table for footnotes.

At least two observations are worthy of further discussion. First, *Yersinia enterocolitica* and *Salmonella enterica* can be detected within 30 seconds when cultured under iron-deficient conditions, but without preselection using FOx as a source of iron, unlike the other three strains. This may be attributed to high levels of constitutive expression of FoxA by *Yersinia* and *Salmonella*, a faster rate of binding for FoxA relative to other FOx receptors, or both. Second, studies with *Yersinia* produced stronger detection signals at 30 seconds when cultured at 4 °C with 0.05 mM bipy, rather than at 37 °C with 3 mM bipy, although the converse was true for signals generated at 5 or 15 minutes. This suggests how differences in culture conditions might influence the expression level or presentation of FoxA by *Yersinia* or other bacteria.

Several charts were constructed from the data presented in Tables 3.2 and 3.3, in order to clarify overall trends and comparisons between different methods of sampling, with separate analyses based on S/N values (Figures 3.7, 3.8) and S/B values (Figures 3.9, 3.10).

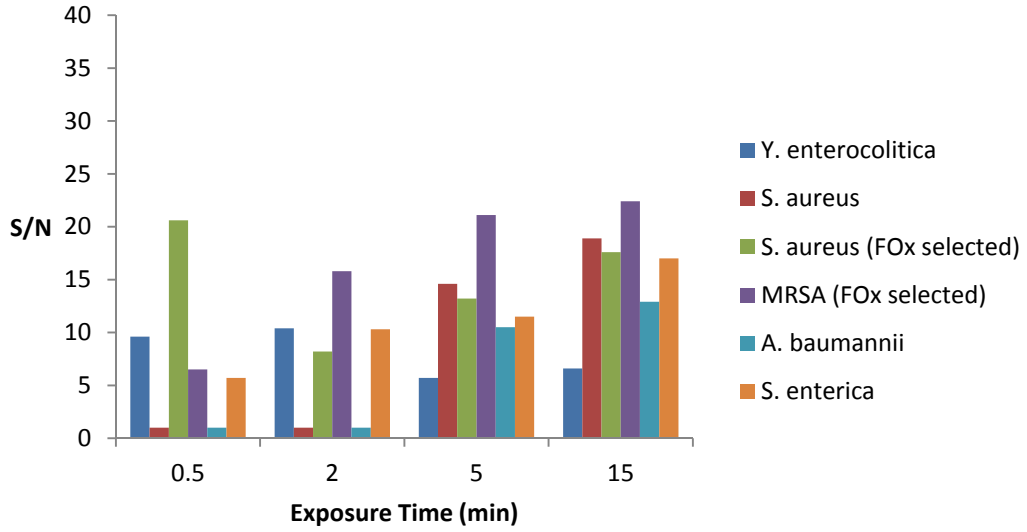

Figure 3.7: S/N ratios as a function of exposure time, using chips patterned with **5** subjected to the horizontal submersion method.

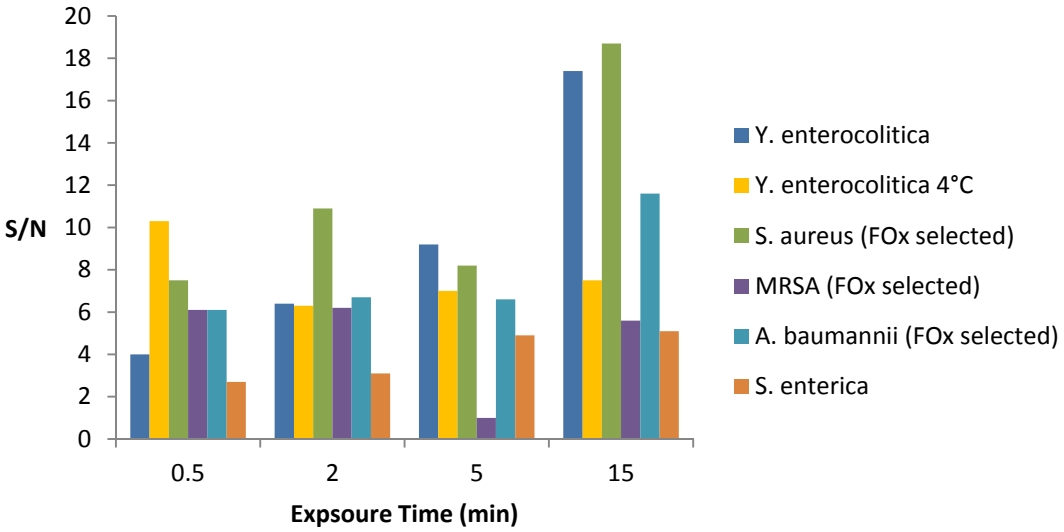

Figure 3.8: S/N ratios as a function of exposure time, using chips patterned with **6** subjected to the horizontal submersion method.

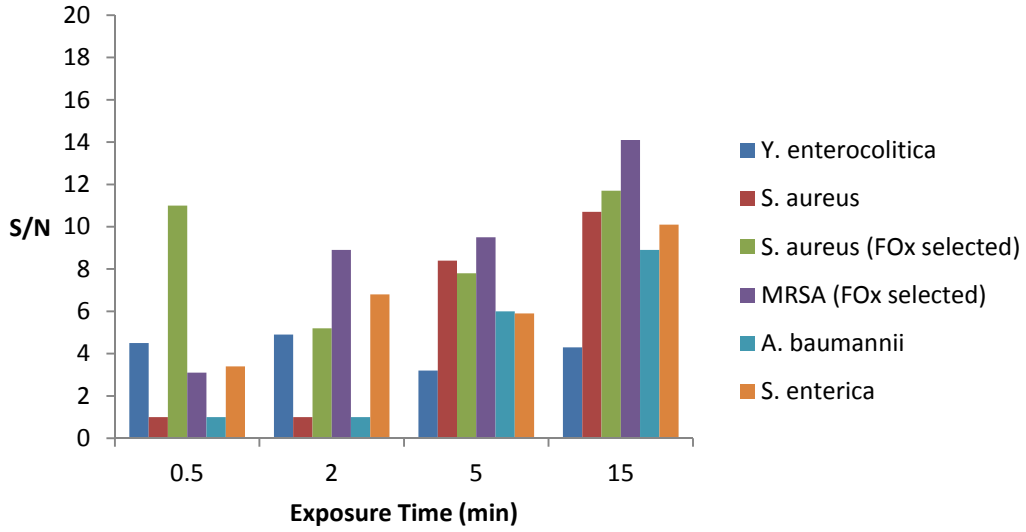

Figure 3.9: S/B ratios as a function of exposure time, using chips patterned with **5** subjected to the horizontal submersion method.

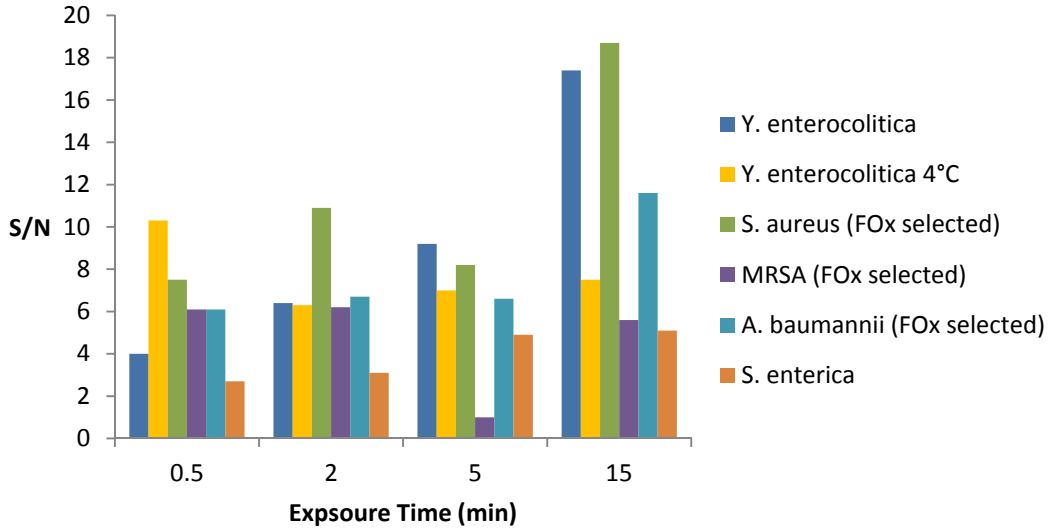

Figure 3.10: S/B ratios as a function of exposure time, using chips patterned with **6** subjected to the horizontal submersion method.

The data was also charted based on each individual strain for analysis of trends. Figures 3.11–3.15 represent all experiments for detection of *Y. enterocolitica*, *S. enterica*, *A. baumannii*, *S. aureus* and MRSA, respectively.

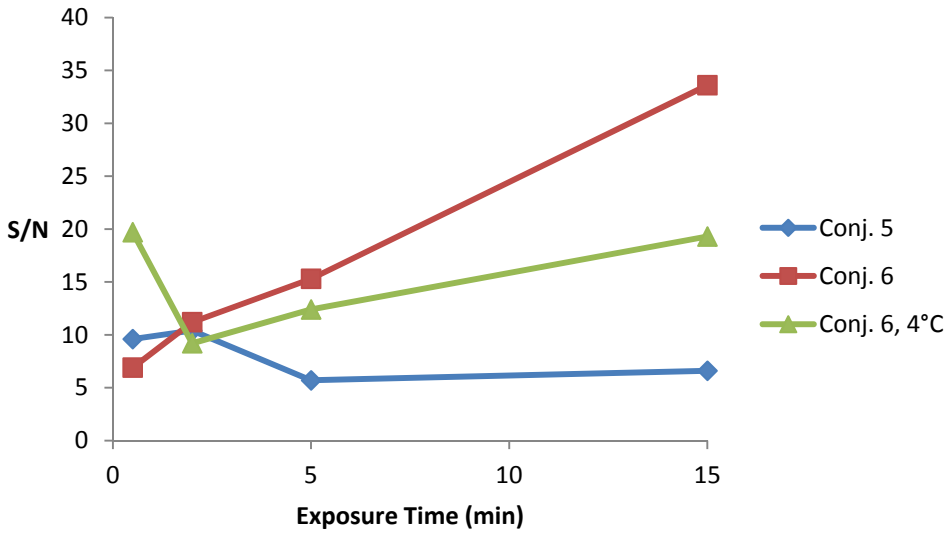

Figure 3.11: S/N ratios as a function of exposure time to *Y. enterocolitica*, for all conditions tested using the horizontal submersion method.

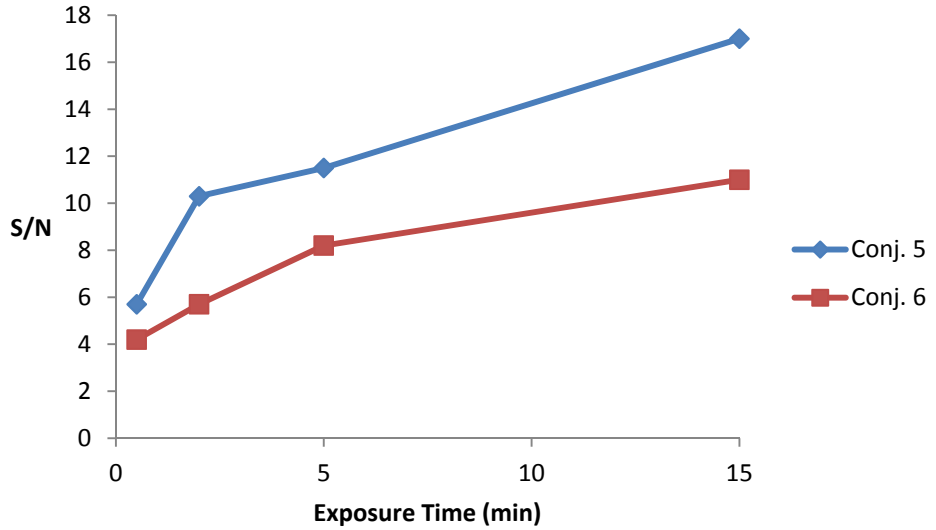

Figure 3.12: S/N ratios as a function of exposure time to *S. enterica*, for all conditions tested using the horizontal submersion method.

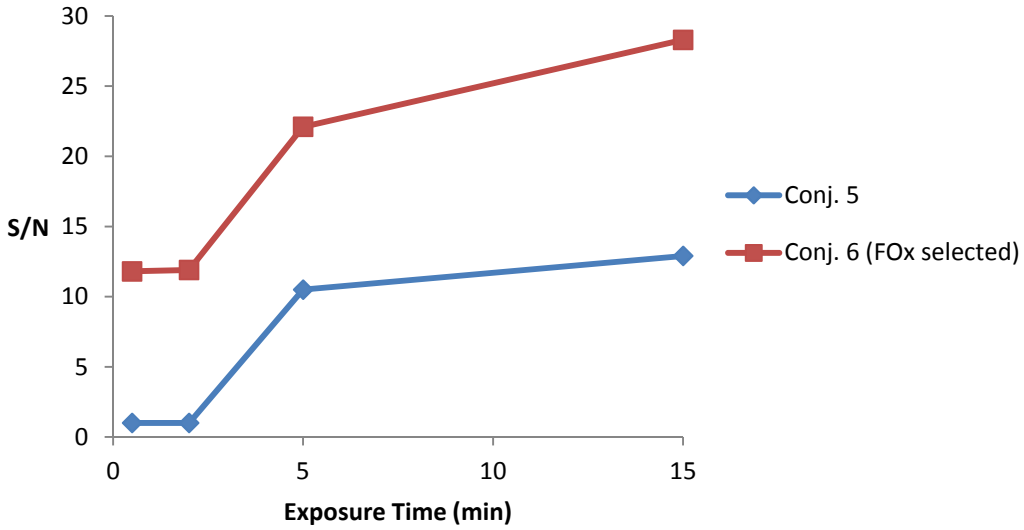

Figure 3.13: S/N ratios as a function of exposure time to *A. baumannii*, for all conditions tested using the horizontal submersion method.

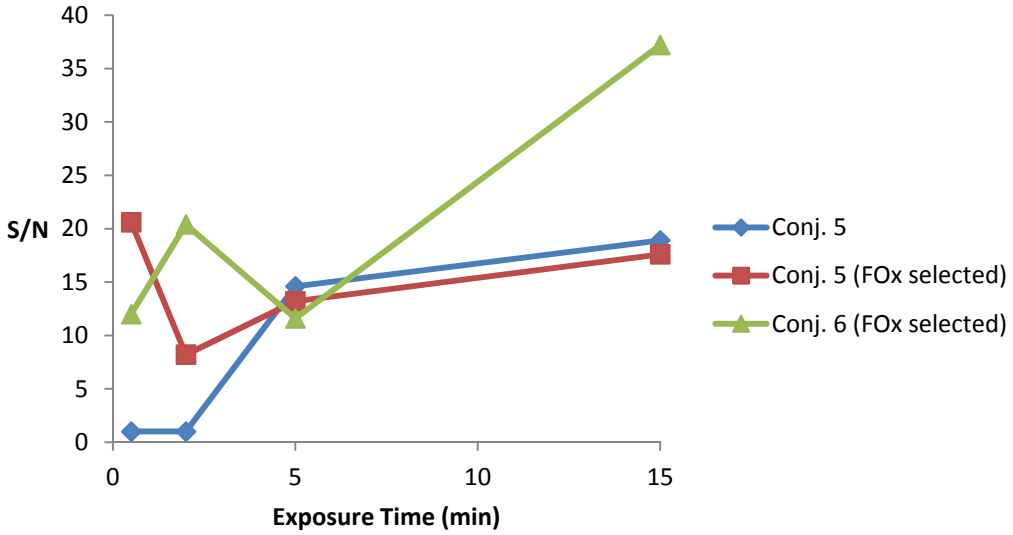

Figure 3.14: S/N ratios as a function of exposure time to *S. aureus*, for all conditions tested using the horizontal submersion method.

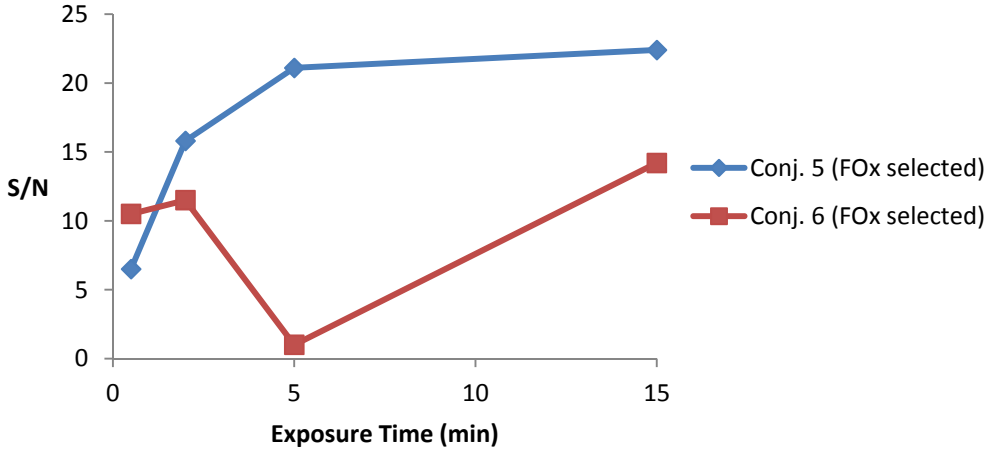

Figure 3.15: S/N ratios as a function of exposure time to MRSA, for all conditions tested using the horizontal submersion method.

Y. enterocolitica shows similar levels of detection in the ultra-rapid domain for both conjugates. However, with increasing exposure time, **6** provides the expected increase in S/N while **5** does not. Detection of *Y. enterocolitica* cultured at 4 °C

provides the best S/N at 30 seconds, and shows promise for the rapid detection of foodborne pathogens at refrigerator temperatures (see below). *S. enterica* shows the greatest consistency between experiments with **5** and **6**; while the shorter linker correlated with higher S/N, both ligands supported similar increases in signal intensity over time. *A. baumannii* also shows a similar trend, although tests with **6** were performed using strains optimized for FOx acquisition. For *S. aureus*, preselection was critical for ultra-rapid capture by FOx conjugates, with **6** having better overall activity; interestingly however, MRSA produced the opposite trend.

3.6 Detection of *Y. enterocolitica* cultured at 4 °C

The horizontal submersion method clearly enhances the capabilities of our pathogen detection system. Previously, the model microorganism *Y. enterocolitica* had been cultured at 37 °C, a standard practice that ensures maximum growth rates and viability in iron-deficient conditions. However, the risk of virulent *Yersinia* in food is more germane at refrigeration temperatures, as competition from other non-psychrotrophic microorganisms is minimal.[3, 10] In addition, it has been shown that *Y. enterocolitica* can persist at low levels even after being sublethally damaged by heating. Cells lie dormant at room temperature or above, but can regain viability and proliferate to harmful levels at refrigerator temperatures.[9] We thus attempted to detect *Y. enterocolitica* cultured under low-temperature conditions.

Y. enterocolitica could be cultured successfully at 4 °C for 48 hours under modestly iron-challenged conditions, using a bipy concentration of 0.05 mM (OD_{600} 0.25, corresponding to 2.5×10^8 cfu/mL). These cultures were less dense than

Yersinia cultured at 37 °C (OD_{600} 0.5–0.9), but sufficient to meet our needs. Bacterial suspensions were concentrated to 10^9 cfu/mL (OD_{600} 1.0), then diluted to 10^7 cfu/mL and left standing at 23 °C prior to exposure using chips patterned with conjugate **6** and the horizontal submersion method, as described in Section 3.4. Gratifyingly, detection was achieved at all tested time points, down to 30 seconds (Figure 3.8 and Table 3.2). Most notably, the S/N ratio at the 30-second time point was higher than those obtained after 2- and 5-minute exposures.

3.7 Conclusions

Building on previous work, we were able to detect five strains of bacteria with different FOx receptors in the ultra-rapid domain, using microarrays of FOx conjugates. Synthesis and careful purification of **5** and **6** as well as transitioning to horizontal submersion method were crucial factors in reaching this milestone. From the data collected several conclusions can be drawn. First, while a chemical linker is known to be necessary for detection, linker length is not a critical factor. This is evidenced by the fact that all five strains were detected within 30 seconds independent of the conjugate used, although evidence suggests in the case of *S. enterica* that detection was enhanced across all time points using **5**. Conjugate **6**, on the other hand, provided better overall response of exposure time versus S/N and S/B data in all cases, other than the already mentioned case of *S. enterica*. This may imply the linker length in **6** is better optimized for screening against a wide variety of strains and associated FOx binding receptors.

Another key finding was that the level of expression and/or presentation of FOx receptors by various bacterial strains can be environmentally dependent, influencing sensitivity or speed of detection. *S. aureus* and MRSA (expressing FhuD2) and *A. baumannii* (expressing FhuE) could not be detected in less than 5 minutes if cultured under iron-deficient conditions. However, by optimizing FOx receptor presentation by the use of FOx-enriched media during growth, all three strains could be detected in 30 seconds. In contrast, FoxA-expressing strains such as *S. enterica* and *Y. enterocolitica* appear to have constitutively high levels of receptor expression, as both species could be detected in 30 seconds if cultured under iron-deficient conditions. Our detection system is thus especially sensitive toward these two bacteria, and has promise as a rapid screening technique for discriminating FOx binding species based on their receptors.

Lastly, *Y. enterocolitica* cultured at 4 °C can also be detected in 30 seconds using FOx microarrays, and at higher S/N levels relative to samples cultured at 37 °C. This has great practical significance, as *Y. enterocolitica* is known to thrive inside refrigerators (4 °C). Our system thus holds promise as a label-free sensor of pathogens lurking in refrigerated foods.

3.8 Materials and Methods

General Procedures. HPLC purification was performed using a Waters 600 controller and waters 2487 dual absorbance detector equipped with Phenomenex reverse phase column 250 x 21 mm. Water was obtained from Millipore Milli-Q Academic purification system equipped with 0.22 μm Millipak filter. Mass spectra were

obtained using a Waters MicromassZQ system. NMR spectra were collected using Varian Inova 300 instrument. UV-vis spectra were obtained using a Varian Cary 50 spectrometer. Infrared (IR) spectra were collected using a Thermo Nexus 670 spectrometer.

Materials. Starting materials were ordered from commercial suppliers and used as received. Deferoxamine (dFO) mesylate, 2,2'-(ethylenedioxy)bis(ethylamine), carbon disulfide, di-*tert*-butyl dicarbonate, and Tween 20 were purchased from Sigma-Aldrich. Epoxy-activated glass slides (Nexterion E) were obtained from Schott. Bovine serum albumin (BSA) was purchased from Jackson Immuno Research. Luria-Bertani broth (LB), nutrient broth (NB), and tryptic soy broth (TS) were obtained as dehydrated powders from Becton-Dickinson. 2,2'-Bipyridyl (bipy) was purchased from Fluka. Iron(III) chloride was obtained from Fisher Scientific. Phosphate buffered saline (1X PBS; Mg- and Ca-free) was purchased from Corning. *Yersinia enterocolitica* (ATCC 51871), *Staphylococcus aureus* (ATCC 10537), *Salmonella enterica* (35664), *Escherichia coli* Nissel (ATCC 25922), MRSA (ATCC BAA-1720), *Pseduomonas aeruginosa* (ATCC 47085), *Klebsiella pneumoniae* (27736) and *Acinetobacter baumannii* (ATCC 19606) were obtained from American Type Culture Collection (ATCC).

Synthesis. Lyophilized conjugate **3a** from freezer stock (5 mg) was dissolved in 100 μL of 0.1 M Na_2CO_3 buffer (pH 11) and allowed to sit at room temperature for 1–2 days. In situ hydrolysis of the ITC to a primary amine was monitored by ESI mass

spectrometry, using the intensity ratio of molecular ion (*m/z*) peaks generated by the ITC and amine. When the apparent ratio stopped increasing, the solution was diluted with deionized water to 1 mL, with a final pH of 10. Reverse-phase HPLC (25–90% acetonitrile in water) yielded the desired amine **5** in pure form (3.5 mg; 70% yield). HPLC chromatogram and mass spectra of **5** are shown in Figure 3.1; the UV-vis spectrum is shown below (Figure 3.16).

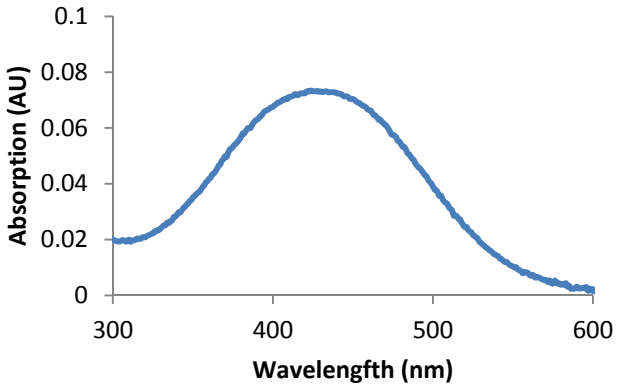

Figure 3.16: UV-vis spectrum of FOx conjugate **5** (in water).

Conjugate **6** was synthesized by dissolving ITC conjugate **3a** (5 mg, 1.0 equiv), 2,2'-(ethylenedioxy)bis(ethylamine) (3.3 µL, 1.1 equiv), and distilled triethylamine (15 µL, 10 equiv) in DMSO (800 µL). The solution was stirred at room temperature for 12 hours. Product formation and disappearance of **3a** was confirmed by ESI mass spectrometry. The reaction mixture was passed through a 0.2-µm membrane filter, then directly injected onto the reverse-phase HPLC system (Figure 3.2). Amine **6** exhibited a strong absorbance at 430 nm (Figure 3.17).

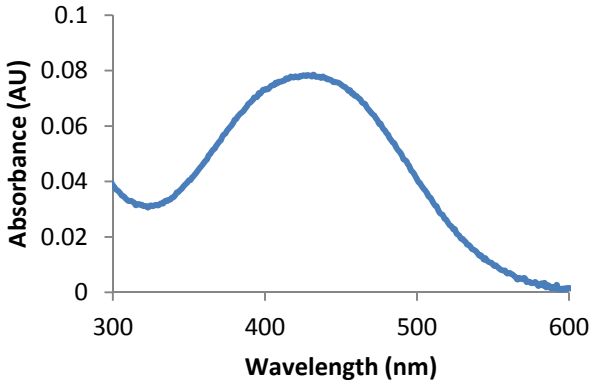

Figure 3.17: UV-vis spectrum of FOx conjugate **6** (in water)

.

Microbiological culture conditions (standard). All strains were grown by thawing crystals from previously frozen stocks (1 mL), diluting them in species-appropriate broth (final volume 10 mL), and incubating the mixture at 37 °C for 16 hours with orbital shaking at 220 rpm. Each strain was cultured in standard media for at least three generations; growth was monitored by using a Genesys 20 spectro-photometer to measure optical density at 600 nm (OD_{600}). When a late stage of the log growth phase was reached (OD_{600} ~1.0), a 0.1-mL aliquot was used to inoculate 10 mL of fresh media to initiate the next generation.

Growth in iron-deficient media (0.05–3 mM bipy) was performed only after 3 generations of normal media growth and suspensions were handled with acid-washed materials to reduce contamination by residual iron. When a high growth density (OD_{600} ~1.0) was achieved, planktonic bacteria cultures were pelleted by centrifugation and redispersed in Mg- and Ca-free PBS buffer followed by three cycles of centrifugation and redispersion in the same buffer. Tenfold serial dilutions in the same buffer were performed to yield suspensions at concentrations ranging from

10^7 to 10^2 cfu/mL. For competitive inhibition studies, 0.25 mM dFOx was added to planktonic bacteria at 10^7 cfu/mL for 5 or 20 minutes, prior to chip exposure.

Optimization of FOx receptor expression. *S. aureus*, MRSA and *A. baumannii* were first cultured under standard conditions as described above, for one generation. The second generation was cultured in the same broth containing 2,2'-bipyridyl (1 mM [bipy] for *S. aureus* and MRSA; 0.1 mM [bipy] for *A. baumannii*) and supplemental FOx (50 μM for *S. aureus* and MRSA; 20 μM for *A. baumannii*), both added prior to autoclaving. The addition of FOx caused the broth to appear bright pink/orange in contrast to its usual pale yellow or salmon color (with bipy added). Subsequent growth cultures were cycled two more times between standard and FOx-supplemented media, then grown again in normal media for a total of seven generations. These were used to inoculate growth cultures in iron-deficient media containing bipy without supplemental FOx for chip-based bacteria detection.

Optical imaging. Bacteria immobilized on periodic conjugate microarrays were imaged under darkfield conditions using an Olympus BX60 with a white light source. Post completion of chip preparation images were acquired as references for background intensities; negative control samples patterned with FOx conjugates but treated with PBS buffer alone were also included. Two-dimensional FFT was performed on all images; linescans of the reciprocal lattices in the k_x direction yield spectra enabling quantitative peak analysis of the principal harmonic ($k = 1/a$).

Microarray printing and blocking (chip preparation). Inkjet printing was performed on 1.25-cm^2 epoxysilane-activated glass substrates (Nexterion E) using a Fujifilm Diamatix Materials Printer (DMP 2800). FOx conjugates **5** or **6** (3 mg) were dissolved in 1 mL of 10 mM Na_2CO_3 buffer (pH 10) containing 0.005% Tween 20 (v/v), and filtered through 0.22-μm membrane filters (PTFE Acrodisc). These mixtures were loaded into compatible cartridges (10 pL drop size) by using a 1 mL disposable syringe and provided flat tipped needle. Square dot-matrix arrays were printed on glass chips using bitmap patterns loaded into the DMP software, with spot sizes and periodicities of approximately 15 and 40 μm, respectively; droplets were jetted using a customized waveform. Once printed, chips were moved immediately into chambers with 75% relative humidity and left at room temperature for at least 12 hours.

Chips were transferred to a petri dish and submerged in PBS containing 0.25% Tween 20, placed on a rotary shaker at 40 rpm for 15 minutes, followed by two rounds of submerged shaking in water before blocking chips with 0.1% BSA in PBS at room temperature for 1 hour. Chips were rinsed twice again in water, then dried on both sides with a gentle stream of nitrogen. The passivated chips could be stored in a desiccator under a dry, inert atmosphere for up to 30 days (quality control tests beyond this time window were not performed).

Handling of chips during detection experiments. For both drop-on-chip and horizontal submersion methods, chips were labeled on the printed face in one corner, which also served as the contact surface with forceps during transfers between petri

dishes and vials. In the horizontal submersion method, exposure times were established by rapidly decanting bacterial suspensions from vials; in the drop-on-chip method, exposure times were established by lifting or tilting chips at one end, forcing most of the bacterial suspension to run off into the petri dish. Chips were then gripped by one corner using forceps, and subjected to backside rinsing with patterned side facing down. This was repeated once more before the chip was dried with a stream of nitrogen and laid patterned side up in a clean petri dish.

3.9 References

1. Walderhaug, M., *Bad Bug Book; Foodborne Pathogenic Microorganisms and Natural Toxins*. 2nd Edition ed.; 2012.

2. Scallan, E.; Hoekstra, R. M.; Angulo, F. J.; Tauxe, R. V.; Widdowson, M.-A.; Roy, S. L.; Jones, J. L.; Griffin, P. M., Foodborne illness acquired in the United States--major pathogens. *Emerg Infect Dis.* **2011,** *17* (1), 7-15.

3. Palonen, E.; Lindström, M.; Korkeala, H., Adaptation of enteropathogenic *Yersinia* to low growth temperature. *Crit Rev Microbiol.* **2010,** *36* (1), 54-67.

4. Ye, Y. W.; Ling, N.; Han, Y. J.; Wu, Q. P., Detection and prevalence of pathogenic *Yersinia enterocolitica* in refrigerated and frozen dairy products by duplex PCR and dot hybridization targeting the virF and ail genes. *J Dairy Sci.* **2014,** *97* (11), 6785-6791.

5. el-Sherbini, M.; al-Agili, S.; el-Jali, H.; Aboshkiwa, M.; Koha, M., Isolation of *Yersinia enterocolitica* from cases of acute appendicitis and ice-cream. *East Mediterr Health J* **1999,** *5* (1), 130-5.

6. Ackers, M.-L.; Schoenfeld, S.; Markman, J.; Smith, M. G.; Nicholson, M. A.; DeWitt, W.; Cameron, D. N.; Griffin, P. M.; Slutsker, L., An Outbreak of *Yersinia enterocolitica* 0:8 Infections Associated with Pasteurized Milk. *J Infect Dis.* **2000,** *181* (5), 1834-1837.

7. Bresolin, G.; Neuhaus, K.; Scherer, S.; Fuchs, T. M., Transcriptional Analysis of Long-Term Adaptation of *Yersinia enterocolitica* to Low-Temperature Growth. *J Bacteriol.* **2006,** *188* (8), 2945-2958.

8. Kapperud, G., *Yersinia enterocolitica* in food hygiene. *Int J Food Microbiol.* **1991,** *12* (1), 53-65.

9. Zadernowska, A.; Chajęcka-Wierzchowska, W.; Łaniewska-Trokenheim, Ł., *Yersinia enterocolitica*: A Dangerous, But Often Ignored, Foodborne Pathogen. *Food Rev Int.* **2014,** *30* (1), 53-70.

10. Bottone, E. J., *Yersinia enterocolitica*: overview and epidemiologic correlates. *Microbes Infect.* **1999,** *1* (4), 323-333.

11. Bottone, E. J., *Yersinia enterocolitica*: the charisma continues. *Clin Microbiol Rev.* **1997,** *10* (2), 257-76.

12. Doshi, R. K.; Patel, G.; Mackay, R.; Wallach, F., Healthcare-associated Infections: epidemiology, prevention, and therapy. *Mt Sinai J Med.* **2009,** *76* (1), 84-94.

13. Eili, K.; David, L. S.; Ramanan, L., Hospitalizations and Deaths Caused by Methicillin-Resistant *Staphylococcus aureus*, United States, 1999–2005. *Emerg Infect Dis.* **2007,** *13* (12), 1840.

14. Khan, H. A.; Ahmad, A.; Mehboob, R., Nosocomial infections and their control strategies. *Asian Pac J Trop Biomed.* **2015,** *5* (7), 509-514.

15. Boucher, H. W.; Talbot, G. H.; Bradley, J. S.; Edwards, J. E.; Gilbert, D.; Rice, L. B.; Scheld, M.; Spellberg, B.; Bartlett, J., Bad Bugs, No Drugs: No ESKAPE! An Update from the Infectious Diseases Society of America. *Clin Infect Dis.* **2009,** *48* (1), 1-12.

16. Pendleton, J. N.; Gorman, S. P.; Gilmore, B. F., Clinical relevance of the ESKAPE pathogens. *Expert Rev Anti Infect Ther.* **2013,** *11* (3), 297-308.

17. Barenfanger, J.; Drake, C.; Kacich, G., Clinical and Financial Benefits of Rapid Bacterial Identification and Antimicrobial Susceptibility Testing. *J Clin Microbiol.* **1999,** *37* (5), 1415-1418.

18. Harbarth, S.; Garbino, J.; Pugin, J.; Romand, J. A.; Lew, D.; Pittet, D., Inappropriate initial antimicrobial therapy and its effect on survival in a clinical trial of immunomodulating therapy for severe sepsis. *Am J Med.* **2003,** *115* (7), 529-535.

19. Shorr, A. F.; Micek, S. T.; Welch, E. C.; Doherty, J. A.; Reichley, R. M.; Kollef, M. H., Inappropriate antibiotic therapy in Gram-negative sepsis increases hospital length of stay. *Crit Care Med* **2011,** *39* (1), 46-51.

20. Kumar, A.; Ellis, P.; Arabi, Y.; Roberts, D.; Light, B.; Parrillo, J. E.; Dodek, P.; Wood, G.; Kumar, A.; Simon, D., et al., Initiation of Inappropriate Antimicrobial Therapy Results in a Fivefold Reduction of Survival in Human Septic Shock. *Chest* **2009,** *136* (5), 1237-1248.

21. Shlaes, D. M., *Antibiotics: The Perfect Storm*. Springer Netherlands: 2010.

22. Umesha, S.; Manukumar, H. M., Advanced Molecular Diagnostic Techniques for Detection of Food-borne Pathogens; Current Applications and Future Challenges. *Crit Rev Food Sci Nutr.* **2016**, 00-00.

23. Law, J. W.-F.; Ab Mutalib, N.-S.; Chan, K.-G.; Lee, L.-H., Rapid methods for the detection of foodborne bacterial pathogens: principles, applications, advantages and limitations. *Front Microbiol.* **2014,** *5*, 770.

24. Chen, J.; Park, B., Recent Advancements in Nanobioassays and Nanobiosensors for Foodborne Pathogenic Bacteria Detection. *J Food Prot.* **2016,** *79* (6), 1055-69.

25. Deshmukh, R. A.; Joshi, K.; Bhand, S.; Roy, U., Recent developments in detection and enumeration of waterborne bacteria: a retrospective minireview. *Microbiologyopen* **2016**.

26. *Antimicrobial Resistance: Global Report on Surveillance*. World Health Organization. 2014; p 257.

27. *National Action Plan for Combating Antibiotic-Resistant Bacteria*. The White House. 2015; p 63.

28. *At United Nations Global Leaders Commit to Act on Antimicrobial Resistance.* World Health Organization. 2016.

29. Adak, A. K.; Leonov, A. P.; Ding, N.; Thundimadathil, J.; Kularatne, S.; Low, P. S.; Wei, A., Bishydrazide Glycoconjugates for Lectin Recognition and Capture of Bacterial Pathogens. *Bioconjugate Chem.* **2010,** *21* (11), 2065-2075.

30. Adak, A. K.; Boley, J. W.; Lyvers, D. P.; Chiu, G. T.; Low, P. S.; Reifenberger, R.; Wei, A., Label-Free Detection of *Staphylococcus aureus* Captured on Immutable Ligand Arrays. *ACS Appl Mater Interfaces* **2013,** *5* (13), 6404-6411.

31. Maltais, T. R.; Adak, A. K.; Younis, W.; Seleem, M. N.; Wei, A., Label-Free Detection and Discrimination of Bacterial Pathogens Based on Hemin Recognition. *Bioconjugate Chem.* **2016,** *27* (7), 1713-1722.

32. Kim, Y.; Lyvers, D. P.; Wei, A.; Reifenberger, R. G.; Low, P. S., Label-free detection of a bacterial pathogen using an immobilized siderophore, deferoxamine. *Lab Chip* **2012,** *12* (5), 971-976.

33. Báumler, A. J.; Hantke, K., Ferrioxamine uptake in *Yersinia enterocolitica*: characterization of the receptor protein FoxA. *Mol Microbiol.* **1992,** *6* (10), 1309-1321.

34. Deiss, K.; Hantke, K.; Winkelmann, G., Molecular recognition of siderophores: A study with cloned ferrioxamine receptors (FoxA) from *Erwinia herbicola* and *Yersinia enterocolitica*. *Biometals* **1998,** *11* (2), 131-137.

35. Funahashi, T.; Tanabe, T.; Mihara, K.; Miyamoto, K.; Tsujibo, H.; Yamamoto, S., Identification and Characterization of an Outer Membrane Receptor Gene in *Acinetobacter baumannii* Required for Utilization of Desferricoprogen, Rhodotorulic Acid, and Desferrioxamine B as Xenosiderophores. *Biol Pharm Bull.* **2012,** *35* (5), 753-760.

36. Kingsley, R. A.; Reissbrodt, R.; Rabsch, W.; Ketley, J. M.; Tsolis, R. M.; Everest, P.; Dougan, G.; Bäumler, A. J.; Roberts, M.; Williams, P. H., Ferrioxamine-Mediated Iron(III) Utilization by *Salmonella enterica*. *Appl Environ Microbiol.* **1999,** *65* (4), 1610-1618.

37. Sebulsky, M. T.; Speziali, C. D.; Shilton, B. H.; Edgell, D. R.; Heinrichs, D. E., FhuD1, a Ferric Hydroxamate-binding Lipoprotein in *Staphylococcus aureus*: A case of gene duplication and lateral transfer *J. Biol. Chem.* **2004,** *279* (51), 53152-53159.

38. Arifin, A. J.; Hannauer, M.; Welch, I.; Heinrichs, D. E., Deferoxamine mesylate enhances virulence of community-associated methicillin resistant *Staphylococcus aureus*. *Microbes Infect.* **2014,** *16* (11), 967-972.

39. Podkowa, K. J.; Briere, L.-A. K.; Heinrichs, D. E.; Shilton, B. H., Crystal and Solution Structure Analysis of FhuD2 from *Staphylococcus aureus* in Multiple Unliganded Conformations and Bound to Ferrioxamine-B. *Biochemistry* **2014,** *53* (12), 2017-2031.

40. Soyer, M.; Duménil, G., Introducing Shear Stress in the Study of Bacterial Adhesion. *J Vis Exp.* **2011,** (55), 3241.

41. Zagorodko, O.; Bouckaert, J.; Dumych, T.; Bilyy, R.; Larroulet, I.; Serrano, A.; Dorta, D.; Gouin, S.; Dima, S.-O.; Oancea, F., et al., Surface Plasmon Resonance (SPR) for the Evaluation of Shear-Force-Dependent Bacterial Adhesion. *Biosensors* **2015,** *5* (2), 276.

42. Viegas, K. D.; Dol, S. S.; Salek, M. M.; Shepherd, R. D.; Martinuzzi, R. M.; Rinker, K. D., Methicillin resistant *Staphylococcus aureus* adhesion to human umbilical vein endothelial cells demonstrates wall shear stress dependent behaviour. *Biomed Eng OnLine* **2011,** *10* (1), 1-18.

43. Mohamed, N.; Rainier, T. R.; Ross, J. M., Novel experimental study of receptor-mediated bacterial adhesion under the influence of fluid shear. *Biotechnol Bioeng.* **2000,** *68* (6), 628-636.

44. Reddy, K.; Ross, J. M., Shear Stress Prevents Fibronectin Binding Protein-Mediated *Staphylococcus aureus* Adhesion to Resting Endothelial Cells. *Infect Immun.* **2001,** *69* (5), 3472-3475.

VITA

VITA

Nigam was born on August 18th, 1990 in Indianapolis, Indiana. He graduated from Hamilton Southeastern High School in 2008. He attended Indiana University Purdue University Indianapolis (IUPUI) from 2008 – 2011 where he obtained a B.S. in Interdisciplinary Science with honors. In Fall of 2011 he entered the Purdue Interdisciplinary Life Sciences (PULSe) Ph.D. program at Purdue University. In May of 2012 he joined Professor Alex Wei's research group. His work in Dr. Wei's laboratory focused mainly on design and optimization of biosensors for rapid detection of pathogenic bacteria. He defended his Ph.D. work in November 2016.

PUBLICATION

Preprint

How to Capture Ferrioxamine-Binding Bacteria in 30 Seconds or Less

Nigam B. Arora, John H. Sides, and Alexander Wei*

Department of Chemistry, Purdue University, 560 Oval Drive, West Lafayette, IN 47907, USA

Supporting Information Placeholder

ABSTRACT: Methods for live pathogen analysis often seek to reduce the limits of detection as a function of time or concentration. In either case, the method of sampling can be vital for establishing practical limits, particularly if a virulence mechanism is involved. Here we show that detection methods based on bacterial receptor–ligand recognition are highly dependent on the method of exposure, using ferrioxamine (FOx) microarrays as the substrate and a label-free imaging method for quantitative analysis. When extrinsic factors are accounted for, pathogen adhesion to patterned substrates can take place in 30 seconds, the practical lower limit of this study.

Keywords: Bacteria, optical biosensors, pathogens, siderophores, ferrioxamine, detection

INTRODUCTION

Time is a critical factor in the detection of actively virulent pathogens like *S. enterica,* the single largest cause of bacterial foodborne illness in the United States;[1-2] *Y. enterocolitica,* which thrives at refrigerator temperatures;[3-11] and drug resistant ESKAPE bacteria such as *A. baumannii* and *S. aureus.*[12] Early detection affords the opportunity to respond to these threats in a timely and targeted fashion,[13-14] reducing the overreliance on blanket remedies such as broad-spectrum antibiotics, which only serve to exacerbate the issues of poor patient outcomes[15-16] and the creation of multidrug-resistant strains.[17] However, standard methods of detection using bacterial culture are plagued by slow turnaround time. Other methods using polymerase chain reaction or antibody based detection also have pitfalls including potential contamination and vulnerability to nonfunctional mutations respectively. The use of siderophores such as FOx provides a valuable entry point for the development of new rapid pathogen detection methods.[18-20]

Siderophores are a class of small molecules that bacteria utilize for acquisition of iron, an element critical to numerous cellular and subcellular processes.[21-24] Siderophores are generally low molecular-weight species (mw 400–1000), chelate ferric ions (Fe^{3+}) via hexadentate coordination with formation constants ranging from 10^{12}–10^{52}, and are highly soluble in water.[25-27] Bacteria often secrete siderophores in response to environmentally low levels of iron.[28] Upon chelation of iron, siderophores are recovered by parent bacteria via cognate receptors presented on their outer membranes.[29] Deferoxamine B (commercially available as deferrioxamine mesylate), the cognate siderophore of *Streptomyces pilosus*,[30] offers perhaps the best combination of biological activity and accessibility. It also has a free primary amine for ready modification, using standard bioconjugate chemistry methods, and the molecule itself is stable in a variety of chemical environments.

Ferrioxamine, the iron chelated form of Deferoxamine B (dFOx), offers much promise as a low-molecular weight ligand for pathogen detection. As with all siderophores, chelation with iron is achieved readily by simple exposure to solutions containing Fe^{3+} ions. Several receptors for FOx have been identified and some well-studied such as (i) FoxA, which is used by *Yersinia enterocolitica*[31-32] and also by *Salmonella enterica*;[33] (ii) FhuE, which is expressed by *A. baumannii*[34] and several strains of *Escherichia coli*; and (iii) FhuD1/2, whose isoforms are found primarily in *Staphylococcus aureus* but also in certain bacilli.[35-36] These receptors as well as FOx itself contribute directly to the pathogenicity of the parent bacteria and are considered to be virulence factors.[31, 34, 37-42] For this reason, as long as these bacteria remain pathogenic they must also bind FOx making it an immutable ligand for detection.

The idea of exploiting bacteria's affinity for siderophores has been around for some time.[43,44] We and others have used siderophores as ligands for detecting pathogenic bacteria.[19, 45-47] The use of immutable ligands for detecting pathogenic bacteria offers several fundamental benefits, not the least being their low vulnerability to nonfunctional mutations. In previous studies, time points for detection were held constant at 30 or 60 minutes in some cases.[46] In this study, we systematically studied bacterial detection as a function of exposure time to determine the time to detection (TTD) for each strain. In particular, we considered the rates of binding between FOx and specific bacterial receptors, to better understand the molecular aspects of siderophore-mediated bacterial adhesion in our detection platform. We found that detection can be easily achieved within 30 seconds and that the method of sample preparation is crucial for enabling this ultra-rapid detection.

EXPERIMENTAL SECTION

Bacteria were cultured (37 °C, 220 rpm shaking) from previously frozen (–80 °C) stocks; subsequent generations were inoculated as 1% (v/v) solutions (10 mL) using active strains. *Y. enterocolitica*, was the singular exception as it was found this strain could also be cultured at 4 °C for 48 hours under modestly iron-challenged conditions. These cultures were less dense than *Yersinia* cultured at 37 °C (OD_{600} 0.5–0.9), but sufficient to meet our needs. For *S. aureus*, MRSA and *A. baumannii* strains had been previously subjected to a selective culturing technique for expression of FOx receptors (FOx selected). Strains were grown out for a minimum of three generations prior to inoculation in iron restricted media treated with 2,2'-bipyridyl (bipy). Strains were cultured individually in broth with variable bipy concentrations ranging from 0.05–3 mM, to determine the highest restriction of iron while still permitting steady growth (Table SI). This was done to achieve maximal expression of FOx-binding receptors. Cultures were monitored for changes in optical density at 600 nm (OD_{600}). At the end of their log growth phase, bacteria were centrifuged to pellets and thrice rinsed and resuspended with phosphate buffered saline (PBS). Finally, bacterial suspensions were diluted with PBS to desired concentration and exposed to chips for pathogen detection experiments.

Patterning of periodic arrays onto activated glass slides (Nexterion H) for production of chips used in detection experiments was performed using a standardized method. FOx conjugates (synthesis described in SI) were dissolved at 3 mg/mL in 10 mM Na_2CO_3 buffer containing 0.005% Tween-20 (v/v) to formulate inks. Inks were loaded into cartridges (10 pL nozzles) for piezoelectric deposition using a Dimatix materials printer (DMP-2800). Droplets were deposited onto 1.25-cm^2 activated substrates and incubated overnight in a 75% relative humidity chamber to allow complete bonding of the printed conjugate to the epoxy-coated substrate. After curing, substrates are washed and blocked against nonspecific binding using bovine serum albumin (0.1% w/v). Chips were used immediately or stored under argon for later use.

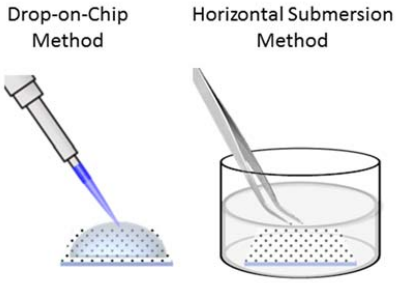

Figure 1. Methods for exposure of chips to bacterial suspension during time to detection experiments

Chip exposure to bacteria was performed using one of two described methods (Figure 1). In drop-on-chip method (DoCM) bacterial suspension (0.2 – 0.4 mL) was pipetted directly onto the patterned face of the chip. In horizontal submersion method (HSM) bacterial suspension was placed into a 3-dram vial with a final volume of 3–4 mL and left standing without further disturbance for a minimum of 20 minutes, prior to the pathogen detection experiment. Chips were then gripped by forceps on a predesignated corner and lowered vertically into the vial, edge-first, with minimum mechanical disturbance. The submerged chip was then released and allowed to rest horizontally on the vial floor with patterned side facing up. For both methods, following exposure, chips were rinsed with water and dried under a stream of nitrogen.

Bacterial adhesion onto patterned chips could be imaged in a label-free manner using optical darkfield microscopy, based on the light scattering from the bacteria themselves.[19] Chips without exposure to bacteria should appear essentially blank when viewed under darkfield conditions, whereas those exposed to bacteria expressing FOx receptors should support a periodic pattern commensurate with concentration. Darkfield images can be analyzed by fast Fourier Transform (FFT) to convert periodic signals into reciprocal lattice peaks allowing signals to be compared quantitatively against noise or local background intensities. A 2D-FFT algorithm was applied using WSxM software,[48] followed by a linescan along the *x*-direction to produce a one-dimensional Fourier spectrum. Background (B) intensities were estimated after applying a logarithmic weighting function to suppress low-frequency ($1/f$) noise. Signal (S) to noise (N) ratios were calculated using equation $S/N = (S-B) / \sigma_B$.

RESULTS AND DISCUSSION

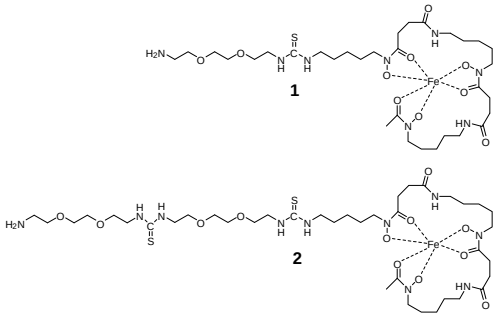

Figure 2. FOx conjugates used in detection studies

Chips patterned with FOx conjugate **1** (Figure 2) performed well in detection studies. Chips patterned were shown to be capable of detecting *Y. enterocolitica* at a concentration of 10^2 cfu/mL given one hour TTD using drop on chip method (Figure S2 and S3). Propidium iodide staining of these chips confirmed the presence of bacterial cells bound to the printed periodic array (Figure S4). Negative control studies successfully showed lack of binding due to competitive inhibition of FOx binding receptors, lack of binding with a bacterium not expressing FOx receptors (*E. coli* Nissel 1917) and lack of binding when treated with only buffer used in suspending bacteria during exposure. These results support the hypothesis that sensitive detection of pathogenic bacteria expressing FOx receptors is a receptor mediated event. Further control studies showed lack of binding when FOx alone (not conjugated to a linker) was used to pattern chips. This indicates that not only is binding receptor mediated but presentation of the ligand is important. Conjugate **2** (Figure 2) was synthesized to determine if linker length would impact detection.

As TTD is a critical factor in positive patient outcomes experiments were performed to determine if detection was possible with 15 or even 5 minute exposure times for five FOx binding pathogens (*Y. enterocolitica*, *S. enterica*, *A. baumannii*, *S. aureus* and MRSA), with both **1** (Figure 3) and **2** (Figure 4) patterned chips, using DoCM. As achieving the fastest possible TTD was the primary goal bacterial concentrations of 10^7 cfu/mL was used for these experiments.

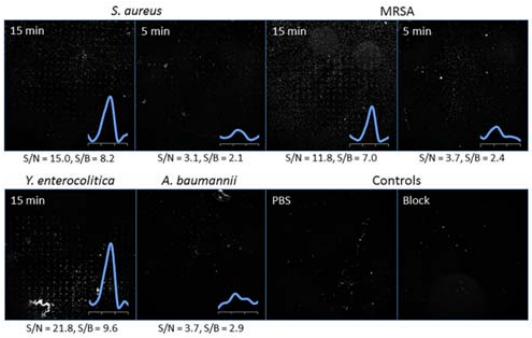

Figure 3. Representative raw images and FFT analysis (where appropriate) from experiments using DoCM with chips patterned with **1**. Appropriate controls appear essentially blank

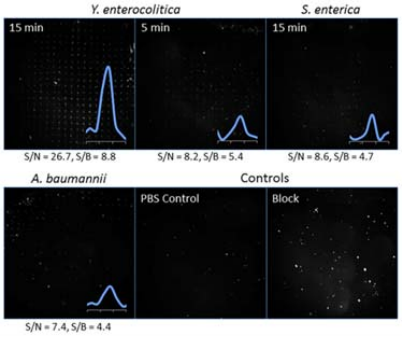

Figure 4. Representative raw images and FFT analysis (where appropriate) from experiments using DoCM with chips patterned with **2**. Appropriate controls appear essentially blank.

Use of the DoCM provided good results during limit of detection studies when all data points were collected at 30 minutes (data not shown), but was less than optimal when data points were collected at 15 minutes or less (Figures 3 and Figure 4). This suggests that planktonic bacteria needed 15–30 minutes to resume their fully active state following pipet transfer. We postulated that the motion associated with pipetting bacterial suspensions onto chips was enough to activate a self-protective response in planktonic cells that suppresses surface adhesion, as shear forces are known to do.[49-50] These types of disturbances should be avoided to keep bacteria primed for adhesion.[51-53] HSM (Figure 1) was designed specifically for this purpose.

Experiments using HSM were performed with exposure times of 15, 5, 2 minutes and 30 seconds to further probe TTD for all five bacterial strains. Chips treated with PBS as well as a competitive inhibition during 30 second exposure (suspensions treated with dFOx 5 minutes prior to testing) were included for each strain as negative controls. For a given pair of conjugate and bacterial strain, chips were employed at each time point and imaged by darkfield optical microscopy at three different regions of interest (ROI). Each image was independently processed by FFT

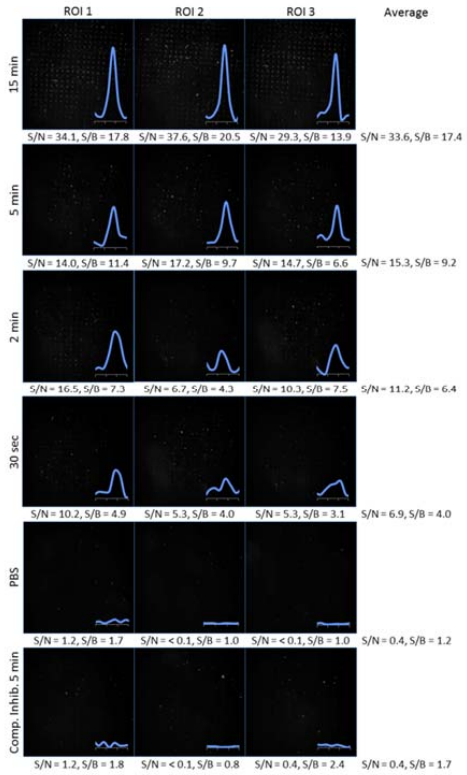

Figure 5. Detection of *Y. enterocolitica* using chips patterned with conjugate **2**, using the HSM. Raw images of three ROIs and their associated FFT signals are depicted for each time point, using S/N and S/B values as quantitative metrics; averages are shown at far right.

analysis to determine both S/N and S/B. These values were then averaged to give a value representative of the entire chip as minor variability was known to exist. Figure 5 shows an example of this process for detection of *Y. enterocolitica* using chips patterned with **2**. The same process was repeated for each strain and conjugate combination. Figure 6 and Figure 7 show a summary of all results.

Overall these experiments proved to be successful as detection (S/N > 3) was achieved in nearly every condition tested. Furthermore, control experiments involving competitive inhibition with excess free ligand confirmed the specificity of bacterial adhesion to be mediated by FOx–receptor interactions. For these experiments, separate bacterial suspensions were first treated with 250 μM dFOx, 5 or 20 minutes prior to chip exposure, with the hypothesis that excess dFOx would saturate bacterial receptors and reduce binding to tethered conjugates. In all cases except one, chips exposed to

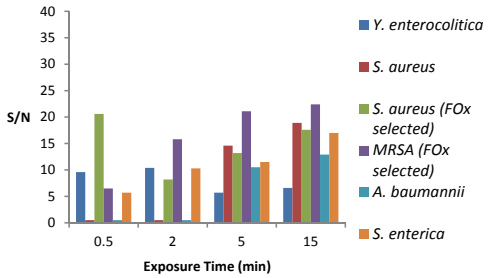

Figure 6. S/N ratios as a function of exposure time, using chips patterned with **1** subjected to the horizontal submersion method.

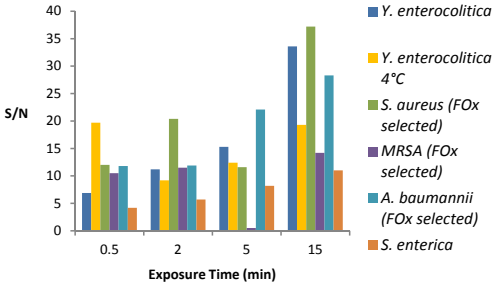

Figure 7. S/N ratios as a function of exposure time, using chips patterned with **2** subjected to the horizontal submersion method.

dFOx-treated bacteria did not demonstrate detection within 30 seconds. In the singular case of *A. baumannii*, pre-incubation with dFOx for 5 minutes was not sufficient to suppress pathogen adhesion, however inhibition was achieved with 20 minutes of pre-incubation.

Previously, the model microorganism *Y. enterocolitica* had been cultured at 37 °C, a standard practice that ensures maximum growth rates and viability in iron-deficient conditions. However, the risk of virulent *Yersinia* in food is more germane at refrigeration temperatures, as competition from other non-psychrotrophic microorganisms is minimal.[3, 10] In addition, it has been shown that *Y. enterocolitica* can persist at low levels even after being sublethally damaged by heating. Cells lie dormant at room temperature or above, but can regain viability and proliferate to harmful levels at refrigerator temperatures.[9] We thus attempted to detect *Y. enterocolitica* cultured under low-temperature conditions.

In the cases of *S. aureus* and MRSA, we applied an additional culturing technique prior to performing TTD experiments. These strains were selected over several generations utilizing FOx as a source of iron. This was achieved by cycling growth media between stock TS broth and TS broth dosed with both bipy (1 mM) and FOx (50 µM) several times. FOx-selected cultures were then cultured in a standard iron-deficient media (TS with 1 mM bipy) for use in TTD experiments. This method of selection was also employed for *A. baumannii*, but only for the TTD experiment performed using **2**. Detection of *S. aureus*, MRSA and *A. baumannii* within 15 minutes is still possible without FOx selection pressure. However, we have found that selective feeding is important to lower the TTD, to ensure that receptors of interest were being expressed. In contrast, neither *Y. enterocolitica* (37 °C or 4 °C) nor *S. enterica* were subject to any type of selection; both were grown in standard LB broth prior to inoculation of iron-deficient media, prior to TTD experiments.

At least two observations are worthy of further discussion. First, *Yersinia enterocolitica* and *Salmonella enterica* can be detected within 30 seconds when cultured under iron-deficient conditions, but without preselection using FOx as a source of iron, unlike the other three strains. This may be attributed to high levels of constitutive expression of FoxA by *Yersinia* and *Salmonella*, a faster rate of binding for FoxA relative to other FOx receptors, or both. Second, studies with *Yersinia* produced stronger detection signals at 30 seconds when cultured at 4 °C with 0.05 mM bipy, rather than at 37 °C with 3 mM bipy, although the converse was true for signals generated at 5 or 15 minutes. This suggests how differences in culture conditions might influence the expression level or presentation of FoxA by *Yersinia* or other bacteria.

CONCLUSION

With all parameters optimized, accounting for extrinsic factors, patterned chips were able to detect five pathogenic bacterial strains within 30 seconds of exposure to bacteria. This was achieved by targeting FOx receptors with conjugates designed to present ligand FOx in an optimal fashion. A critical factor in detection of pathogenic bacteria, TTD, was improved significantly by using HSM rather than DoCM indicating exposure method directly impacts rate of binding. Finally detection of *Y. enterocolitica* cultured at 4°C was successful at all tested time points showing promise for detection of pathogens lurking at refrigerator temperatures.

ASSOCIATED CONTENT

Supporting Information

The Supporting Information is available free of charge on the Publications website:

AUTHOR INFORMATION

Corresponding Author

E-mail: alexwei@purdue.edu

Notes

The authors declare no competing financial interests.

ACKNOWLEDGMENT

The authors gratefully acknowledge financial support from the National Science Foundation (CMMI-1449358) and a fellowship from the Indiana Manufacturing Consortium (N.B.A.). We also thank professors Phil Low and Ron Reifenberger for helpful discussions over the years.

REFERENCES

1. Walderhaug, M., *Bad Bug Book; Foodborne Pathogenic Microorganisms and Natural Toxins*. 2nd Edition ed.; 2012.
2. Scallan, E.; Hoekstra, R. M.; Angulo, F. J.; Tauxe, R. V.; Widdowson, M.-A.; Roy, S. L.; Jones, J. L.; Griffin, P. M., Foodborne illness acquired in the United States--major pathogens. *Emerg Infect Dis.* **2011,** *17* (1), 7-15.

3. Palonen, E.; Lindström, M.; Korkeala, H., Adaptation of enteropathogenic *Yersinia* to low growth temperature. *Crit Rev Microbiol.* **2010,** *36* (1), 54-67.
4. Ye, Y. W.; Ling, N.; Han, Y. J.; Wu, Q. P., Detection and prevalence of pathogenic *Yersinia enterocolitica* in refrigerated and frozen dairy products by duplex PCR and dot hybridization targeting the virF and ail genes. *J Dairy Sci.* **2014,** *97* (11), 6785-6791.
5. el-Sherbini, M.; al-Agili, S.; el-Jali, H.; Aboshkiwa, M.; Koha, M., Isolation of *Yersinia enterocolitica* from cases of acute appendicitis and ice-cream. *East Mediterr Health J* **1999,** *5* (1), 130-5.
6. Ackers, M.-L.; Schoenfeld, S.; Markman, J.; Smith, M. G.; Nicholson, M. A.; DeWitt, W.; Cameron, D. N.; Griffin, P. M.; Slutsker, L., An Outbreak of *Yersinia enterocolitica* 0:8 Infections Associated with Pasteurized Milk. *J Infect Dis.* **2000,** *181* (5), 1834-1837.
7. Bresolin, G.; Neuhaus, K.; Scherer, S.; Fuchs, T. M., Transcriptional Analysis of Long-Term Adaptation of *Yersinia enterocolitica* to Low-Temperature Growth. *J Bacteriol.* **2006,** *188* (8), 2945-2958.
8. Kapperud, G., *Yersinia enterocolitica* in food hygiene. *Int J Food Microbiol.* **1991,** *12* (1), 53-65.
9. Zadernowska, A.; Chajęcka-Wierzchowska, W.; Łaniewska-Trokenheim, Ł., *Yersinia enterocolitica*: A Dangerous, But Often Ignored, Foodborne Pathogen. *Food Rev Int.* **2014,** *30* (1), 53-70.
10. Bottone, E. J., *Yersinia enterocolitica*: overview and epidemiologic correlates. *Microbes Infect.* **1999,** *1* (4), 323-333.
11. Bottone, E. J., *Yersinia enterocolitica*: the charisma continues. *Clin Microbiol Rev.* **1997,** *10* (2), 257-76.
12. Pendleton, J. N.; Gorman, S. P.; Gilmore, B. F., Clinical relevance of the ESKAPE pathogens. *Expert Rev Anti Infect Ther.* **2013,** *11* (3), 297-308.
13. Barenfanger, J.; Drake, C.; Kacich, G., Clinical and Financial Benefits of Rapid Bacterial Identification and Antimicrobial Susceptibility Testing. *J Clin Microbiol.* **1999,** *37* (5), 1415-1418.
14. Harbarth, S.; Garbino, J.; Pugin, J.; Romand, J. A.; Lew, D.; Pittet, D., Inappropriate initial antimicrobial therapy and its effect on survival in a clinical trial of immunomodulating therapy for severe sepsis. *Am J Med.* **2003,** *115* (7), 529-535.
15. Shorr, A. F.; Micek, S. T.; Welch, E. C.; Doherty, J. A.; Reichley, R. M.; Kollef, M. H., Inappropriate antibiotic therapy in Gram-negative sepsis increases hospital length of stay. *Crit Care Med* **2011,** *39* (1), 46-51.
16. Kumar, A.; Ellis, P.; Arabi, Y.; Roberts, D.; Light, B.; Parrillo, J. E.; Dodek, P.; Wood, G.; Kumar, A.; Simon, D., et al., Initiation of Inappropriate Antimicrobial Therapy Results in a Fivefold Reduction of Survival in Human Septic Shock. *Chest* **2009,** *136* (5), 1237-1248.
17. Shlaes, D. M., *Antibiotics: The Perfect Storm*. Springer Netherlands: 2010.
18. Adak, A. K.; Leonov, A. P.; Ding, N.; Thundimadathil, J.; Kularatne, S.; Low, P. S.; Wei, A., Bishydrazide Glycoconjugates for Lectin Recognition and Capture of Bacterial Pathogens. *Bioconjugate Chem.* **2010,** *21* (11), 2065-2075.
19. Adak, A. K.; Boley, J. W.; Lyvers, D. P.; Chiu, G. T.; Low, P. S.; Reifenberger, R.; Wei, A., Label-Free Detection of Staphylococcus aureus Captured on Immutable Ligand Arrays. *ACS Appl Mater Interfaces* **2013,** *5* (13), 6404-6411.
20. Maltais, T. R.; Adak, A. K.; Younis, W.; Seleem, M. N.; Wei, A., Label-Free Detection and Discrimination of Bacterial Pathogens Based on Hemin Recognition. *Bioconjugate Chem.* **2016,** *27* (7), 1713-1722.
21. Messenger, A. J. M.; Barclay, R., Bacteria, iron and pathogenicity. *Biochem Educ.* **1983,** *11* (2), 54-63.
22. Andrews, S. C.; Robinson, A. K.; Rodríguez-Quiñones, F., Bacterial iron homeostasis. *FEMS Microbiol Rev.* **2003,** *27* (2-3), 215-237.
23. Dlouhy, A. C.; Outten, C. E., The Iron Metallome in Eukaryotic Organisms. *Met Ions Life Sci.* **2013,** *12*, 241-278.
24. Frawley, E. R.; Fang, F. C., The Ins and Outs of Bacterial Iron Metabolism. *Mol Microbiol.* **2014,** *93* (4), 609-616.
25. Neilands, J. B., Microbial Envelope Proteins Related to Iron. *Annu Rev Microbiol.* **1982,** *36* (1), 285-309.
26. Crosa, J. H.; Walsh, C. T., Genetics and Assembly Line Enzymology of Siderophore Biosynthesis in Bacteria. *Microbiol Mol Biol Rev.* **2002,** *66* (2), 223-249.
27. Oves-Costales, D.; Kadi, N.; Challis, G. L., The long-overlooked enzymology of a nonribosomal peptide synthetase-independent pathway for virulence-conferring siderophore biosynthesis. *Chem. Commun.* **2009,** (43), 6530-6541.
28. Ratledeg, C.; Dover, L. G., Iron Metabolism in Pathogenic Bacteria. *Annu Rev Microbiol.* **2000,** *54*, 881.
29. Stintzi, A.; Barnes, C.; Xu, J.; Raymond, K. N., Microbial Iron Transport via a Siderophore Shuttle: A Membrane Ion Transport Paradigm. *Proc Natl Acad Sci USA* **2000,** *97* (20), 10691-10696.
30. Müller, G.; Raymond, K. N., Specificity and mechanism of ferrioxamine-mediated iron transport in *Streptomyces pilosus*. *J Bacteriol.* **1984,** *160* (1), 304-312.
31. Báumler, A. J.; Hantke, K., Ferrioxamine uptake in *Yersinia enterocolitica*: characterization of the receptor protein FoxA. *Mol Microbiol.* **1992,** *6* (10), 1309-1321.
32. Deiss, K.; Hantke, K.; Winkelmann, G., Molecular recognition of siderophores: A study with cloned ferrioxamine receptors (FoxA) from *Erwinia herbicola* and *Yersinia enterocolitica*. *Biometals* **1998,** *11* (2), 131-137.
33. Kingsley, R. A.; Reissbrodt, R.; Rabsch, W.; Ketley, J. M.; Tsolis, R. M.; Everest, P.; Dougan, G.; Bäumler, A. J.; Roberts, M.; Williams, P. H., Ferrioxamine-Mediated Iron(III) Utilization by *Salmonella enterica*. *Appl Environ Microbiol.* **1999,** *65* (4), 1610-1618.
34. Funahashi, T.; Tanabe, T.; Mihara, K.; Miyamoto, K.; Tsujibo, H.; Yamamoto, S., Identification and Characterization of an Outer Membrane Receptor Gene in *Acinetobacter baumannii* Required for Utilization of Desferricoprogen, Rhodotorulic Acid, and Desferrioxamine B as Xenosiderophores. *Biol Pharm Bull.* **2012,** *35* (5), 753-760.
35. Sebulsky, M. T.; Shilton, B. H.; Speziali, C. D.; Heinrichs, D. E., The Role of FhuD2 in Iron(III)-Hydroxamate Transport in *Staphylococcus aureus*. *J. Biol. Chem.* **2003,** *278* (50), 49890-49900.
36. Podkowa, K. J.; Briere, L.-A. K.; Heinrichs, D. E.; Shilton, B. H., Crystal and Solution Structure Analysis of FhuD2 from *Staphylococcus aureus* in Multiple Unliganded Conformations and Bound to Ferrioxamine-B. *Biochemistry* **2014,** *53* (12), 2017-2031.
37. Chambers, C. E.; Sokol, P. A., Comparison of siderophore production and utilization in pathogenic and environmental isolates of *Yersinia enterocolitica*. *J Clin Microbiol.* **1994,** *32* (1), 32-39.
38. Mishra, R. P. N.; Mariotti, P.; Fiaschi, L.; Nosari, S.; Maccari, S.; Liberatori, S.; Fontana, M. R.; Pezzicoli, A.; De Falco, M. G.; Falugi, F., et al., *Staphylococcus aureus* FhuD2 Is Involved in the Early Phase of Staphylococcal Dissemination and Generates Protective Immunity in Mice. *J Infect Dis.* **2012,** *206* (7), 1041-1049.
39. Mariotti, P.; Malito, E.; Biancucci, M.; Lo Surdo, P.; Mishra, Ravi P. N.; Nardi-Dei, V.; Savino, S.; Nissum, M.; Spraggon, G.; Grandi, G., et al., Structural and functional characterization of the *Staphylococcus aureus* virulence factor and vaccine candidate FhuD2. *Biochem. J.* **2013,** *449* (3), 683-693.
40. Arifin, A. J.; Hannauer, M.; Welch, I.; Heinrichs, D. E., Deferoxamine mesylate enhances virulence of community-associated methicillin resistant *Staphylococcus aureus*. *Microbes Infect.* **2014,** *16* (11), 967-972.
41. Bottone, E. J., *Yersinia enterocolitica*: Revisitation of an Enduring Human Pathogen. *Clin Microbiol Newsl.* **2015,** *37* (1), 1-8.
42. Hassan, A.; Naz, A.; Obaid, A.; Paracha, R. Z.; Naz, K.; Awan, F. M.; Muhmmad, S. A.; Janjua, H. A.; Ahmad, J.; Ali, A., Pangenome and immuno-proteomics analysis of *Acinetobacter baumannii* strains revealed the core peptide vaccine targets. *BMG Genomics* **2016,** *17*, 732.
43. Braun, V.; Pramanik, A.; Gwinner, T.; Koberle, M.; Bohn, E., Sideromycins: tools and antibiotics. *Biometals* **2009,** *22* (1), 3-13.
44. Page, M. G. P., Siderophore conjugates. *Ann N Y Acad Sci.* **2013,** *1277* (1), 115-126.
45. Doorneweerd, D. D.; Henne, W. A.; Reifenberger, R. G.; Low, P. S., Selective Capture and Identification of Pathogenic Bacteria Using an Immobilized Siderophore. *Langmuir* **2010,** *26* (19), 15424-15429.
46. Kim, Y.; Lyvers, D. P.; Wei, A.; Reifenberger, R. G.; Low, P. S., Label-free detection of a bacterial pathogen using an immobilized siderophore, deferoxamine. *Lab Chip* **2012,** *12* (5), 971-976.
47. Pandey, R. K.; Jarvis, G. G.; Low, P. S., Chemical synthesis of staphyloferrin A and its application for *Staphylococcus aureus* detection. *Org Biomol Chem.* **2014,** *12* (11), 1707-1710.
48. Horcas, I.; Fernandez, R.; Gomez-Rodriguez, J. M.; Colchero, J.; Gomez-Herrero, J.; Baro, A. M., WSXM: a software for scanning

probe microscopy and a tool for nanotechnology. *Rev Sci Instrum* **2007,** *78* (1), 013705.
49. Soyer, M.; Duménil, G., Introducing Shear Stress in the Study of Bacterial Adhesion. *J Vis Exp.* **2011,** (55), 3241.
50. Zagorodko, O.; Bouckaert, J.; Dumych, T.; Bilyy, R.; Larroulet, I.; Serrano, A.; Dorta, D.; Gouin, S.; Dima, S.-O.; Oancea, F., et al., Surface Plasmon Resonance (SPR) for the Evaluation of Shear-Force-Dependent Bacterial Adhesion. *Biosensors* **2015,** *5* (2), 276.
51. Viegas, K. D.; Dol, S. S.; Salek, M. M.; Shepherd, R. D.; Martinuzzi, R. M.; Rinker, K. D., Methicillin resistant *Staphylococcus aureus* adhesion to human umbilical vein endothelial cells demonstrates wall shear stress dependent behaviour. *Biomed Eng OnLine* **2011,** *10* (1), 1-18.
52. Mohamed, N.; Rainier, T. R.; Ross, J. M., Novel experimental study of receptor-mediated bacterial adhesion under the influence of fluid shear. *Biotechnol Bioeng.* **2000,** *68* (6), 628-636.
53. Reddy, K.; Ross, J. M., Shear Stress Prevents Fibronectin Binding Protein-Mediated *Staphylococcus aureus* Adhesion to Resting Endothelial Cells. *Infect Immun.* **2001,** *69* (5), 3472-3475.

Supporting Information

How to Capture Ferrioxamine-Binding Bacteria in 30 Seconds or Less

Nigam B. Arora, John H. Sides, and Alexander Wei*

Department of Chemistry, Purdue University, 560 Oval Drive, West Lafayette, IN 47907, USA

Correspondence to alexwei@purdue.edu

Optimized culture of bacteria under iron restricted conditions. As standard practice, strains were grown out for a minimum of three generations prior to inoculation in bipy-treated media. These cultures were handled exclusively with acid-washed materials to eliminate the possibility of iron contamination. For optimization, strains were cultured in broth with variable bipy concentrations ranging from 0.05–3 mM, to determine the highest restriction of iron while still permitting steady growth. For many strains, a clear concentration threshold could be determined above which bacteria did not proliferate. Other strains could proliferate at even the highest bipy concentrations; in these cases, optimal conditions were determined by consistency of culture growth and/or by the quality of the detection experiments. Optimized bipy levels for each strain are shown in table S1.

Table S1. List of bacterial strains optimized for growth under iron-restricted conditions

Bacterial strain	Broth	Max. [bipy], in mM
Y. enterocolitica	Luria-Bertani	3
Y. enterocolitica (4 °C)	Luria-Bertani	0.05
S. aureus	Tryptic Soy	1
MRSA	Tryptic Soy	1
P. aeruginosa	Luria-Bertani	0.3
S. enterica	Luria-Bertani	0.1
A. baumannii	Nutrient Broth	0.1
K. pneumoniae	Nutrient Broth	0.1

Synthesis of FOx conjugates for patterning of chips. Synthesis of 2,2'-(ethylenedioxy)bis(ethylisothiocyanate). To a solution of 2,2'-(ethylenedioxy)bis(ethylamine) (322 µL in 5 mL dry methanol) was added triethylamine (612 µL) and carbon disulfide (400 µL). The reaction was stirred at room temperature and monitored for changes in optical extinction using Cary 50 UV-vis spectrometer. Formation of the bis-dithiocarbamate (DTC) intermediate was observed at 5 minutes; the reaction was deemed complete at 15 minutes. The reaction vessel was cooled to 0 °C in an ice bath. Di-*tert*-butyl dicarbonate (1.19 g in 1.25 mL dry methanol) was added to the reaction mixture, followed by 4-dimethylaminopyridine (DMAP; 8.1 mg in 1mL dry methanol), and the reaction was warmed to room temperature. UV spectroscopy showed reduction in DTC absorption at 255 and 290 nm within 5 minutes at room temperature, and emergence of an absorption band at 225 nm corresponding to the isothiocyanate. The reaction mixture was stirred for 1 hour, then concentrated by rotary evaporation to a clear yellow oil (418 mg, 82% yield). ITC formation was confirmed by ^{13}C NMR. Bis-ITC was used without further purification.

Synthesis of FOx-ITC conjugate. A solution of iron(III) chloride (4.9 mg in 1 mL DMSO) was treated with 18.5 mg of dFOx to form the corresponding iron chelate (FOx). The dark red reaction was mixed for 10 min at room temperature until a homogeneous solution was obtained, then treated with dry triethylamine (15 µL) and 2,2'-(ethylenedioxy)bis(ethylisothiocyanate) (14 µL) and allowed to stir for

at least 12 hours. Product formation and the disappearance of FOx were monitored by ESI mass spectrometry. Purification was performed by HPLC (Waters) using a C18 reverse-phase column (Phenomenex 250 x 21 mm) with a gradient of 25–75% acetonitrile in water, at a constant flow rate 10 mL/min. Fractions containing the desired conjugate were concentrated first by rotary evaporation (to remove acetonitrile), followed by lyophilization. The conjugates were obtained as orange powders, with isolated yields on the order of 60%.

Synthesis of conjugate **1**. Lyophilized FOx-ITC conjugate from freezer stock (5 mg) was dissolved in 100 µL of 0.1 M Na_2CO_3 buffer (pH 11) and allowed to sit at room temperature for 1–2 days. In situ hydrolysis of the ITC to a primary amine was monitored by ESI mass spectrometry, using the intensity ratio of molecular ion (*m/z*) peaks generated by the ITC and amine. When the apparent ratio stopped increasing, the solution was diluted with deionized water to 1 mL, with a final pH of 10. Reverse-phase HPLC (25–90% acetonitrile in water) yielded the desired amine **1** in pure form (3.5 mg; 70% yield).

Synthesis of conjugate **2.** Lyophilized FOx-ITC (5 mg, 1.0 equiv), 2,2'-(ethylenedioxy)bis(ethylamine) (3.3 µL, 1.1 equiv), and distilled triethylamine (15 µL, 10 equiv) were dissolved in DMSO (800 µL). The solution was stirred at room temperature for 12 hours. Product formation and disappearance of starting material was confirmed by ESI mass spectrometry. The reaction mixture was passed through a 0.2-µm membrane filter, then directly injected onto the reverse-phase HPLC system. Amine **2** exhibited a strong absorbance at 430 nm

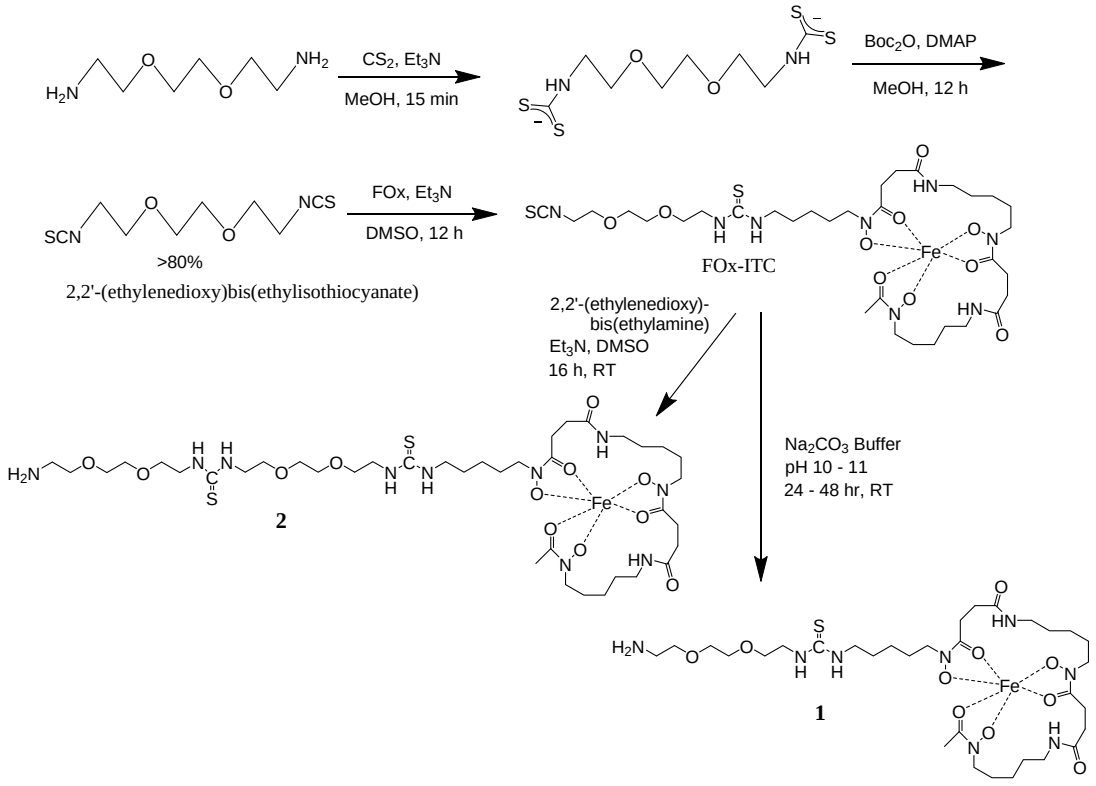

Figure S1. Synthesis of FOx conjugates **1** and **2**

Limit of detection studies with Y. enterocolitica using DoCM . To determine the limit of detection (LOD) for *Y. enterocolitica*, five chips were exposed to bacterial suspensions at concentrations between 10^6 and 10^2 cfu/mL. A negative control chip was exposed to PBS buffer and also carried through all parts of the experiment. Chip exposure time was 1 hour using the drop-on-chip method. Chips were imaged under darkfield conditions (Figure S2), then subjected to FFT analysis for an objective determination of positive capture (Figure S3). In some cases, bacteria-treated chips were treated with propidium iodide (PI) to confirm that optical scattering was primarily due to immobilized *Y. enterocolitica*. Chips were first sterilized with UV light irradiation (254 nm) for four hours, then exposed to 3 µg/mL PI in a pH 7 sodium chloride/sodium citrate buffer for 10 minutes before rinsing with water, drying with compressed air, and imaging with a fluorescence microscope (Figure S4). PI staining confirmed that the patterns visualized by darkfield imaging were in fact due to scattering from immobilized bacteria. This was reinforced by images taken with the 100X objective, showing individual stained cells clustered on printed spots. We can thus conclude that the LOD for *Y. enterocolitica* is 10^2 cfu/mL, given an exposure time of one hour.

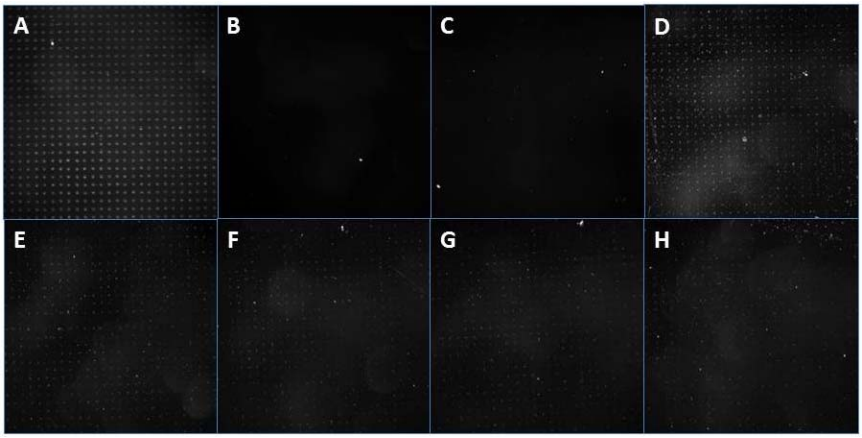

Figure S2. Darkfield images depicting chips from LOD study with *Y. enterocolitica*. (A) post print, (B) post block, (C) after exposure to PBS only, and (D–H) after exposure to bacteria at concentrations of 10^6 – 10^2 cfu/mL respectively.

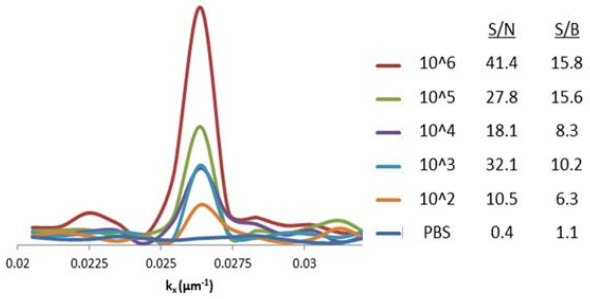

Figure S3. FFT signals from darkfield images of LOD experiment, with associated S/N and S/B values.

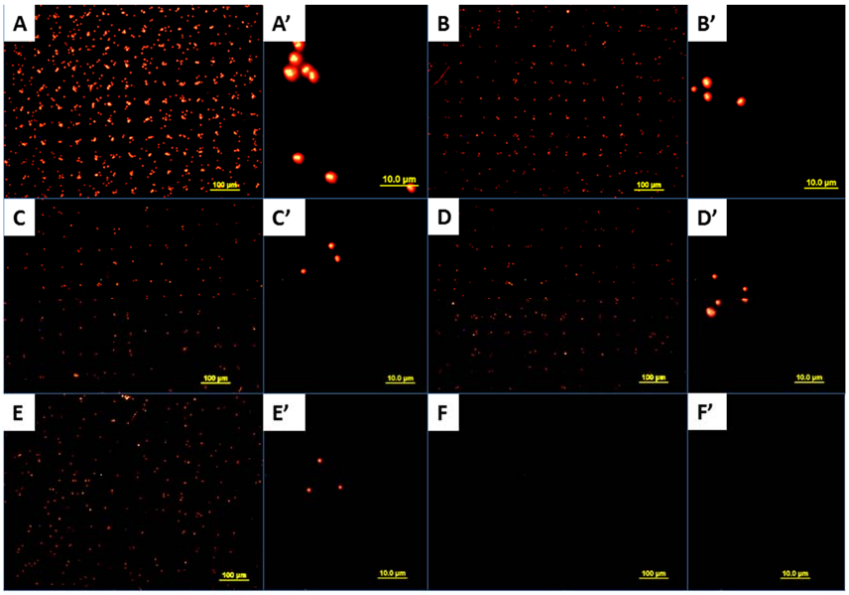

Figure S4. Fluorescence images of all chips used in LOD experiment, after treatment with PI. Low-magnification images with 10X objective (A–E) and images of individual array elements spots with 100X objective (A'–E') are represented for chips exposed to bacteria at 10^6, 10^5, 10^4, 10^3, and 10^2 cfu/mL, respectively. Negative control chips treated with PBS buffer (F and F') appear blank, indicating absence of immobilized bacteria.